Virginia Commonwealth University

VCU Scholars Compass

2008

A Capillary-Based Microfluidic System for Immunoaffinity Separations in Biological Matrices

Michael Peoples
Virginia Commonwealth University

www.manaraa.com

A CAPILLARY-BASED MICROFLUIDIC SYSTEM FOR IMMUNOAFFINITY

SEPARATIONS IN BIOLOGICAL MATRICES

A Dissertation submitted in partial fulfillment of the requirements for the degree of
Doctor of Philosophy at Virginia Commonwealth University.

by

MICHAEL CHAD PEOPLES
Bachelor of Science, Virginia Commonwealth University, 1998

Director: H. THOMAS KARNES, Ph.D.
PROFESSOR, DEPARTMENT OF PHARMACEUTICS

Virginia Commonwealth University
Richmond, Virginia
May 2008

This work is dedicated to my family for continued support during the lows, middles, and highs. A special dedication is reserved for my loving wife and son, who endured the long journey of this part-time student.

Acknowledgement

Table of Contents

List of Tables

List of Figures

Abstract

A CAPILLARY-BASED MICROFLUIDIC SYSTEM FOR IMMUNOAFFINITY

SEPARATIONS IN BIOLOGICAL MATRICES

By Michael Chad Peoples

A Dissertation submitted in partial fulfillment of the requirements for the degree of Doctor
of Philosophy at Virginia Commonwealth University.

Virginia Commonwealth University, 2008

Major Director: H. Thomas Karnes, Ph.D.
Professor, Department of Pharmaceutics

The analysis of biological samples in clinical or research settings often requires measurement of analytes from complex and limited matrices. Immunoaffinity separations in miniaturized formats offer selective isolation of target analytes with minimal reagent consumption and reduced analysis times. A prototype capillary-based microfluidic system has been developed for immunoaffinity separations in biological matrices with laser-induced fluorescence detection of labeled antigens or antibodies. The laboratory-constructed device was assembled from two micro syringe pumps, a microchip mixer, a

micro-injector, a diode laser with fused-silica capillary flow cell, and a separation capillary column. The columns were prepared from polymer tubing and packed under negative pressure with a stationary phase that consisted of biotinylated antibodies attached to streptavidin-silica beads. A custom software program controlled the syringe pumps to perform step gradient elution and collected the signal as chromatograms. The system performance was evaluated with flow accuracy, mixer proportioning, pH gradient generation, and assessment of detectability. A direct labeling/direct capture immunoaffinity separation of C-reactive protein (CRP) was demonstrated in simulated serum. CRP, a biomarker of inflammation and cardiovascular disease risk assessment, was fluorescently labeled in a one-step reaction and directly injected into the system. A quadratic calibration model was selected and precision and accuracy were reported. Parathyroid hormone was also analyzed by the direct capture approach, but displayed nonspecific binding of human plasma matrix components that limited the useful assay range. Capillary sandwich assays of CRP in human serum and cerebrospinal fluid were performed using both capture and detection antibodies. The detection antibody was labeled and purified offline to minimize signal from labeled matrix components. Four parameter logistic functions were used to model the data and precision and accuracy were evaluated. During the study, 250 nL injection volumes 2.0 µL/min flow rates were employed, minimizing sample and reagent consumption. The microfluidic system was capable of separating antigens from biological matrices and is potentially portable for patient point-of-care settings. Additionally, the flexible design of the separation capillary

allows for the analysis of different clinical markers by changing the antibodies and the low

assay volume requirements could lead to less invasive patient sampling techniques.

CHAPTER 1 Microfluidic Immunoaffinity Separations for Bioanalysis

Drawn from manuscript published in Journal of Chromatography B (2008) 866: 14-25

1.1 Introduction

The measurement of analytes from complex and limited matrices is frequently required for analysis of biological samples. There is an increasing need for analytical instrumentation capable of minimal sample consumption and reduced analysis times, while providing selective separation of target compounds from the sample matrix. The reduction of sample requirements is advantageous for the analysis of scarce or valuable biological test materials, including research, clinical, and archived samples (Phillips and Smith 2002). Miniaturized analytical devices address this requirement for reduced reagent consumption and fast time of analysis, while offering the potential for portability and patient point-of-care testing. Target analytes in biological samples are often present in low concentrations relative to the surrounding matrix components, necessitating effective separation techniques. Immunoaffinity-based separation techniques have been used to separate analytes of interest from complex biological samples based on the selective binding of antibodies to their respective antigens (Phillips and Smith 2002). Immunoaffinity microfluidic devices employing antibodies as immobilized ligands may be applied to capture and concentrate target analytes from small volumes (microliters and below) of biological matrices. The combination of miniaturized instrumentation with an

1

immunoaffinity separation approach allows for potentially rapid and selective isolation of low concentration analytes from biological samples.

Immunoaffinity separations have been reviewed with respect to their use in sample preparation/extraction (Hennion and Pichon 2003; Delaunay-Bertoncini and Hennion 2004), post-column immunodetection (Tang and Karnes 2000), capillary electrophoresis (Yeung, Luo et al. 2003; Guzman and Phillips 2005), microfluidic immunosensors (Luppa, Sokoll et al. 2001; Bange, Halsall et al. 2005), and conventional scale affinity/immunoaffinity chromatography (Hage 1998; Hage 1999; Weller 2000). In the current review, recent literature will be discussed as it pertains to immunoaffinity separations, with small-scale biological sample analysis using miniaturized instrumental components and involving pumped-based systems with capillaries or microchips. The term "microfluidics" will be used to describe the movement of liquids through microchip channels or capillaries having internal dimensions less than 1 mm and the term "immunoaffinity" will encompass flow-based immunoassays as well as immunoaffinity chromatography.

1.2 Immunoaffinity background

1.2.1 Antibodies

Antibodies are large glycoproteins produced in response to a material identified as foreign by the body and immunoglobulin G (IgG) is the most commonly used antibody in immunoaffinity techniques. IgG is approximately 150 kDa, consisting of four polypeptides with two 25 kDa identical light chains and two 50 kDa identical

glycosylated heavy chains (Guzman and Phillips 2005). Figure 1 shows a schematic of an antibody with common functional groups diagrammed. Disulfide bonds join light and heavy chains together, as well as linking the two heavy chains to form the hinge area. The FAb (fragment antibody binding) portion is located at the N-terminus and contains a region of variable amino acid content responsible for antigen specificity. The Fc (fragment crystallizable) portion spans the C-terminus to the hinge region and maintains a constant amino acid sequence within the same class of antibody. Primary amines of lysine residues are located throughout the entire antibody and carbohydrate groups are mainly located in the Fc region (Subramanian 2002). The carbohydrate residues and primary amines are targeted attachment sites for linking antibodies to solid supports or attaching labels for detection. Two types of antibodies employed for immunoaffinity separations are polyclonal and monoclonal. Polyclonal antibodies are natural antibodies from multiple cell lines that may bind different recognition sites or epitopes with varying strengths, whereas monoclonal antibodies are produced from a single cell line and bind to a single epitope with the same strength (Hage 1998).
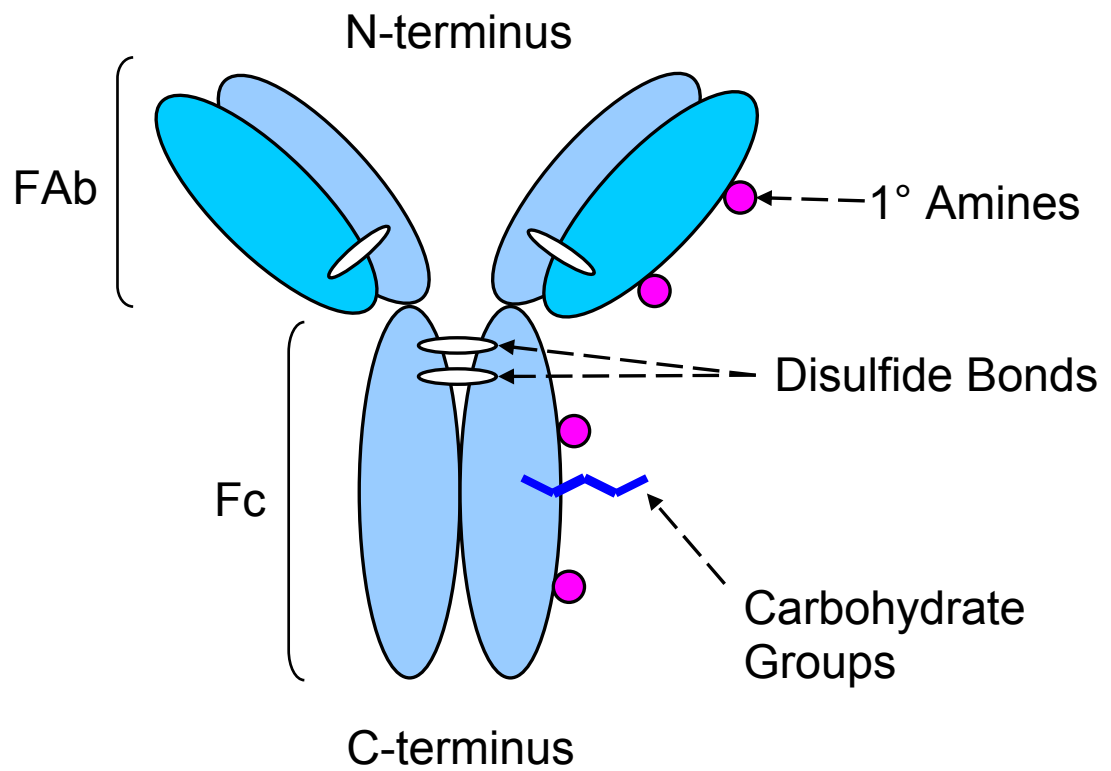
Figure 1: Antibody structure and functional groups for labeling or solid phase attachment.
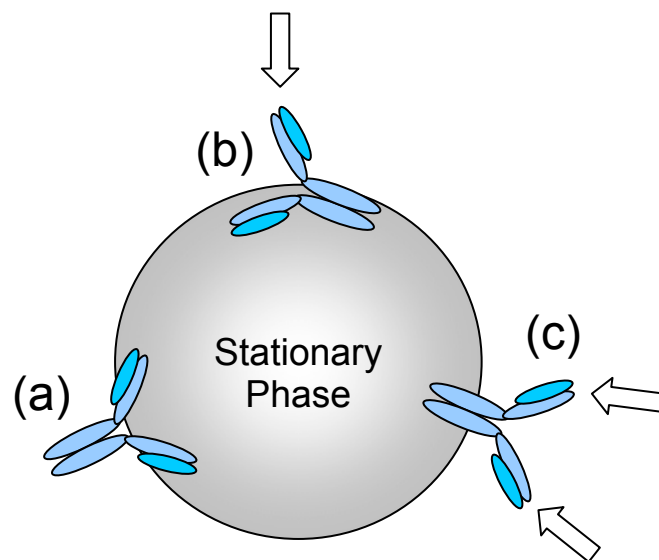
Figure 2: Effect of immobilized IgG on antigen recognition. Arrows indicate available antigen binding sites.

1.2.2 Antibody immobilization

Immunoaffinity-based separations typically employ immobilized antibodies as a stationary phase to capture antigens of interest from sample matrices. The unbound material is washed to waste before an elution buffer is applied to dissociate the antigen for detection (Subramanian 2002). The heart of an immunoaffinity analysis system is the separation column or channel, which consists of an immunosorbent of immobilized antibodies. The orientation of the stationary antibodies is critical to the binding activity (Hage 1998). Figure 2 shows the possible orientations of an immobilized IgG on a solid support material. In (a), the antibody is attached through the FAb section and both antigen biding sites are unavailable. In (b) the binding sites are partially available and in (c) the antibody is attached through the Fc region with both binding sites fully available. Immobilization strategies that anchor the antibody with the FAb portions facing away from the stationary support result in a higher degree of active antibody per unit of stationary support.

Antibodies may be attached directly to the walls of a capillary column or microchip channel. Antibodies can also be linked to solid phase supports and packed into columns or channels. Solid supports may consist of particles or beads made from plastic, silica or glass, and magnetic materials (Hage 1998; Hayes, Polson et al. 2001; Rhemrev-Boom, Yates et al. 2001). The stationary phase should possess the following characteristics (Guzman and Stubbs 2001; Rhemrev-Boom, Yates et al. 2001; Subramanian 2002):

      a) Chemical stability

b) Low nonspecific binding

c) Mechanical stability for favorable flow rates

d) Sufficient surface area for antibody-antigen binding.

The choice of solid phase material and method of antibody attachment are important factors for developing an immunoaffinity separation. A simple approach for antibody immobilization is through direct attachment to a solid support. Antibodies may be physically adsorbed to plastic chips or beads through noncovalent bonding (Nisnevitch and Firer 2001; Cho, Paek et al. 2007) or free amine groups may be reacted through activated surfaces. Immobilization of the antibodies by direct adsorption or through primary amines results in a random orientation and potentially lowered binding activity. This likely results from attachment of the antibody through the FAb arms, which can occur when linking antibodies to supports using free amino groups. Carbohydrate groups of the Fc region can be oxidized to aldehyde functional groups with periodate and reacted with hydrazide supports to give the proper orientation for antigen binding. Polyclonal antibodies are reported to have better success binding antigen versus monoclonal antibodies after periodate oxidation (Lu, Smyth et al. 1996). This may be due to differences in the degree of glycosylation between the two types of antibodies. Additionally, FAb fragments produced from enzymatic cleavage of IgG can be coupled through free sulfhydryl groups to chemically modified supports. This method results in monovalent antibody fragments with antigen receptors oriented toward the solution and away from the stationary support.

Attachment of antibodies to secondary molecules has been used for optimizing antibody orientation and also providing a protective protein coat to the solid phase material. Bacterial cell wall proteins A and G are secondary molecules that selectively bind many antibodies at the Fc region. These proteins maintain antibody binding at physiological pH, but will release antibodies in weakly acidic conditions (Hage 1998; Weller 2000). The straightforward coupling of antibodies to protein A and G is an advantage, but the antibodies must be reapplied to the column. Multiple injections on this type of column could consume large quantities of valuable antibodies; however, additional reactions may be performed to cross-link protein A or G to the antibody for a less reversible attachment (Hage 1998; Nisnevitch and Firer 2001).

Avidin is a protein from egg white that has a high affinity for the vitamin biotin ($K_a = 10^{15}$/M), forming strong noncovalent bonds (Chilkoti and Stayton 1995; Strachan, Mallia et al. 2004). Streptavidin is a bacterial form of avidin with similar binding sites for biotin, but is also a form that has less nonspecific interaction with proteins. Unlike the antibody binding of protein A or G, the streptavidin-biotin bond is nearly irreversible. Antibodies must be linked to biotin in order to react with streptavidin, but their activity is unlikely to be affected due to the small size of biotin (244 Da) (Strachan, Mallia et al. 2004). Numerous biotin derivatives for linkage to antibodies are available. Biotinylation of antibodies may be achieved through primary amine groups using *N*-hydroxysuccinimide groups or through aldehydes using a hydrazide linker. The biotin hydrazide reagents will react with oxidized carbohydrates in the Fc region to form a hydrazone bond. The use of hydrazine has the same advantage as using protein A or G,

which is that antibody attachment does not interfere with antigen binding sites (Nisnevitch and Firer 2001). Biotinylation of antibodies through oxidized carbohydrates or sulfhydryl groups of Fab fragments have been shown to yield stationary supports with higher degrees of antibody activity when compared to supports from amino-biotinylated antibodies (Lu, Smyth et al. 1996; Cho, Paek et al. 2007). Alternatively, many antibodies may be purchased biotinylated, although this is most often via primary amine attachment. It should be noted that biotinylated IgG has been reported to display instability in human plasma after prolonged exposure (4 hour incubation) (Bogusiewicz, Mock et al. 2004). Figure 3 shows a solid phase bead with antibodies attached by FAb sulfhydryl groups and secondary compounds. Protein A/G, avidin/streptavidin, and secondary antibody-coated beads are commercially available in polystyrene and magnetic polystyrene from numerous vendors. Sources of activated supports suitable for high performance immunoaffinity applications (i.e., silica or glass) are shown in Table 1.
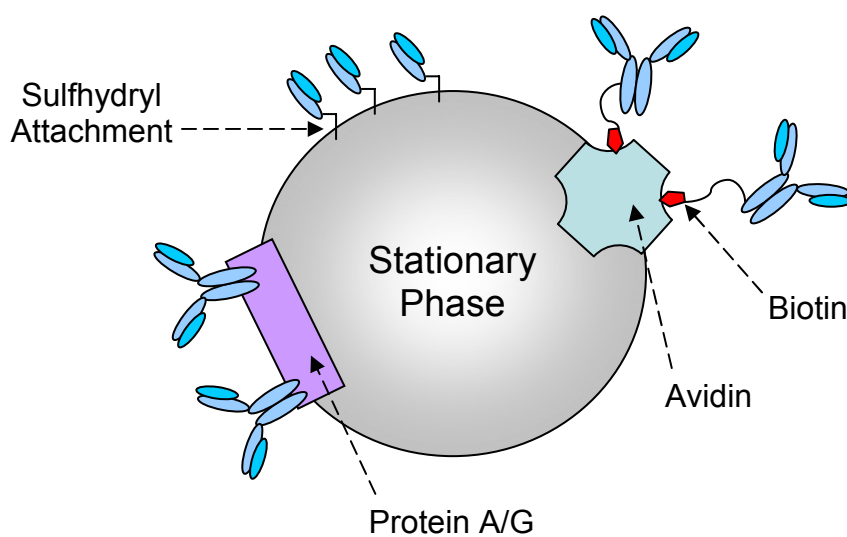
Figure 3: Antibody immobilization strategies. Antibodies may be linked through secondary compounds such as Protein A/G and biotin/avidin or covalently attached through sulfhydryl groups of FAb fragments.

Table 1: High performance supports suitable for immobilizing antibodies through

secondary compounds.

Material	Coating	Vendor
Silica microspheres	Avidin	Kisker[a]
Silica microspheres	Streptavidin	Bangs Labs[b] Kisker[a] Polysciences[c]
Silica microspheres	Protein A or G	Kisker[a]
Glass particles	Streptavidin	Xenopore[d]

[a] www.kisker-biotec.com, [b] www.bangslabs.com, [c] www.polysciences.com,
[d] www.xenopore.com

1.3. Immunoaffinity separations

1.3.1. Antibody-antigen complexes and immunoaffinity chromatography

Antibody-antigen complexes form as the result of several intermolecular forces, the main four being:

1. Hydrogen bonding

2. Coulombic, i.e., NH_3^+ and COO^-

3. Van der Waals

4. Hydrophobic interactions.

Collectively, these forces result in strong binding at physiological conditions (Phillips 1985; Subramanian 2002). In immunoaffinity chromatography, it is desirable to elute the analyte quickly by dissociating the antibody-antigen complex without damaging

the immobilized antibody. The sample containing the antigen is introduced to the antibody in an application buffer with conditions to allow for maximum binding. Application buffers are typically near physiological pH and salt concentrations and phosphate or tris-based buffers are often used. During this antigen capture step all nonreactive sample components are washed from the separation column. Recovery of the isolated antigen for detection is achieved by the application of an appropriate elution buffer. Alternatively, detection of the antibody-bound antigen may occur directly on-chip or on-capillary; however, the antigen must still be dissociated if the system is intended to be reusable.

The selection of an effective elution buffer can vary based on the antigen under investigation and empirical tests are frequently required (Yarmush, Antonsen et al. 1992; Subramanian 2002). The most commonly used scheme involves lowering the pH of the running buffer down to 2 or below. Many solid supports such as silica can degrade when exposed to sharp changes from neutral to acidic conditions. Protein coatings such as protein A or streptavidin offer some protection in this regard (Phillips 1985). Acidic elution buffers may lead to poor antigen recovery in cases where the antibody-antigen complex is held together predominately with hydrophobic interactions. Chaotropic agents, such as thiocyanates, are also used as elution buffers with less damaging effects to the stationary phase compared to low pH acidic buffers (Phillips and Dickens 2000). Chaotropes disturb the structure of water molecules and reduce hydrophobic interactions between proteins (Moelbert, Normand et al. 2004; Salvi, De Los Rios et al. 2005). Other dissociation reagents have been utilized, including ionic strength modifications,

denaturants, and polarity-reducing organic modifiers (Phillips 1985; Yarmush, Antonsen et al. 1992).

With any elution scheme, a short step-wise or linear gradient of the dissociating buffer may be introduced into the running buffer. Step gradients have the potential of providing faster antigen dissociation and shorter analysis times versus linear gradients (Hage 1998). The type of gradient may also have an effect on the shape of the eluted antigen peak; it has been reported that linear gradient elution produces sharper, more resolved peaks versus stepwise gradients (Phillips and Dickens 2000). For pH and chaotropic elution buffers, linear gradients are also reported to be gentler on the immobilized antibody and support material (Phillips 1985; Phillips and Dickens 2000).

Different modes of immunoaffinity separations using immobilized antibody columns and microchips may be performed, including:

1. Competitive

2. Non-competitive

3. Direct capture.

A competition assay may be employed, where sample antigen and a labeled antigen of known concentration compete for limited antibody binding sites. The amount of labeled antigen bound to the antibody will decrease with increasing amounts of sample antigen. A competitive assay is commonly used for smaller univalent antigens (Sapsford, Charles et al. 2002). A non-competitive sandwich immunoassay requires two antibodies with affinity for the antigen. The first antibody is immobilized to capture the antigen and a second, labeled antibody is added before or after injection of the sample. The dual

antibody system offers a higher selectivity, but requires that the antigen be large enough to bind two antibodies through distinct epitopes. The sandwich assay format may also take more time to perform due to two antibody binding steps (Sapsford, Charles et al. 2002). The most straightforward approach is a direct capture assay. In this technique the sample is injected onto the immunoaffinity column and the antigen binds to the antibody in neutral buffer. The antigen is often pre-labeled (i.e. with a fluorescent conjugate) to improve detectability of low concentration samples (Hage 1998). The unbound material is pumped to waste and then the elution buffer is applied to dissociate the antigen for measurement. This results in a large initial chromatographic peak corresponding to the unbound material and excess label. The antigen peak will be a sharper, purified second peak. An inherent advantage is there is no need to purify the labeled analyte prior to analysis. An example of a typical direct capture format immunoaffinity chromatogram is shown in Figure 4. A 250 nL injection of human parathyroid hormone (111 nM in phosphate buffer containing 0.1% human serum albumin) labeled with a laser dye was separated on a 0.175 x 19 mm capillary column and detected with a 650 nm diode laser LIF detector. Elution was achieved with a step gradient from a pH 7.0, 100 mM phosphate application buffer to a 2.5 M NaSCN elution buffer. The instrumentation used has been described in Chapter 2 (Peoples, Phillips et al. 2007).
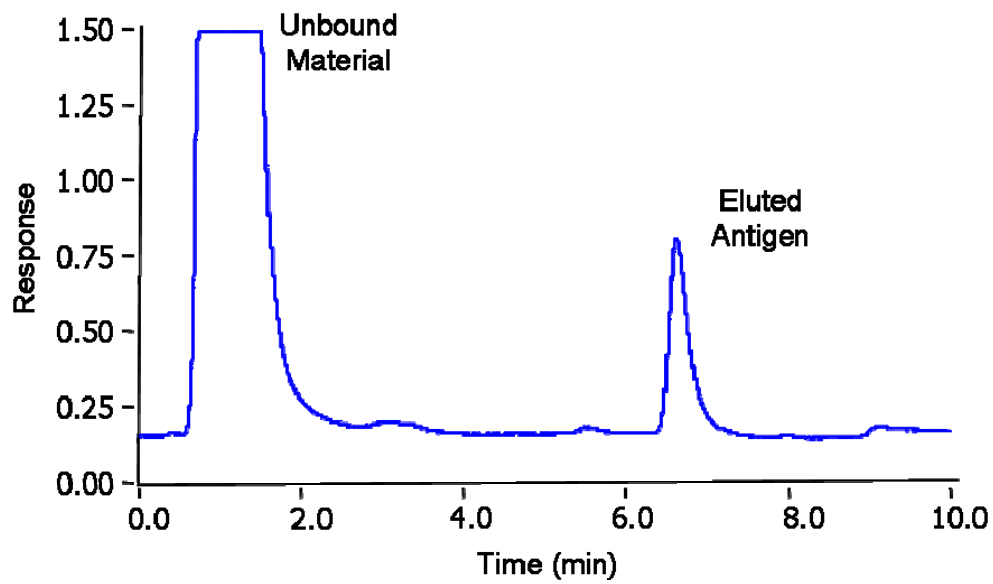
Figure 4: Typical immunoaffinity chromatogram. The first off-scale peak corresponds to unreacted material washing off the column during the antigen capture step. After application of a dissociation buffer, the antigen is eluted as the second peak. Conditions are described in the text.

1.3.2. Working lifetime of immunoaffinity devices

The working lifetime of immunoaffinity systems is important where repeat analyses are desired. Reducing the amount of material required to repeatedly prepare separation devices is an advantage considering the associated high costs of immunoassay reagents. Column and microchip lifetimes are often reported in terms of cycles, representing sample injection, elution, and/or regeneration. The useful lifetime is related to degradation of assay performance or loss of binding activity and dependent upon running/storage conditions of the system. The sample matrix, flow rate, elution conditions, and operating and storage temperature all affect the system's life expectancy. Nonspecific binding of matrix components from repeat sample injections and incomplete elution can contaminate the system (Yarmush, Antonsen et al. 1992) and cause increased back pressure (Hage, Taylor et al. 1992). The immobilized antibody may be damaged or removed from the stationary support in the presence of high flow and pressure (Phillips and Dickens 2000). Flow rate also affects antigen recovery, as slower flows allow more time for antibody-antigen reactions. Harsh elution buffers may damage antibodies since the targeted forces holding antibody-antigen complexes together are the same as those responsible for maintaining the tertiary structure and binding ability of the antibody (Phillips 1985). Yang et al. reported that 150 cycles were possible for microfluidic chips using 10 mM glycine-HCl at pH 2.0 for elution (Yang, Brooks et al. 2005). Additionally, the temperature of the immunoaffinity device can affect the performance and refrigerated (4°C) conditions are reported to extend active life. Immunoaffinity column lifetimes of up to 200 cycles have been reported for columns both stored (Rhemrev-Boom, Yates et

al. 2001), and stored/operated (Phillips and Smith 2002) at refrigerated temperatures; although 200-250 cycles have also been reported for columns operated at room temperature (Hage, Taylor et al. 1992).

1.3.3. Biological samples and complex matrices

Complex sample matrices require extensive sample preparation to become compatible with microfluidic systems and small-scale instrument components (Whitesides 2006). Biological samples for clinical and research purposes are problematic for microfluidic devices due to nonspecific binding of biomolecules, particularly proteins. Nonspecific adsorption to surfaces of capillary tubing and microchip materials, including stationary supports, can lead to increased system pressures and obstruction of small dimension flow paths. Immunoaffinity separations are adversely affected by nonspecific binding of biomolecules, which can cause higher background signals (Dai, Baker et al. 2006). Blood proteins have been reported to quench fluorescently labeled antigens upon binding. Hatch et al. have reported spiking iophenoxate into human whole-blood samples to preferentially bind serum albumin and reduce this quenching effect (Hatch, Kamholz et al. 2001). Syringe filtration of human plasma has also been reported for sample pretreatment prior to immunoaffinity chromatography (Hage, Taylor et al. 1992). Filtration removes particulate matter that can clog pores of retaining frits or connecting tubing. Molecular weight cutoff filters (MWCO) have been employed for removing proteins and macromolecules from biological samples that could interfere with immunoaffinity separations (Phillips and Wellner 2006a). These filters are available in

centrifugal devices capable of processing small volumes of fluid. Filter selection is based upon the molecular weight of the target antigen; compounds of a larger molecular weight are retained on the filter and the desired analyte passes through to the filtrate. Biological fluids have been diluted in buffers prior to introduction into microfluidic devices to minimize matrix effects. The total protein content of samples has been adjusted to a constant amount to better control fluorescent labeling reactions (Phillips and Wellner 2006a; Phillips and Wellner 2006b). This type of normalization maintains consistent reaction conditions for conjugation reactions that are dependent on the amount of excess reagents. For example, a fluorescent dye that reacts with primary amines would potentially label all protein material present in a biological sample, requiring large concentrations of excess dye.

Capillary columns and connecting tubing for microfluidic devices are often made of fused-silica and polyetheretherketone (PEEK). Salim et al. have studied the effects of nonspecific protein binding on glass capillaries, fused-silica tubing, and PEEK tubing, noting the latter two as common microfluidic transfer lines (Salim, O'Sullivan et al. 2007). Adsorption of the human blood plasma protein fibrinogen was monitored by an enzyme-linked immunosorbent assay (ELISA) using an anti-fibrinogen antibody conjugated to horseradish peroxidase. The ELISA reagents were introduced into capillaries of each material after incubation with fibrinogen and flushed into microplate wells for measurement. It was determined that in addition to glass capillaries, PEEK tubing and fused-silica capillaries exhibited significant amounts of fibrinogen adsorption. The use of these materials in microfluidic immunoaffinity devices may contribute to

nonspecific binding. Moreover, targeted antigens that are proteinaceous in nature may also bind to transfer tubing prior to separation, resulting in a loss of detectable analyte.

Microfluidic chips are commonly made from polymeric materials that are mechanically and chemically stable, as well as inexpensive to manufacture. Materials such as polystyrene and poly(dimethylsiloxane) (PDMS) are popular polymers for microfluidics, but have an inherent disadvantage of nonspecific protein binding (Phillips and Cheng 2005; Sibarani, Takai et al. 2007). The surfaces of these devices are often modified to reduce their hydrophobic nature, which is believed to be involved in the nonspecific interaction of biomolecules. Sibrani et al. have reported the use of phospholipid polymers to modify PDMS microchip channels for reduced nonspecific protein adsorption (Sibarani, Takai et al. 2007). Human serum albumin conjugated with fluorescein isothiocyanate (FITC) was incubated in the PDMS channels, washed, and the channel-bound albumin conjugate was measured with fluorescence microscopy. The polymer modification contained hydrophilic phosphorylcholine groups, which reduced nonspecific adsorption of the albumin and also facilitated sample loading versus unmodified PDMS. A similar study involved coating poly(methyl methacrylate) (PMMA) microchannels with phospholipid polymers to reduce nonspecific interactions (Bi, Zhong et al. 2006). In this study, FITC-bovine serum albumin (BSA) was shown to be bound to unmodified PMMA microchannels, but this binding was significantly reduced when incubated with the phospholipid coated surface. Additionally, human serum and rabbit plasma were incubated on the modified PMMA substrates and scanning electron microscopy images showed minimized nonspecific adsorption. The authors note

that high water content of phospholipid modified polymers helps prevent hydrophobic interactions between biomolecules and the substrate. A microfluidic immunoassay for glucagon has been demonstrated using antibodies anchored to mobile polymer chains of poly(ethylene glycol) (PEG) acrylate (Sebra, Masters et al. 2006). The polymer chain was reported to reduce nonspecific binding of proteins to the substrate materials and also increase accessibility by extending the antibody into the sample solution. A detection limit of 1×10^{-13} M was reported for glucagon in phosphate buffered saline and no blocking steps were required. However, the sensitivity was decreased 53 and 66% for assays in 20% plasma and 20% whole blood, respectively.

In addition to sample filtering, MWCO devices, and microchip surface modification, reagents may also be added to immunoassay buffers to reduce nonspecific binding. Proteins, polymers, and surfactants have been employed in immunoassays as blocking reagents to prevent nonspecific binding of proteins and matrix components (Gardas and Lewartowska 1988; Butler 2000; Studentsov, Schiffman et al. 2002; Brogan, Shin et al. 2004). Protein solutions such as BSA, casein, gelatin, and milk are typically added as incubation steps in static assays and allowed to react with the platform surface (Vogt, Phillips et al. 1987; Butler 2000; Dai, Baker et al. 2006). Protein blocking agents act by filling spaces on the solid support between immobilized antibodies (Butler 2000). In flow-based assays such as immunoaffinity chromatography, surfactants may be added to the application and elution mobile phase buffers to reduce nonspecific binding. Nonionic surfactants commonly used include Triton, Tween, and Brij, which are all effective in reducing hydrophobic protein aggregation and adsorption to solid support

materials (Phillips and Krum 1998; Butler 2000). Additionally, surfactants may provide a favorable hydrophobic-hydrophilic environment for antibody-antigen binding and therefore increase the measured response (Wood 1993). Polymers have been used to block nonspecific binding to polystyrene beads (Waterboer, Sehr et al. 2006) and microplate surfaces and offer advantages versus protein and surfactant blockers (Studentsov, Schiffman et al. 2002). Polymer solutions are stable, inexpensive, homogenous, and free of potential protein interferences. Polyvinyl alcohol, polyvinylpyrrolidone, and polyethylene glycol have been reported to reduce nonspecific background. Polymers may also enhance binding in immunoassays by stabilizing antibodies and protein antigens (Studentsov, Schiffman et al. 2002).

1.4. Microfluidic immunoaffinity instrumentation

The ideal lab-on-a-chip system is a microfluidic device that allows complete analysis, from sample introduction to detection, all on-chip (Lim and Zhang 2007). As discussed previously, biological samples may require extensive pretreatment before introduction into a microfluidic system. Additionally, fluid manipulation and detection are often performed by off-chip external equipment (Whitesides 2006). Miniaturized instrument components facilitate microfluidic analyses and may fit onto mobile laboratory carts for potential point-of-care applications. Instrumentation used in the construction and operation of pump-based immunoaffinity microfluidic devices typically

involves fluid control, sample introduction, separation columns or channels, and detectors.

1.4.1. Pumping systems and mixers

Immunoaffinity separations for capillary electrophoresis and capillary electrochromatography involve the use of electrokinetic flow and have been reviewed elsewhere (Yeung, Luo et al. 2003; Amundsen and Siren 2007; Okanda and El Rassi 2007). Pressure-driven, flow-based immunoassays and immunoaffinity chromatography in microfluidic platforms use pumps to push or pull liquids through the device. Syringe pumps (Liu and Li 2001; Sato, Yamanaka et al. 2002) and peristaltic pumps (Lim and Matsunaga 2001; Yacoub-George, Hell et al. 2007) are frequently used to generate flow and introduce reagents. These pumps are available in micro-formats capable of µL/min to nL/min flow rates. Simple or disposable systems may require only one pump to deliver antigens into a capture/detection zone with an application buffer. When antigen elution or regeneration of the microfluidic device is desired, a second buffer or elution solvent is introduced. A single syringe pump, for example, would require the syringe to be changed mid-run for antigen elution. Simple step gradients can be generated using a switching valve connected to two buffer reservoirs and a single pump; however, flexible linear gradients require two pumping sources and a mixing device (Phillips and Dickens 2000). Mixing of buffers occurs in tees or microfluidic chips with branching channels. Gradient mixers are placed in-line between the pumps and the separation column or channel. Dual syringe pumps (Peoples, Phillips et al. 2007) and microdialysis pumps

(Phillips and Smith 2002) have been successfully used to produce immunoaffinity gradients with microfluidic mixing chips. Capillary action has also been applied for immunoassay fluid movement in microchannels (Wolf, Juncker et al. 2004). Devices employing capillary action forces do not require external pumping equipment or power to generate flow and are therefore well suited for portable applications. Capillary flow is manipulated by the shape of the flow path and the hydrophobic/hydrophilic character of the surface (Soo Ko, Yoon et al. 2003). Wolf et al. have described a microfluidic system using capillary action force to perform a C-reactive protein sandwich immunoassay on polymer substrates (Wolf, Juncker et al. 2004). A capillary pump was created by setting a piece of clean room paper over the exit channels. A flow rate of approximately 0.6 µL/min was achieved using the tissue for flow promotion. Examples of representative pumping mechanisms and separation devices are given in Table 2.

Table 2: Types of pump-based flow for immunoaffinity devices.

Flow control	Separation device	Ref
Syringe pumps	Packed fused-silica capillary Packed PEEK/fused-silica capillary PDMS/glass channel	[Phillips and Smith 2002] [Peoples et al. 2007] [Hahn et al. 2007]
Peristaltic pumps	PEEK capillary/stainless steel Fused-silica capillary chip	[Lim and Matsunaga 2001] [Yacoub-George et al. 2007]
Capillary action	PDMS/PMMA channel PDMS/silicon channel Glass capillary	[Soo Ko et al. 2003] [Wolf et al. 2004] [Torabi et al. 2007]

1.4.2. Sample introduction

The analysis of limited biological samples often involves processing a small volume of material, and sample introduction into microfluidic devices requires instrumentation capable of sub-microliter injections. Manual injection valves suitable for micro-and nanoliter volumes of fluid may be fitted with laboratory-constructed sample loops on a capillary scale. PEEK and fused-silica capillary tubing can be cut to desired lengths corresponding to loop volumes based on the calculation for the volume of a cylinder. The chief limitation with manual injectors is limited automation and throughput; however, many clinical and point-of-care tests only require testing small numbers of samples. Micro-syringes may be used to transfer samples to wells or ports of microchips and syringe pumps have been applied as well. Sato et al. have described a syringe pump connected to a microchip outlet hole with a capillary to pull samples from the inlet into the reaction region (Sato, Yamanaka et al. 2002). As commercial autosamplers for liquid chromatography become miniaturized (i.e. nano-LC), microfluidic immunoaffinity separations will benefit from a higher degree of automation and increased throughput.

1.4.3. Separation column or channel

Capillary columns or microchip channels serve as the reaction area for immunoaffinity microfluidic separations. Resolution of the unbound peak and antigen peaks in immunoaffinity chromatography is controlled by the elution step, not necessarily the column dimensions (Erxleben and Ruzicka 2005). Immunoaffinity columns are

therefore amenable to miniaturization as long as the separation zone is large enough to provide adequate antigen binding capacity. For clinical samples, a 50:1 ratio of capture antibody to potential antigen amount has been suggested for efficient binding (Phillips and Wellner 2006a). This could be due to an increased amount of matrix components that may interfere (compete) with antigen binding. In a flow-through system, this excess ratio of antibody to antigen may be necessary to increase the chances of antibody-antigen interaction due to the speed at which the antigen is traveling through the column.

Separation capillaries and channels may be open with antibodies attached to the inner surfaces or packed with an immunosorbent such as beads. The use of reduced-dimension open channels or packed bead beds has inherent advantages over conventional scale immunoassay platforms. Compared to microtiter wells commonly used in immunoassays, the reactive surface area to solution volume ratio is larger and diffusion distances are reduced in capillaries and microchannels (Johns, Rosengarten et al. 1996). These effects are more pronounced when beds of packed microbeads are used for antigen capture in microfluidics (Verpoorte 2003; Lim and Zhang 2007). Increasing the reactive binding surface and reducing the internal volume required for antibody-antigen recognition enables the concentration of dilute antigens in small sample volumes (Dodge, Fluri et al. 2001; Verpoorte 2003). In flow-through systems, sample volumes greater than the volume of the packed bed may be injected and eluted in a concentrated, smaller volume. The increased reactive surface area and reduced diffusion distances in immunoaffinity microfluidics result in a faster time of analysis versus conventional immunoassay techniques (Lim and Zhang 2007). For example, the analysis time of

human immunoglobulin A on a polystyrene bead-packed microchip was reduced to 1/90 of the time needed for an immunoassay in a microplate (Sato, Tokeshi et al. 2000).

Capillary columns used in microfluidic immunoaffinity separations have been constructed from fused-silica (Phillips 2001; Hodgson, Brook et al. 2005; Yacoub-George, Hell et al. 2007), PEEK (Salim, O'Sullivan et al. 2007), and PEEK-coated fused-silica (PEEKsil) (Peoples, Phillips et al. 2007). These materials are commercially available in a variety of internal and outer diameters and may be cut to desired lengths. Retaining frits are required for bead-based separations and have been made by heat annealing silica particles to form porous glass frits (Phillips 2001; Phillips and Smith 2002). Alternatively, capillary-scale stainless steel frits may be purchased and attached to micro-column end fittings (Peoples, Phillips et al. 2007). Capillary columns made from monolithic stationary supports do not require the use of retaining frits (Hodgson, Brook et al. 2005) and offer reduced back pressures with fast mass transfer properties (Mallik and Hage 2006). Fused-silica capillaries have been used for the direct attachment of antibodies to the inner walls of the column (Liu and Li 2001; Yacoub-George, Hell et al. 2007). Open capillary tubes would have less back pressure in pump-based systems versus packed capillaries and could be operated at faster flow rates.

Increasing the flow rate in immunoaffinity separations may result in incomplete antibody-antigen reactions; however, it is not always possible or necessary to reach equilibrium of antibody-antigen binding in microfluidic systems. Wolf et al. have noted that the binding step can be optimized by picking the time that produces an adequately large measured response (Wolf, Juncker et al. 2004). In flow-through devices, this means

choosing the fastest flow rate that still allows enough antigen binding to provide a desired signal.

Microfluidic immunoaffinity separations have been performed on chips made from silicon, glass, and polymeric materials, such as PDMS, PMMA, and polystyrene (Lim and Zhang 2007; Sibarani, Takai et al. 2007). PDMS has been most commonly used (Bange, Halsall et al. 2005; Sibarani, Takai et al. 2007), but as discussed previously requires surface treatments or blocking steps to inhibit high nonspecific protein interactions. Microchips may contain antibodies immobilized to the surface of the substrate or to beads packed in channels. Antibody Fab fragments have been directly attached to ports of glass chips for immunoaffinity-CE of neuropeptides (Phillips and Wellner 2006a) and cytokines (Phillips 2004) in clinical samples. Beads are retained in microchips by creating weirs or physical barriers to trap beads that are larger than the outlet channel (Dodge, Fluri et al. 2001; Verpoorte 2003). Magnetic beads do not require alterations of channel dimensions and are instead held in place by use of an external magnet (Verpoorte 2003; Lim and Zhang 2007). In the bead-based chips, the stationary support is typically back flushed from the weirs (Sato, Tokeshi et al. 2001) or the magnetic field is removed (Hayes, Polson et al. 2001) to release the beads and reuse the device. Although this eliminates the need for regeneration of the immunoaffinity solid phase, the beads must be reapplied with each sample, which may consume valuable materials.

Capillaries and chips that use beads for antibody-antigen reactions must be packed to form separation zones. Positive pressure is often applied via syringe pumps to

pack slurries of beads into microfluidic devices (Sato, Tokeshi et al. 2001), although high pressures may lead to damage of the immobilized antibody (Phillips 1985). Negative pressure may also be used for packing bead solutions using vacuum or syringe pumps to pull the slurry from the end of the column or channel (Sato, Yamanaka et al. 2002; Peoples, Phillips et al. 2007; Shin, Lee et al. 2007). Slurries of beads may also be introduced into columns by a series of injections under positive or negative pressure (Clarke and Hage 2001; Piyasena, Buranda et al. 2004). Packed beds using magnetic beads are made by pumping or pulling the beads past a magnet located at the desired location of the capillary or chip (Hayes, Polson et al. 2001).

1.4.3.1. Open systems

Antibodies may be attached to internal walls of capillaries or channels by direct adsorption or through functional group modifications. For example, an "immunostack" of reagents was formed in the channels of plastic chips by first directly adsorbing C-reactive protein from human serum (Bhattacharyya and Klapperich 2007). The blocking buffer, primary antibody, and secondary detection antibody were then added sequentially. This procedure was simple and took 25 minutes to complete versus several hours for an ELISA of the same antigen. Open glass capillaries were used to perform sandwich immunoassays of myocardial proteins in diluted human plasma (Torabi, Mobini Far et al. 2007). The capture antibodies were immobilized to silane or silane/glutaraldehyde-modified capillaries and the effects of sonication were studied. The silane surface

treatment of the internal walls was enhanced by sonication, although the antibody-antigen binding step was negatively affected.

Fused-silica capillary columns (250 µm internal diameter (i.d.)) have been modified with glutaraldehyde for the immobilization of anti-*E. coli* O157:H7 antibodies (Liu and Li 2001). A sandwich immunoassay was demonstrated using a syringe pump to deliver reagents and off-line absorbance detection of an enzymatic reaction product was employed. A separate sandwich immunoassay for *E. coli* O157:H7 was performed in 530 µm i.d. fused-silica capillaries using fluorescence detection (Ho, Hsu et al. 2004). The capture antibody was immobilized to the internal capillary wall through a protein A modification and covalently anchored with dimethyl pimelidate. The detection antibodies were conjugated to 250 nm liposomes that encapsulated a fluorescent dye. Once the sandwich complex was formed, a detergent was added to lyse the bound liposome and release the dye for detection.

1.4.3.2. Packed systems

Microfluidic chips and capillaries are frequently packed with solid particles that have been modified with immobilized antibodies or antigens. Polystyrene beads coated with anti-C-reactive protein have been used in a PDMS chip for a competitive chromatographic immunoassay (Shin, Lee et al. 2007). The beads were held in a chamber by a frit structure and a 20-fold amplification of the fluorescence signal was achieved compared to the assay without beads. Polystyrene beads trapped in weirs of a PDMS chip were demonstrated for a sandwich immunoassay of tacrolimus with on-chip

fluorescence detection (Murakami, Endo et al. 2004). The assay was performed using a single channel and took 15 minutes to complete versus 2 to 4 hours for commercial systems. It should be noted that microchip time was for one sample and the commercial systems were capable of processing 24 to 48 samples. Malmstadt et al. have reported a temperature-responsive stationary phase in poly(ethylene terephthalate) (PET) channels for a competitive immunoassay of digoxin (Malmstadt, Hoffman et al. 2004). Biotinylated antibodies were immobilized to streptavidin anchored to the beads through a biotin-PEG linkage. The beads were also coated with a temperature sensitive polymer, poly (N-isopropylacrylamide) (PNIPAAm). A hydrophilic-to-hydrophobic phase transition of the polymer occurs at temperatures above the lower critical solution temperature (about 28 °C). The temperature of the microfluidic device was maintained at 33-37 °C, which caused aggregation of the beads and adhesion to the channel walls. When the temperature was adjusted below 28 °C the beads were no longer in a hydrophobic phase and were released for fluorescence measurement of the bound antigen. The advantages of the reversible immobilized beads were that one device platform could be reused multiple times and different antigens could be assayed by applying different immobilized antibody beads.

A direct capture microfluidic immunoaffinity chromatography system was demonstrated for the analysis of substance P in human plasma, serum, urine, cerebral spinal fluid, tissue lymph, and cell lysates (Phillips and Smith 2002). Biotinylated antibodies were attached to glass beads and packed into 12 mm long fused-silica capillaries with a 50 μm internal diameter. A dual syringe microdialysis pump was used

to deliver buffers and only 50 nL injection volumes were required. HPLC microcolumns were reported for fast separations of fluorescein and BSA using a packed bed of immunoaffinity beads sandwiched between layers of diol-bonded silica (Clarke and Hage 2001). Although the size of the columns was 2.1 mm i.d. x 1.0 cm, the length of active stationary support used in the study varied from 60 μm to 1.1 mm. A competitive chromatographic immunoassay of BSA required only 5 to 25 seconds for signal measurement. In a similar study by the same research group, affinity microcolumns were demonstrated using monolithic disks as the stationary support (Jiang, Mallik et al. 2005). Anti-FITC antibodies immobilized on a 4.5 mm i.d. x 0.95 mm monolithic support were used to measure fluorescein in phosphate buffer. A 95% extraction of fluorescein was achieved when the residence time in the column was 100 milliseconds using a flow rate of 3 mL/min. The authors note that nonspecific binding could be reduced in small-scale columns that employ relatively high flow rates. The monolithic columns also exhibited lower back pressures and greater stability to higher flow rates versus the silica bead-packed sandwich microcolumns.

Monolithic supports in 250 μm i.d. x 10 cm fused-silica capillaries were reported for immunoaffinity separation of fluorescein with laser-induced fluorescence detection (Hodgson, Brook et al. 2005). The antigen was concentrated prior to detection by applying 150 column bed volumes of an aqueous solution and eluted with 20% methanol in a neutral buffer. Affinity microcolumns in PDMS channels have been demonstrated for simultaneous on-column measurement of multiple analytes (Piyasena, Buranda et al. 2004). Affinity receptors included immobilized fluorescein-labeled anti-

carninoembryonic antigen, FLAG peptide, and biotin. The fluorescence resonance energy transfer of the receptor beads to bound analytes was measured. Glass receptor beads were packed into 600 μm segments separated by uncoated beads to form approximately 5.4 mm columns. The columns were mounted vertically and scanned up and down with a laser so that each analyte segment provided a distinct signal.

1.4.3.3. Magnetic systems

Magnetic particles may be modified with immunoaffinity ligands and used as solid supports that are manipulated by placing a magnet near channels or capillaries. Paramagnetic beads coated with streptavidin were used to demonstrate a flow immunoassay for inerleukin-5 and parathyroid hormone (Hayes, Polson et al. 2001). The beads were conjugated with biotinylated primary antibodies and pulled by vacuum into 50 μm i.d. fused-silica capillaries. A rare earth magnet placed near the capillary allowed the beads to form a partially-packed bed. The packed bed did not cross the entire capillary, which resulted in lower pressure and potentially higher flow rates versus a densely packed bed. Magnetic beads have also been employed for mixing in microfluidic devices. Herrmann et al. have reported the use of streptavidin magnetic beads in a stop-flow ELISA for anti-streptavidin antibodies on PDMS chips (Herrmann, Veres et al. 2006). The beads served not only as a reactive stationary support, but also as an internal mixing element. A rare earth magnet was used to trap the beads in the reaction chamber to form a loose bed. During the stop-flow incubation period, the magnet was moved back and forth along the channel to mix reagents and improve the reaction.

Hahn et al. have demonstrated a novel magnetophoretic immunoassay for human IgE in a PDMS-based microfluidic chip (Hahn, Jin et al. 2007). The antigen, dust mite allergen, was conjugated to 5.6 μm microbeads and used to capture allergen-specific human IgE. A sandwich complex was formed by adding 9 nm superparamagnetic particles conjugated with anti-human IgG. The superparamagnetic particle-microbead sandwich was pumped through a microchannel parallel to a nickel microstructure under external magnetic field. The deflection velocity of the microbeads to the nickel was measured with a charge coupled device (CCD) camera on an inverted microscope. The microbead velocity (μm/sec) was proportional to the amount of superparamagnetic particles and thus the IgE. For two dust mites, *Dermatophagoides farinae* and *Dermatophagoides pteronyssinus*, the detection limits of IgE in human serum were 565 and 268 fM, respectively.

1.4.3.4. Devices for multiple assays

Some biomedical applications require the measurement of many analytes from a single small volume of sample. The analysis of multiple analytes or multiple samples simultaneously by microfluidic immunoaffinity devices requires more complex system designs. These typically involve the use of multiple reaction channels or capillary columns. For example, 30 fused-silica columns were connected in series to analyze multiple analytes from a single 10 μL human serum sample (Phillips 2001). Each capillary was packed with antibody-coated glass beads corresponding to a specific antigen for a direct capture assay. The antigens were fluorescently labeled and detected

on-column by laser-induced fluorescence (LIF). In another study, four samples were simultaneously assayed for interferon using glass chips containing branching channels packed with antibody-coated polystyrene beads (Sato, Yamanaka et al. 2002). A similar eight-channel system has been developed in PDMS chips for parallel ELISA using a magnetic bead separation (Herrmann, Veres et al. 2006). The branching channels and columns connected in series have the advantage of using a single pumping system to deliver reagents and samples. A unique system for the analysis of biological warfare agents has been developed by combing antibody-coated capillary columns with chips (Yacoub-George, Hell et al. 2007). Fused silica capillary columns were glued into grooves of a polymer chip to create ten separate channels. Ten simultaneous sandwich immunoassays for one antigen each and multiplexed sandwich immunoassays for three antigens were demonstrated in aqueous solutions. Microperistaltic pumps and a multianode-photomultiplier array were used for fluid control and detection in each of the channels. Immunosensors have also been reported for monitoring multiple antigens using three (Petrou, Kakabakos et al. 2002) or four (Mastichiadis, Kakabakos et al. 2002) distinct antibody bands in a single plastic capillary.

1.4.4. Detection

Detectors for microfluidic systems must be capable of providing sensitive measurements in low volumes and small physical dimensions are a significant advantage. Common detection methods for microfluidic immunoaffinity separations include fluorescence and LIF, electrochemical detection, and chemiluminescence (Bange, Halsall

et al. 2005). Labeling of the antigen or a secondary antibody is often performed to enhance the detectable signal (Hage 1998; Bange, Halsall et al. 2005). Enzyme labels have been used in microfluidic immunoaffinity systems with absorbance (Liu and Li 2001), fluorescence (Murakami, Endo et al. 2004; Herrmann, Veres et al. 2006), and chemiluminescence (Bhattacharyya and Klapperich 2007; Torabi, Mobini Far et al. 2007) detection. Table 3 lists some representative detection methods for microfluidic immunoaffinity separations.

Immunoaffinity devices involve directly measuring the antibody-bound antigen on the solid support or in a moving liquid after elution occurs. On-chip measurements typically require focusing detectors onto a small, transparent detection zone. Fused-silica capillaries can be made into flow cells by burning off the polyimide coating and connecting to the outlet of chips or capillary columns (Hodgson, Brook et al. 2005; Peoples, Phillips et al. 2007). Square capillaries are available in 50, 75, and 100 μm internal diameters (Polymicro Technologies, Phoenix, AZ) and may be used to construct low-volume flow cells. On-column detection zones for fused-silica capillaries have been created by removing the outer coating (Hayes, Polson et al. 2001; Phillips 2001). When the detection zone is made of packed beads, background scatter may be problematic in optical measurements. Alternatively, offline sample fractions have been collected post-system and measured using absorbance (Liu and Li 2001) or fluorescence (Malmstadt, Hoffman et al. 2004) spectrophotometers.

Table 3: Detection methods used in microfluidic immunoaffinity separations.

Detection	Antigen	Matrix	Detectability*	Ref
Absorbance	*E. coli.* O157:H7	Buffer	5.0×10^2 cfu/mL (LLOQ)	[Liu and Li 2001]
Fluorescence	C-reactive protein	Human plasma	30 ng/mL	[Wolf et al. 2004] [Shin et al. 2007]
	C-reactive protein	Buffer	1.4 nM	[Herrmann et al. 2006]
	Anti-streptavidin Antibodies	Buffer	0.1 pg/mL (LLOQ)	
Laser-induced fluorescence	Substance P	Unclear	< 500 fg/mL	[Phillips and Smith 2002]
	Fluorescein	Aqueous	0.1 nM	[Hodgson et al. 2005]
	Cholera toxin	Unclear	~210 pM	[Phillips and Cheng 2005]
	Naproxen	Human plasma or buffer	5 ng/mL	[Phillips and Wellner 2006]
Chemiluminescence	Myoglobin Creatine kinase mb Troponin I Fatty acid-binding protein	Human plasma diluted 1:8 in buffer containing 12.5% plasma	1.2 ng/mL 0.6 ng/mL 5.6 ng/mL 4 ng/mL	[Torabi et al. 2007]
	Staphylococcal enferotoxins C-reactive protein	Aqueous	0.1 ng/mL	[Yacoub-George et al. 2007]
		Human serum	100 ng/mL	[Bhattacharya and Klapperich 2007]
Surface plasmon resonance	Interleukin-8	Buffer Human saliva	2.5 pM 184 pM	[Yang et al. 2005] [Kurita et al. 2006]
	B-type natriuretic peptide	Buffer	5 pg/mL (LLOQ) 75 nM (LLOQ)	[Nelson et al. 2007]
	Phenytoin	Buffer		
Thermal lens microscope	Carcinoembryonic antigen Interferon-γ	Human serum	~0.03 ng/mL	[Sato et al. 2001] [Sato et al. 2002]
		Buffer	~0.01 ng/mL	
Electrochemical	Human α-fetoprotein	Buffer	0.1 ng	[Nashia et al. 2007]

* Detectability reported as limit of detection (LOD), unless noted otherwise. LLOQ refers to the lowest reported level of calibration.

Fluorescence and LIF are the most commonly used methods of detection and can be measured by simple instrumentation including an excitation source, microscope, and photomultiplier tube (PMT) or CCD (Jiang, Attiya et al. 2000; Schwarz and Hauser 2001; Bange, Halsall et al. 2005). Many microscope approaches employ lamp-based sources,

such as xenon or mercury lamps that provide a broad range of excitation wavelengths (Kuswandi, Nuriman et al. 2007). Laser-induced fluorescence is a highly sensitive technique, well suited for analyzing analytes in small volumes of fluid in capillary or chip formats. Laser beams are monochromatic, coherent, and capable of being focused onto miniaturized flow cells or microchips (Johnson and Landers 2004). Lasers are high intensity sources and can provide improved detection sensitivity since fluorescence is proportional to excitation power. Commercial LIF detectors intended for capillary electrophoresis or capillary LC detection are compatible with microfluidic devices. Manufacturers of these detectors include Beckman Coulter, Agilent, and Picometrics.

Two common optical arrangements in both laboratory-constructed and commercial LIF detection systems include orthogonal and collinear or confocal arrangements. In the orthogonal configuration, the fluorescent signal is collected at an angle offset from the excitation light path. The collection angle is commonly 90° for capillary flow cells and less than 90° for microchips (Johnson and Landers 2004). A confocal arrangement uses the same path for both excitation and emission. The confocal optical design was reported to have advantages over the orthogonal design, including ease of alignment, stability, and improved sensitivity (Malek and Khaledi 1999; Johnson and Landers 2004). The increased sensitivity in the confocal optical arrangement results from the use of high numerical aperture objectives, while the orthogonal design restricts the use of such objectives because of their inherently small working distances (Bhoopathy and Karnes 2002; Johnson and Landers 2004). Optical filters are commonly used to remove scattered light with both orthogonal and confocal arrangements.

Reducing laser scatter from the fluorescence signal lowers the background and improves detectability (Rahavendran and Karnes 1993). Most fluorescent dyes in the red region of the spectrum have short stokes shifts and require combinations of filters to discriminate fluorescence from scatter (Johnson and Landers 2004).

Diode lasers are compact, stable, and inexpensive (Rahavendran and Karnes 1993), and are more compatible with portable microfluidic devices than larger lasers, such as gas lasers (Jiang, Attiya et al. 2000). Commercially available diode lasers are currently limited to the far red and infrared regions of the spectrum (Schwarz and Hauser 2001). The analysis of biological matrices by visible diode LIF is advantageous because of the minimal biological sample background exhibited in the far-red (>620 nm) spectrum (Rahavendran and Karnes 1996). Since most sample antigens do not fluoresce in the far-red region of the spectrum, derivatization of functional groups with fluorochrome labels is often required (Nagaraj and Karnes 2000). Amine-reactive dyes excitable by lasers may be used to label protein antigens, antibodies, or peptides for immunoaffinity separations. The use of labeled antibodies in immunoaffinity assays provides a measurable signal for antigens that do not posses a readily labeled functional group. Fluorescence detection in microfluidic and miniaturized portable systems may also benefit from the use of light-emitting diodes (LED) as excitation sources. LEDs are compact, inexpensive, available in a broad range of wavelengths, and have minimal power requirements (Gotz and Karst 2007). Therefore, an LED excitation source may be directly integrated into a microfluidic device for portable fluorescence measurements.

Chemiluminescence detection is increasingly being applied to microfluidic immunoassays and offers the potential for portable field use or point-of-care devices. Light is generated from the chemiluminescent reaction itself and therefore no light sources are required as in fluorescent techniques. In addition to the low background signal, power requirements and external equipment are reduced, making miniaturization more feasible (Wang, Hofmann et al. 2007). Bhattacharyya et al. have reported chemiluminescence detection for C-reactive protein in human serum using cyclic polyolefin chips (Bhattacharyya and Klapperich 2007). Secondary antibodies labeled with horseradish peroxidase (HRP) were exposed to luminol as a substrate in the presence of hydrogen peroxide and the chemiluminscence light was measured on either photographic film or using a commercial imaging device. The assay provided detection limits of 100 ng/mL in serum using the imaging device. Although no quantitative data was given, the use of photographic film shows potential for point-of-care applications by reducing the amount of external equipment required for analysis. The instrumentation needed to measure chemiluminescent signals has also been miniaturized. A photodiode chip was used to measure several cardiac proteins in diluted human plasma based on the reaction of HRP-conjugated secondary antibodies with luminol (Torabi, Mobini Far et al. 2007). A multi-channel immunodetector was reported for a sandwich assay of biological agents using a portable chip system containing a multianode-photomultiplier array to measure the response of HRP-labeled secondary antibodies (Yacoub-George, Hell et al. 2007).

Electrochemical detection has also been applied in microfluidics, with amperometric methods reported as the most common (Schwarz and Hauser 2001; Bange, Halsall et al. 2005). The instrumentation used is simple to miniaturize and inexpensive; however, the electrodes may be difficult to control in reduced dimensions and the system may require shielding (Schwarz and Hauser 2001; Bange, Halsall et al. 2005; Kurita, Yokota et al. 2006). Cyclic voltammetry has been applied to affinity separations using gold electrodes on a polymer substrate (Soo Ko, Yoon et al. 2003). The sensing surface was comprised of gold electrodes modified with immobilized biotin or ferritin as models. HRP-conjugated streptavidin or HRP-conjugated anti-IgG were introduced into the device to form complexes with biotin or anti-ferritin/ferritin, respectively. Adding 4-chloro-1-naphthol to the HRP conjugates resulted in an enzyme-catalyzed precipitation reaction and the insoluble products were measured. Lim et al. have reported the use of ferrocene-conjugated IgG for a flow immunoassay of human chorionic gonadotropin with electrochemical detection (Lim and Matsunaga 2001). Antibody-antigen complexes were separated from unreacted ferrocene-labeled antibodies by an inline cation exchange column. Current from the ferrocene label was measured by pumping the samples into a three-electrode flow cell. The authors note that in addition to the simplicity of the assay, the time of analysis is reduced versus other electrochemical immunoassays because no enzyme-catalyzed reactions were necessary.

Surface plasmon resonance (SPR) detectors for immunoaffinity separations offer an alternative technology that is well-suited for detection on microfluidic platforms. SPR measurements are based upon changes in optical properties on the surface of chips coated

with immobilized ligands, such as antibodies. The binding of associated antigens and formation of an immunocomplex causes changes in the refractive index and shifts the SPR angle (Yang, Brooks et al. 2005). SPR is a fast, simple technique and does not require the use of labeled reagents (Kurita, Yokota et al. 2006; Nelson, Foley et al. 2007). A commercial SPR system was used to perform a sandwich immunoassay of interleukin-8 (IL-8) in human saliva in microfluidic channels (Yang, Brooks et al. 2005). A capture antibody immobilized on the surface of the sensor chip was exposed to the antigen and secondary antibody, sequentially. A detection limit of 184 pM was reported for IL-8 in centrifuged saliva. To reduce nonspecific interactions on the carboxymethyl dextran surface of the sensor, carboxymethyl dextran sodium salt was added to samples prior to analysis. Nonspecific adsorption of biomolecules to the sensor surface in SPR is problematic since the technique responds to refractive index changes produced by specific or nonspecific binding (Kurita, Yokota et al. 2006). Kurita et al. have reported that heating of human serum was necessary to reduce nonspecific interference with an SPR immunoassay for B-type natriuretic peptide (BNP) (Kurita, Yokota et al. 2006). Antibodies labeled with acetylcholine esterase were exposed to acetylthiocholine, which produced thiocholine. The thiocholine was then pumped to a gold film sensor for measurement. Plasma diluted 1:10 contained pseudocholinesterase and caused large amounts of thiocholine production. Heat treatment of the plasma inactivated the esterase and allowed recovery of BNP from 10 pg/mL to 100 ng/mL in diluted plasma.

Other detection methods have been used for microfluidic immunoaffinity separations. Thermal lens microscopy (TLM), which is a technique based on detection of

heat generated by the absorption of light (Yamauchi, Mawatari et al. 2006), has been reported for chip-based immunoassays. Colloidal gold has been used as a label for TLM to detect human IgA (Sato, Tokeshi et al. 2000), carcinoembryonic antigen (Sato, Tokeshi et al. 2001), and interferon (Sato, Yamanaka et al. 2002) in polystyrene bead-packed channels. The use of mass spectrometry (MS) has been reported for micro-immunoaffinity chromatography of various amino acids (Zeleke, Smith et al. 2006). Stereo-selective antibodies were immobilized to silica beads packed in PEEK columns and used for isocratic chiral separations. Direct analysis of antigens in immunoaffinity chromatography commonly involves nonvolatile buffers, such as phosphate, which are not compatible with MS analysis. An ammonium bicarbonate buffer was used that had the advantages of good buffering capacity at a neutral pH suitable for antibody-antigen reactions and volatility for MS detection.

1.5. Conclusions

Microfluidic devices are capable of performing a wide range of analytical functions with low reagent and sample requirements. Miniaturization of analytical instrumentation towards portable platforms is beneficial for point-of-care testing or other field applications. The combination of immunoaffinity separation techniques with microfluidic systems offers selective measurement of target analytes based on antibody-antigen interactions. Specific compounds of interest may be isolated from limited sample sources and immunoaffinity concentration facilitates measurement of trace levels.

Research in clinical and biomedical fields commonly requires analysis of complex biological matrices. Directly introducing biological material in to a microfluidic system may result in unwanted nonspecific binding of proteins or other compounds. Much of the published work reviewed here has been conducted in aqueous systems and may not be easily transferable to real biologic samples. Sample pretreatment, buffer additives, and modifications of device surfaces are frequently required to make biological samples compatible with small-scale instrumentation. Some published works have demonstrated application to real samples by analyte quantification in diluted real matrix. The corresponding effect on the lower limit of quantification in undiluted samples should be understood by those who attempt to reproduce this work.

Microfluidic chips and capillary systems using immunoaffinity separations range from simple to elegant in design. Many of these systems are based on pressure-driven fluid control and are assembled from several external miniaturized and conventional scale components, including components for sample introduction and detection. Compared to immunoassays performed in microplates, microfluidic immunoaffinity devices provide the potential for faster analysis times and reduced sample size.

CHAPTER 2 A Capillary-based Microfluidic Instrument Suitable for Immunoaffinity Chromatography

2.1 Introduction

The analysis of complex biological sample matrices for clinical and research purposes requires the use of selective analytical technology for measurement of target analytes. Additionally, limited sample quantities and the potential need for patient point-of-care testing have necessitated the development of miniaturized instrumentation and microfluidic devices (von Lode 2005). Immunoaffinity separation techniques, capable of isolating specific analytes by formation of an antibody-antigen complex, have been applied in a variety of formats suitable for small-scale bioanalysis. Immunoassay-based solid phase supports have been used for sample extraction and purification prior to a secondary separation step, such as chromatography or capillary electrophoresis (Tang and Karnes 2000; Guzman 2003; Hennion and Pichon 2003; Su, Zhang et al. 2005). Immunoaffinity extraction can provide greater selectivity than traditional solid phase extraction supports due to the nature of the antibody-antigen binding (Hennion and Pichon 2003). Immunoassays and immunoaffinity separations have been presented in several miniaturized systems, including microchips and capillary-based instruments. Microfluidic chips may involve electroosmotic or hydrodynamic pumping for fluid

44

control with immunoaffinity separation in open or packed channels, and several platforms have been demonstrated (Chiem and Harrison 1998; Cheng, Skinner et al. 2001; Dodge, Fluri et al. 2001; Sato, Tokeshi et al. 2001; Wang, Ibanez et al. 2001; Murakami, Endo et al. 2004; Phillips 2004; Wolf, Juncker et al. 2004; Phillips and Wellner 2006). Immunoaffinity capillary electrophoresis has been demonstrated for single and multiple analyte analyses in fused-silica capillaries (Phillips 1998; Jia, He et al. 2002). Immunoaffinity chromatographic systems and flow immunoassays have been employed as well, with micro-separations occurring in capillary columns or channels (Hayes, Polson et al. 2001; Lim and Matsunaga 2001; Phillips and Smith 2002). Several reviews and reports have been recently published on immunoextraction sample preparation, immunoaffinity capillary electrophoresis, and immunoaffinity chromatography (Hage 1998; Tang and Karnes 2000; Weller 2000; Guzman and Stubbs 2001; Hennion and Pichon 2003; Yeung, Luo et al. 2003; Guzman and Phillips 2005).

Immunoaffinity chromatography systems for micro-scale separations involve the use of pumps to force fluids through capillaries and channels either open or packed with solid particles, such as beads. Pumps capable of μL/min flow rates are often required and peristaltic or syringe pumps have been used. Bead-based immunoassays using immobilized antibodies have been used for qualitative and quantitative biomedical analysis (Bangs 1996). Beads may also be utilized as solid supports to attach antibodies for immunoaffinity stationary phases. Separation capillaries packed with beads offer the advantage of reduced diffusion distances for mass transport and the ability to concentrate samples online in a fluidic system over open tubular capillaries (Buranda, Huang et al.

2002; Verpoorte 2003).   Antibody-coated bead supports also create reduced interstitial volumes for antibody-antigen recognition.   Sample antigen may be loaded onto and captured by immobilized antibody beads and released in a reduced volume, thereby enhancing the signal.

A number of different supports including magnetic, plastic, glass and silica beads as well as monolithic supports have been applied for immunoaffinity chromatography. A magnetic bead-based flow immunoassay was demonstrated in both microchannel and capillary formats for sandwich immunoassays of parathyroid hormone and interleukin-5 (Hayes, Polson et al. 2001). A glass bead direct capture immunoaffinity separation of substance P in multiple biological sample matrices was achieved with a liquid chromatography system made from microdialysis pumps and a fused-silica separation capillary (Phillips and Smith 2002). Polystyrene antibody-coated beads packed into chip-based microchannels have been employed for analysis of human carcinoembryonic antigen and Tacrolimus in separate studies (Sato, Tokeshi et al. 2001; Murakami, Endo et al. 2004).   Capillary columns made from monolithic supports containing stationary antibodies were prepared and tested using fluorescein as a model antigen (Hodgson, Brook et al. 2005).   Monolithic disks for immunoaffinity extraction were reported for rapid isolation of rabbit IgG and fluorescein models (Jiang, Mallik et al. 2005).

Syringe pumps or conventional HPLC pumps with unique mixers have been employed to produce gradients for capillary liquid chromatography and microfluidic devices because of their commercial availability and ease of use. Ducret et al. (Ducret, Bartone et al. 1998) reported the use of two syringe pumps to produce gradients for

capillary HPLC with electrospray ionization mass spectrometry. A capillary mixing chamber was constructed using capillary tubing and a steel ball from a ball point pen. Cappiello et al. (Cappiello, Famiglini et al. 2003) described the use of a 14-port switching valve and flow-splitting with conventional HPLC pumps to produce nano- and microflow gradients. The switching valve metered mobile phase mixtures from 6 pre-filled loops for gradient generation. Zhou et al. (Zhou, Rusnak et al. 2000) demonstrated gradient mixing for capillary HPLC with mass spectrometric detection using a single syringe pump and a micro-autosampler. The autosampler was used to generate gradients by injecting programmed volumes of premixed mobile phase solutions from separate vials.

The aim of this work was to design a capillary HPLC system suitable for performing immunoaffinity chromatography separations in biological samples. The system was developed for small volume sample injection with the ability to detect fluorescent laser dye conjugates in the picomolar (pM) range. Additionally, many of the system components are commercially-available and reasonably straightforward to assemble. Two syringe pumps were programmed together in an original format for microfluidic step gradient elution and a detailed design is included for assembly of a capillary scale separation column. The laboratory-built instrumentation and software program are presented here, along with initial results of an immunoaffinity separation as proof-of-principle.

2.2 Experimental

2.2.1 Reagents and materials

Plain 1 μm silica beads were purchased from Polysciences (Warrington, PA). Alexa Fluor 647 succinimidyl dye (λ_{ex} = 650 nm, λ_{em} = 670 nm) was obtained from Invitrogen (Carlsbad, CA). Streptavidin-coated 5.7 μm glass particles were purchased from Xenopore (Hawthorne, NJ). Biotin-conjugated polyclonal rabbit anti-goat IgG (H+L) and Alexa Fluor 647-conjugated polyclonal goat IgG (anti-human) were obtained from Invitrogen. Purified water was made in-house using a Barnstead Nanopure Diamond system (Dubuque, IW). All other chemicals were purchased from Sigma (St. Louis, MO).

2.2.2 Instrumentation

The basic components of the instrumentation are shown in Figure 5. Dual microliter OEM module syringe pumps from Harvard Apparatus, Inc. (Holliston, MA) were mounted side-by-side in a 0.22" clear acrylic housing. Twin LCD display chips were wired to the pump boards to allow for confirmation of power up and flow rate. Glass gastight 1700 series syringes with 22-gauge blunt needle tips (Hamilton, Reno, NV) were used with the pumps. Each syringe needle tip was connected by a union to a length of 360 μm outer diameter (OD) x 100 μm inner diameter (ID) PEEK (polyetheretherketone) capillary tubing (Upchurch Scientific, Oak Harbor, WA). The PEEK capillary was attached to a nano-scale mixer (NanoMixer, Upchurch Scientific)

Diode Laser

Syringe Pumps

LIF Detector

Nano-gradient Mixer

Micro-injector

Column Assembly
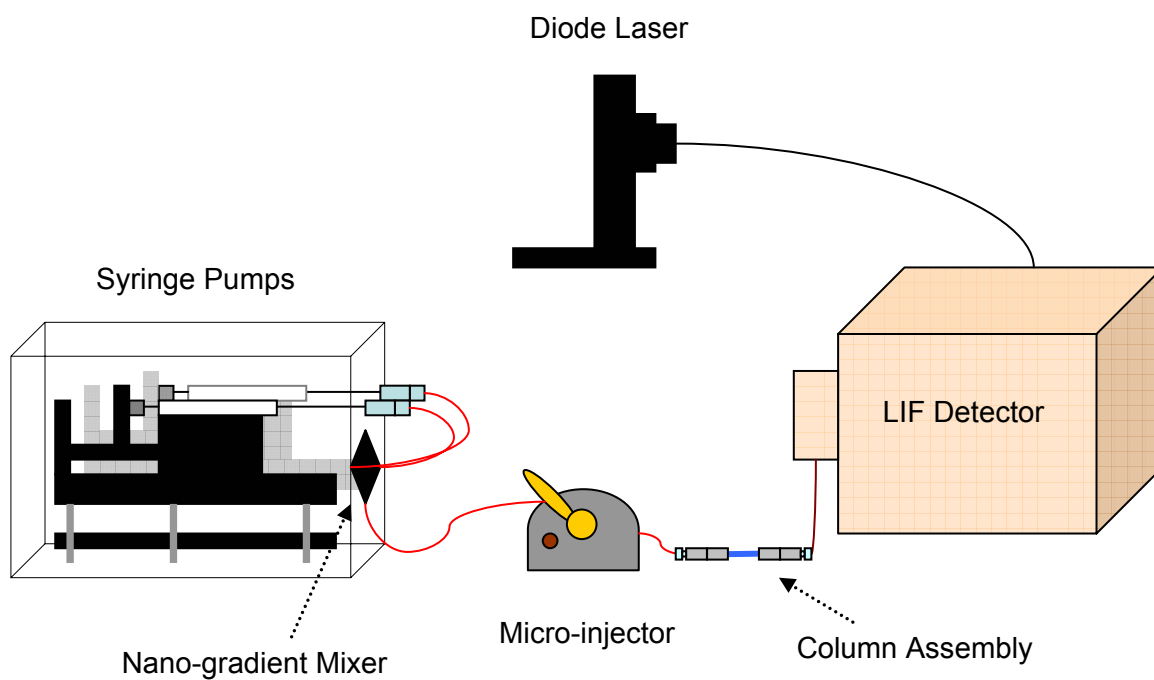
Figure 5: Diagram of capillary LC with laser-induced fluorescence detection.

mounted on the front of the pump cabinet enclosure. The NanoMixer is a gradient mixing chip capable of low and high mixing configurations, requiring 30 nL and 60 nL of fluid, respectively. The mixer was connected by a single length of 100 μm ID PEEK capillary to one of six ports of a Microinjector (Upchurch Scientific). Injection loops were made with capillary PEEK tubing by treating the tubing as a cylinder and cutting the capillary to the appropriate length based on the calculated volume.

A 20 mW 650-nm laser diode (Lasermate Group, Inc., Pomona, CA) was housed in a LDM 4412 laser diode mount (ILX Lightwave, Bozeman, MT) with a collimating lens. Thermoelectric cooling and current control were maintained by an ILX Lightwave model LDC-3722 laser diode controller (20°C; 60 mA). Output power and wavelength were measured with a model OMM-6810B optical multimeter (ILX Lightwave). The laser was operated at a typical power output of 16 mW measured at the optical bench. The front of the laser diode module was attached to a fiber optic that was connected to a Zetalif laser-induced fluorescence detector (Picometrics, Ramonville, France). The laser light in the Zetalif detector is brought to a dichroic mirror and reflected onto a 2 mm ball lens. The excitation beam is focused onto a capillary flow cell and fluorescence is collected back through the ball lens in a collinear arrangement. High pass, spatial, and notch filters (Omega Optical, Inc., Brattleboro, VT) were placed in the light path before the emitted light hit a Hamamatsu model R928 red-sensitive photomultiplier tube (Bridgeport, NJ). The photomultiplier tube was routinely operated at 700 V. The flow cell was made from square fused silica capillary tubing with dimensions of 360 μm OD by 100 μm ID (Polymicro Technologies, Phoenix, AZ). A 2 mm detection window was

created by burning off the polyimide coating with a capillary window maker (MicoSolv Technology Corporation, Long Branch, NJ). The detector signal was acquired with a computer via a National Instruments USB-9215 data acquisition card with 16-bit resolution (Austin, TX).

2.2.3 Column design

Prototype columns were constructed from PEEKsil tubing (Upchurch) with dimensions of 200 μm ID x 1/16" OD. Stainless steel external column endfittings and ferrules were purchased from Valco Instrument Co. Inc. (Houston, TX). A stainless steel 0.5 μm frit in a polymer ring (Upchurch) with dimensions 0.038 in x 0.030 in x 0.062 in was used to retain stationary phase material. PEEKsil is polyetheretherketone-coated capillary tubing with a fused-silica inner core. The polymer outer layer adds protection and rigidity to the fused silica and the material is rated at a pressure of 8,500 psi. The tubing ends are machine cut and level, making them suitable for chromatography columns. The endfittings were wrench-tightened onto the columns with frits attached to set the ferrules. One endfitting assembly and one frit were removed to allow for packing. A detailed view of the column components is shown in Figure 6.

Columns were packed under negative pressure (approximately 600 psi maximum) using a vacuum pump and adding a 3 mg/mL slurry of either silica or immunoaffinity beads to the top of the column body tubing drop-wise. Figure 7 shows a diagram of the packing apparatus. A jewelry engraver was used to periodically vibrate the sides of the column during packing to remove air pockets. When the beads were observed at the top
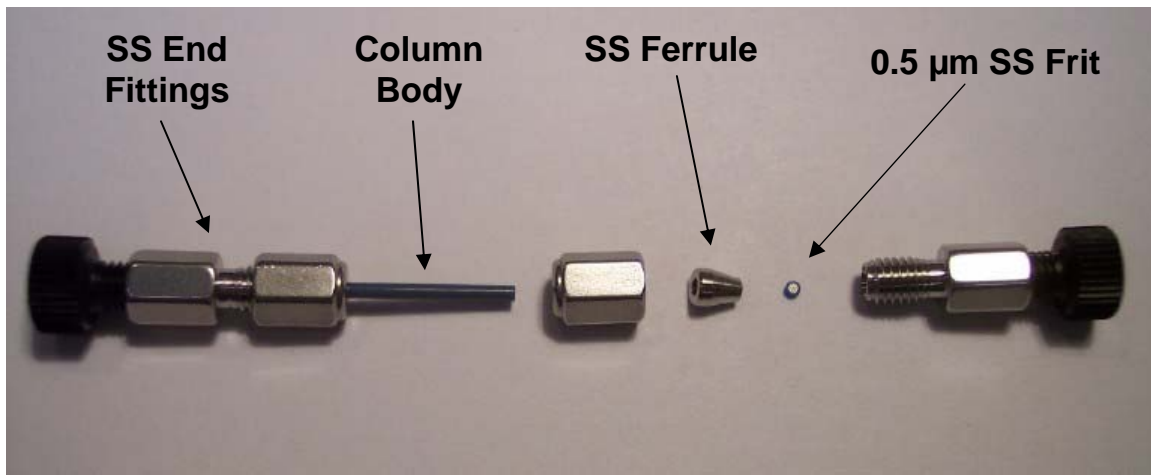
Figure 6: Components of the prototype capillary column. The column body is made of polymer-coated fused-silica and all fitting are stainless steel (SS).
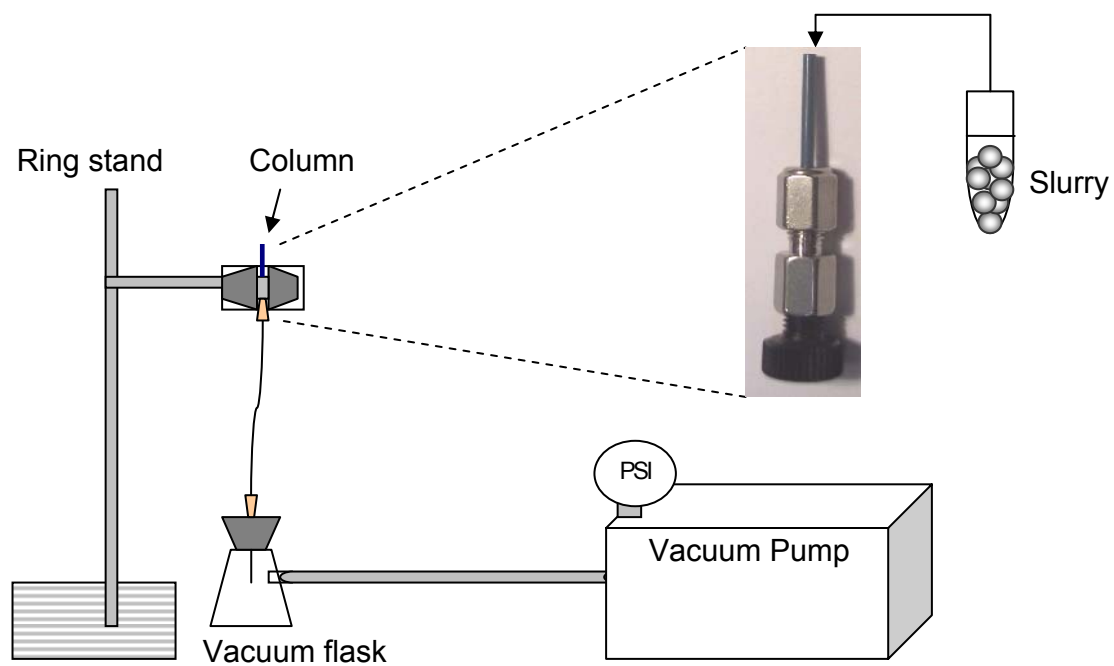
Figure 7: Column packing diagram.

of the column, the assembly was removed and the open end covered with Parafilm. The

column was then gently tapped on the bench top and inspected under magnification. The

procedure was repeated until the stationary phase persisted at the column head. Next, the

top of the column was leveled with a stainless steel spatula and the end fitting containing

the second frit was gently reassembled. Column lengths of 25 and 50 mm were packed

by this procedure and tested as prototype separation columns.

2.2.4 Software design

Two software programs were designed for instrument control/data acquisition and

data analysis using LabVIEW (National Instruments).   For the control/acquisition

program, the dual microliter syringe pumps were connected through computer serial ports

and run simultaneously. The pump user's manual specified the serial port connection

inputs and language commands through HyperTerminal control in Windows-based

computers. These commands and connections form the basis for controlling the dual

pumping system in LabVIEW. The syringe volume and diameter were defined along

with all computer addresses connected to the pumps and detector. A timed events

window was created to allow for changes in flow rate to be input for each pump for a

desired duration of time. There are a total of twenty lines of input, corresponding to 20

possible lines of gradient programming. After a defined time duration in line one, the

data acquisition begins and the LIF signal is displayed as a real time chromatogram from

the USB card interface. Manual injections are made at the end of line one to improve

reproducibility.   Each running of the program requires a file path, where the

chromatogram is stored.   The file can be recalled in the data analysis program which regenerates the chromatogram and relies on user-input threshold values to define a reportable peak. The software requires confirmation of a selected peak and then imports the peak into a window where integration is performed. Both area under the curve and height are reported. In LabVIEW, the front panel screen is part of a virtual instrument with user input fields and functions such as on/off switches and LED's. The actual programming is contained in a second screen called a block diagram. A portion of the front panel screen for the control/acquisition program is shown in Figure 8. A compact disc containing both LabVIEW programs is located in the back cover of this dissertation.

2.2.5 System optimization

        Two prototype columns were packed with 1 µm silica spherical particles and evaluated with respect to measurement of flow rate accuracy. In order to confirm the flow rate water was pumped through each column for 10 minutes at 1.0 µL/min, collected in a 200 µL polypropylene tube, and measured with Hamilton glass syringes. Each column had an inner diameter of 200 µm and lengths of either 25 mm or 50 mm. Additionally, Nucleosil 10 µm C8 particles (Alltech, Deerfield, IL) were packed into a 200 µm by 50 mm column. All tests were performed in triplicate.

        Evaluation of the system mixer was performed by programming a step gradient of pH 7.4, 100 mM phosphate in pump A and 800 pM Alexa Fluor 647 in pH 7.4, 100 mM phosphate for pump B. Observed profiles, in triplicate, were compared to the programmed gradient profile. The plateau of each step was measured and plotted versus

Figure 8: Control and acquisition front panel. This screen allows pump control, gradient programming, and data acquisition settings of duration and sampling rate. The chromatogram is viewed in real time. The first 10 lines of gradient input are shown.

concentration.

The ability of the pumps and mixer to perform a pH gradient was tested by measuring the pH of column effluent after a linear acidic gradient program was run. Pump A contained pH 7.4 100 mM phosphate and pump B contained a pH 1.2 100 mM glycine-HCl solution. Offline measurements of premixed solutions were compared to online measurements at the same proportions using the mixer. Offline measurements were made with an Orion model 920A+ pH meter (Thermo Electron Corporation, Waltham, MA) and online measurements were made with pH paper indicators (Micro Essential Laboratory, Brooklyn, NY).

Various concentrations of Alexa Fluor 647 laser dye were prepared in water and injected into the system to evaluate the detector system. A calibration curve was tested in triplicate at concentrations of 100, 200, 400, 600, and 800 picomolar and a linear regression was used to obtain an equation for the line. A blank was injected n = 3 times and the peak-to-peak noise was measured across the elution window of the dye peak. The limit of detection (LOD) was calculated by the equation LOD = 3 S_b/m, where S_b is the standard deviation of the blank peak-to-peak noise and m is the slope from the calibration curve.

2.2.6 IgG Immunoaffinity Chromatography as Proof-of-Principle

Goat IgG was used as a model antigen and rabbit anti-goat IgG was used as the immobilized capture antibody. Streptavidin-coated glass beads and biotinylated rabbit anti-goat IgG were combined in a ratio of 3 mg: 150 ng in 1 mL of 10 mM phosphate

buffer pH 7.2. The mixture was placed onto a rotary mixer for 1 hour at room temperature and 15 hours at 4 °C. The particles were washed 3 times in 10 mM phosphate buffer, pH 7.2 and incubated with 50 ng/mL of biotin at 4 °C for 2 hours. The particles were then washed 5 times and reconstituted in 10 mM phosphate buffer pH 7.2. The activity of the immunoaffinity stationary support was tested by placing 300 μg of particles and 7.5 ng of Alexa Fluor 647-labeled goat IgG on a rotary mixer for 2 hours at room temperature. Three replicates were prepared along with 3 controls of Alexa Fluor 647 without the immunoaffinity glass particles. The solution was centrifuged at 1200 rpm for 10 minutes and the supernatant was injected into the flow cell of the LIF detector. The stationary phase was found to remove approximately 79% of the Alexa Fluor 647-goat IgG from solution versus controls.

A 0.2 x 25 mm capillary column was packed with the immunoaffinity stationary phase as described above and stored at 4 °C until use. Solutions of Alexa Fluor 647-goat IgG were prepared in 10 mM phosphate, pH 7.2 at 111, 333, 667, and 1000 pM. After injection of the antigen, a 10 mM phosphate buffer solution was applied for 4 minutes, followed by a linear elution gradient of 2.5 M sodium thiocyanate. The column was then equilibrated with 10 mM phosphate buffer. The flow rate was 1.5 μL/min and the column was kept in an ice water jacket while running samples.

2.3. Results and Discussion

In the present work, we have combined two syringe pumps with a nano-gradient mixing chip for the production of gradients with capillary-scale tubing and separation columns. The OEM module microliter syringe pumps are capable of providing a wide range of flow rates from 0.0001 to 791.8 µL/min using syringe sizes from 1 to 1000 µL. Simple serial commands for the RS-232 interface with HyperTerminal control in Windows-based computers can be used to run the pumps and change flow rates with no additional software requirements. For automated gradients, a custom program has been written in LabVIEW software that varies the flow rate of each pump over timed steps. The gradient mixing chip was demonstrated to produce adequate mixing for gradients of fluorescent dye and pH changes.

The column assembly is straightforward to construct and flexible in design. The material, inner diameter, and length of tubing can be changed to create a variety of dimensions for multiple applications. The column packing procedure using a vacuum pump is both gentle and efficient, making it suitable for immunoaffinity and other fragile stationary phases. A similar packing procedure has been reported by Qu et al. (Qu, Hu et al. 2004) for use with capillary electrochromatography with the noted advantage uncomplicated assembly and operation. The syringe pumps, nano-gradient mixer, micro-injector, and capillary column components presented here are all commercially available and relatively simple to construct into a functional chromatography system.

The operational capabilities and limitations of the pumps were determined by the manufacturer specifications for the syringes and syringe pumps. Table 4 was created

using the nominal syringe pump force in pounds and syringe internal diameter in square inches. Dividing the pump force by the syringe internal diameter gives maximum operational pressure ratings in pounds per square inch (psi). The operational pressure rating of syringes and pumps increases with decreasing syringe size. For example, changing from a 500 µL to a 100 µL syringe increases the pump pressure capacity from approximately 500 psi to greater than 2,000 psi. The 100 µL syringe is only rated up to 1,000 psi. The syringe size and corresponding pressure rating are limiting factors for the determination of an overall system pressure threshold. Another important consideration for use with immunoaffinity stationary phases is that such supports can start to degrade at pressures higher than 500 psi (Phillips and Dickens 2000).

Table 4: Syringe and pump pressure with syringe size.

Syringe	Syringe size (µL)	Maximum syringe pressure (psi)[a]	Syringe internal diameter (in.^{2})[a]	Maximum pump pressure (psi)
Hamilton glass gastight	500 100	500 1000	0.012938 0.002595	464 2312

The Harvard Apparatus microliter syringe pump delivers 6 pounds of force. [a]Data from Harvard Apparatus website for Hamilton 1700 series Gastight syringes (www.harvardapparatus.com).

A prototype column was selected by measuring flow rate accuracy while varying particle size and column length. Water pumped at a flow rate of 1.0 µL/min was chosen for all columns for the sake of uniformity. Both a 100 µL and a 500 µL syringe were used to evaluate flow rate accuracy through the prototype columns. Packing the

capillaries with 1 μm beads took approximately 2 hours for the 25 mm column and 6-7 hours for the 50 mm column. Results of the flow rate accuracy evaluation are shown in table 5. The 50 mm column packed with 1 μm silica delivered a volume of pumped water that was 30 ± 6 % less than expected when using a 500 μL syringe. When the same column was reevaluated using a 100 μL syringe, the accuracy improved to 99 ± 4 % of the expected volume. It was concluded that the maximum pressure rating of the 500 μL syringe (500 psi) may have been exceeded with this column. Leakage around the plunger of the 500 μL syringe was observed, indicating syringe failure as the source of flow rate inaccuracy. A 25 mm prototype column packed with 1 μm beads was also evaluated. The flow rate delivered was as expected when using a 500 μL syringe (1.00 μL/min) and no leakage was observed. The 25 mm prototype column was therefore chosen to perform further optimization studies of the instrument. This column allows for the use of the larger (500 μL) syringe, which effectively increases the amount of mobile phase that can be loaded onto the pumps without refilling a syringe during sample analysis. Further optimization of the system was carried out with the 25 mm prototype and a 50 mm column packed with 10 μm C8 particles was also examined. The larger particle size allowed for the use of both the longer column and larger syringe (500 μl), while maintaining flow rate accuracy. These findings agree with the expected relationship between pressure and an HPLC column packed with spherical particles. Pressure is approximately proportional to column length, but inversely proportional to the particle diameter squared (Snyder, Kirkland et al. 1997).

Table 5: Flow rate accuracy with respect to syringe size, column length, and particle size changes.

Column	Syringe Size (µL)	Measured Flow Rate (µL/min)
0.2 x 50mm, 1µm silica	500	0.70 ± 0.06
0.2 x 50mm, 1µm silica	100	0.99 ± 0.04
0.2 x 25mm, 1µm silica	500	1.00 ± 0.00
0.2 x 50mm, 10µm C$_8$	500	1.00 ± 0.02

Mobile phase: water, flow rate: 1.0 µL/min, duration: 10 min, expected flow rate: 1 µL/min.
Values represent the average of 3 replicates ± one standard deviation.

A mixing profile was created by measuring the Alexa Fluor 647 dye signal at different programmed proportions pumped through the 0.2 by 25 mm column packed with 1 µm silica beads (Figure 9 A and B). Pump B contained the dye and was programmed from a starting proportion of 2.5% up to 97.5% in a four step gradient. At 1.5 µL/min there was approximately 3 minutes of lag time between the observed signal and programmed mixing. The height above baseline for the plateau at each step was plotted against the concentration of dye being pumped. The line was fit with a linear regression and the equation was $y = mx + b$. The parameter estimates were $y = 5.5 \times 10^{-4}$ $(9.2 \times 10^{-7})x - 0.0005 (0.0005)$, with an r^2 of 1.0000 (0.0004), where standard error is shown in parenthesis.

A
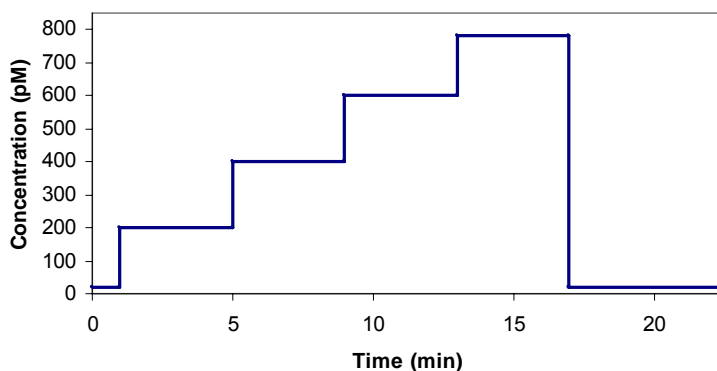
B
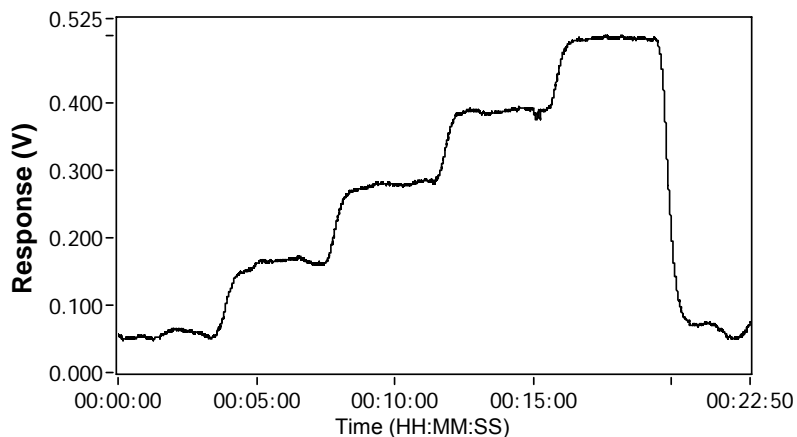
Figure 9: Programmed (A) and observed detector response (B) of a step gradient using Alexa Fluor 647 dye. Pump A contained 100 mM phosphate buffer pH 7.4 and pump B contained 1000 pg/mL Alexa Fluor 647 dye in100 mM phosphate buffer pH 7.4. Flow rate was 1.5 μL/min. The plateau of each step was plotted versus the concentration of dye pumped for n = 3 replicates.

Gradient accuracy was further confirmed by monitoring pH changes through the 0.2 by 25 mm column. A neutral phosphate to acidic glycine-HCl gradient was programmed at 1.0 µL/min using the software. Column effluent was spotted on pH paper every 30 seconds and only visually clear, whole pH unit changes were recorded. The observed pH was plotted versus time and overlaid with the programmed acidic gradient (Figure 10). The observed profile indicated that the system was capable of producing an acid gradient suitable for immunoaffinity elution. The delay in observed pH change versus programmed pH gradient can be attributed to the system dwell volume. The stagnation in pH between minutes 8 and 10 is due to limitations of measuring observed pH using pH paper in whole units. Fixed proportions of pump A to pump B buffers were measured online with pH paper and offline with a pH meter at 30, 35, and 50% glycine-HCl. For the 30, 35, and 50% pH 1.2 100 mM glycine-HCl solutions, the pH meter readings were 6.0, 5.8, and 2.6, respectively. The corresponding post-column measurements with pH paper were 6, 6, and 3, and were limited to whole unit readings.
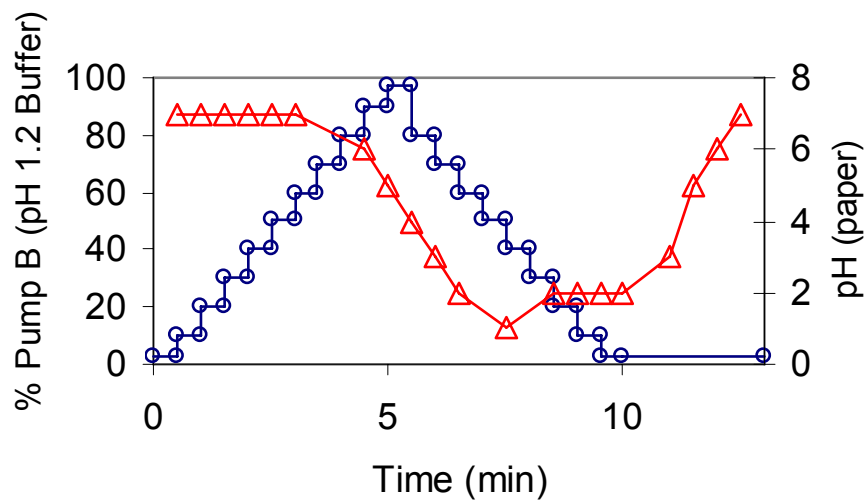
Figure 10: Ability of the system to produce an acid gradient. The line with open circles represents a gradient of Pump B programmed in LabVIEW. The open triangles represent the observed pH values in whole units. Conditions described in text.

Aqueous solutions of Alexa Fluor 647 dye were injected onto the 0.2 by 25 mm column at 1.5 µL/min in a mobile phase consisting of unbuffered water to determine the detection limit of the system. Injection loops of 750 nL, 1.0 µL, and 1.6 µL were evaluated and a 1.0 µL injection loop was chosen for sample introduction. Peak intensity and shape were optimal with the 1.0 µL loop. The parameter estimates for a linear regression fit of the data were y = 0.00031 (0.00002)x – 0.004 (0.008), with an r^2 of 0.992 (0.009), where standard error is shown in parenthesis. The LOD, calculated as three times the standard deviation of the blank divided by the slope of the calibration curve, was determined to be 10 pM or 10 attomoles on column. Neat solutions of Alexa Fluor 647 were used to calculate the theoretical limit of detection. Buffer solutions may display lower nonspecific binding compared to biological samples. Therefore, the detectability of the capillary microfluidic system is more likely to be matrix-limited than instrument-limited. Reducing the nonspecific signal would lead to improved detection limits in biological matrices.

The ability of a system to detect low picomolar concentrations of laser dye-labeled proteins is attractive for clinical applications. The demonstrated low detection limit of dye solutions shows promise in this regard and may be improved further since immunoaffinity chromatography allows online sample concentration. For example, Guzman has developed a solid-phase microdevice capable of concentrating samples 1000-fold online with immunoaffinity capillary electrophoresis (Guzman 2003). Other factors may be changed to further improve the detection limit of the system. In the current microfluidic instrument, the post-column capillary used for the flow cell is 100

μm inner diameter. Reducing this capillary to 75 or 50 μm inner diameter would reduce extra-column band broadening, resulting in lower limits of detection. The maximum flow rate achieved without exceeding the pressure capacity of the syringe was 1.5μL/min. Increasing the flow rate would also help improve peak shape, but was not an option for the 0.2 x 25 mm prototype column packed with 1 μm silica beads due to exceeding the pressure rating for the syringes. Alternatively, the use of larger particle sizes for column packing material would allow for faster flow rates with this system, but also will lead to peak broadening.

To demonstrate that the system was suitable for immunoaffinity chromatography, a 0.2 x 25 mm prototype column was packed with 5.7 μm glass particles coated with rabbit anti-goat polyclonal antibodies. Alexa Fluor 647-goat IgG solutions were injected into the microfluidic system using a 1.0 μL injection loop. Introduction of a sodium thiocyanate gradient had a pronounced effect on the baseline, as is shown for an injection of blank phosphate buffer (Figure 11). The signal decreases as the chaotropic gradient is introduced and rises as the mobile phase returns to the starting phosphate buffer. The reason for the baseline drop with 2.5 M sodium thiocyanate is not known, but may be due to a quenching phenomenon or refractive index change. Chromatograms of goat IgG-fluorescent dye solutions show a large first peak of unbound material and a second peak corresponding to captured antigen. Figure 12 shows a representative chromatogram of goat IgG at 667 pM with the immunoaffinity-purified peak eluting just before the baseline dip induced by the gradient. This chromatogram was the 25th overall injection on the column. A linear regression resulted in a slope of 0.0858 and an r^2 value of 0.9963

using peak areas and concentrations from 111 pM to 1000 pM (single injection curve). Further optimization of this proof-of-principle model would focus on maximizing antigen recovery and minimizing the baseline effect of the chaotropic gradient. Antigen recovery may be improved by varying loading or running buffer conditions. The pH and/or salt concentration of the running buffer will have an effect on the degree of antibody-antigen binding. Instrumental parameters such as flow rate may be varied as well. An optimized flow rate would utilize the fastest runtime that still provided time for the antibody-antigen reaction to occur. The baseline effect can be minimized by using the lowest effective concentration the chaotropic buffer or changing to a different type of elution buffer, for example acid elution. The column was maintained at 15 °C and an approximately 40% decrease in antigen binding capacity was observed gradually between 40 to 50 injections. A new ice water jacket has been constructed from copper tubing that maintains column temperature at 5 °C and it is expected to help increase column lifetime. A peristaltic pump is used to pump ice water through a copper coil wrapped around the separation column. A schematic of the column cooler is shown in Figure 13.
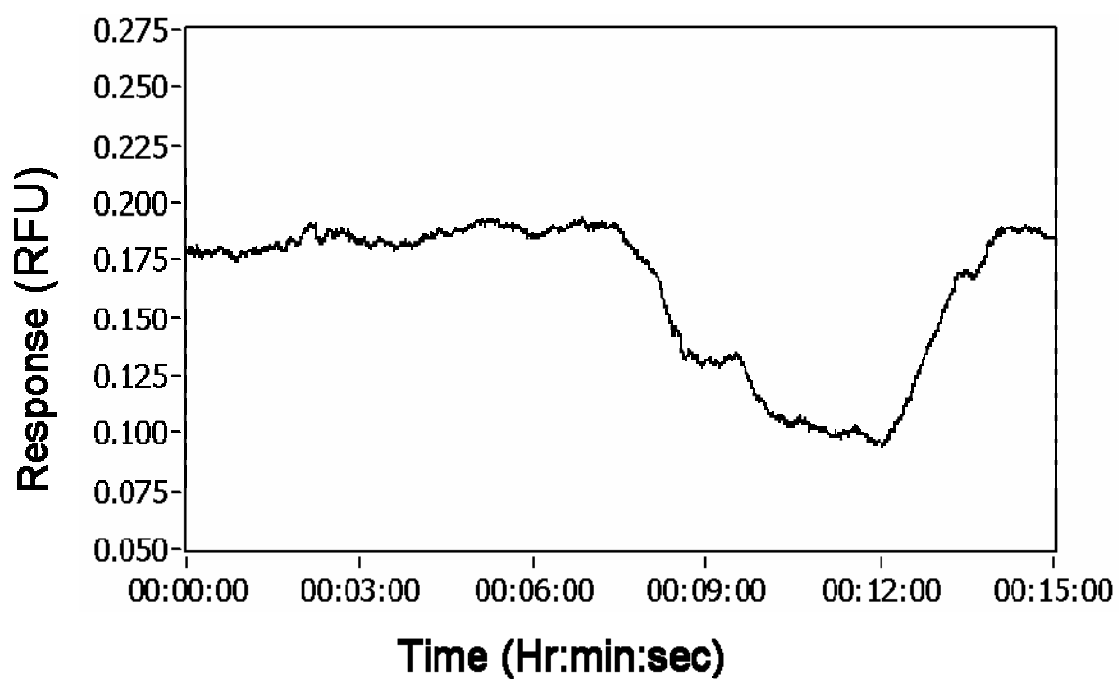
Figure 11: Baseline change during a sodium thiocyanate gradient. A blank injection of

10 mM phosphate buffer was made. Run conditions are as described in the text.
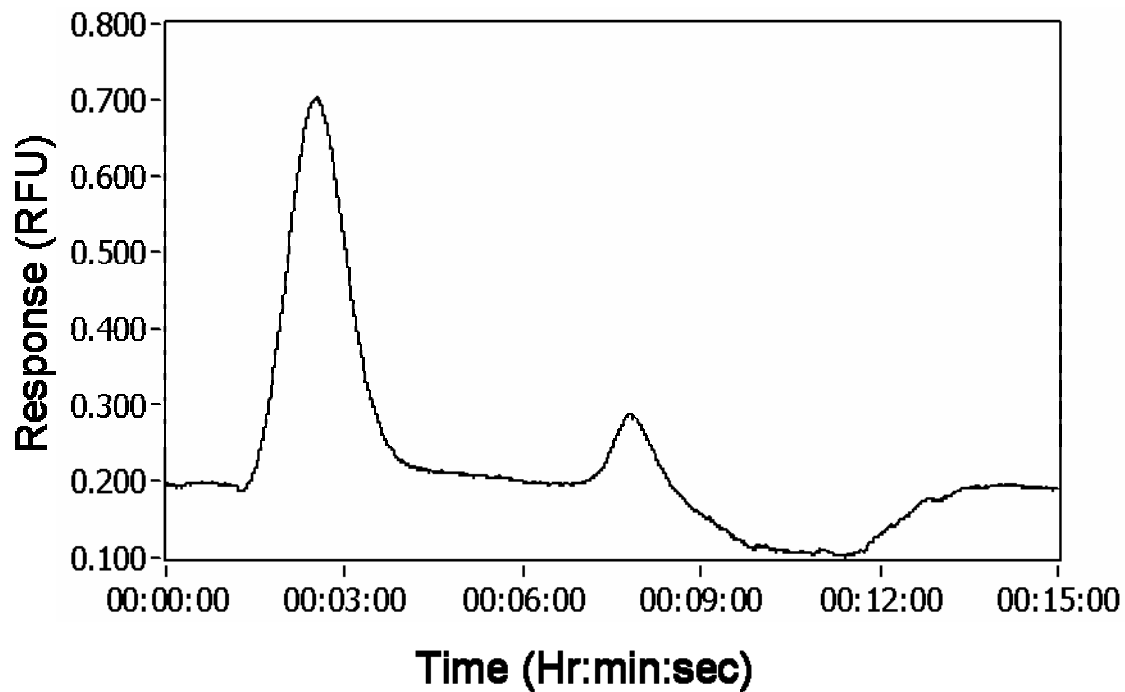
Figure 12:   Representative immunoaffinity chromatogram of 667 pM goat IgG labeled with Alexa Fluor 647 dye. The first peak is the unbound material and the second peak is immunoaffinity purified goat IgG. Conditions are described in the text.

Column Coil

Copper Tubing

Peristaltic Pump

Ice Water
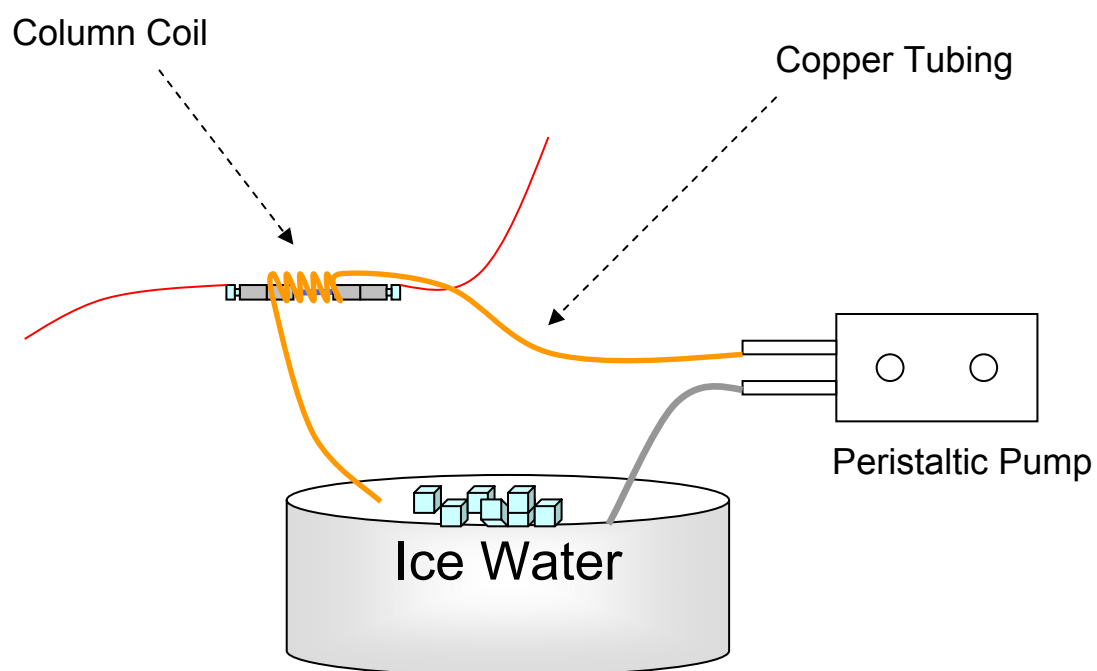
Figure 13: Diagram of column cooling apparatus.

2.4 Conclusions

A laboratory-constructed capillary HPLC with visible diode laser-induced fluorescence detection was presented. Separation columns were designed and optimized with respect to syringe size, column length, and particle size. The prototype column chosen for proof-of-concept testing was a 200 μm by 25 mm polymer-coated fused-silica capillary. The ability of the microliter syringe pumps and nano gradient mixer chip to perform as a microfluidic gradient HPLC has been demonstrated through a series of programmed evaluations. Pumping software-programmed amounts of fluorescent dye through the mixer created response profiles that correlated well with expected concentration increases. Furthermore, an acidic gradient was confirmed by pH readings of column effluent and offline measurements. Throughout the optimization, the software programs were verified by accurately controlling the components to function as a miniaturized chromatography system.

Effective immunoaffinity chromatography requires an elution scheme and instrumentation capable of producing gradients that dissociate the antibody-antigen complex. The system constructed meets this need and requires low amounts of reagents and samples, which can be an advantage when working with expensive immuno-reagents or when rapid results are needed. A goal for the instrument was to reach limits of detection in the low picomolar range. The system was developed in response to the need for rapid and selective assays including intraoperative assays and point-of-surgery tests, or other point-of-care applications. Many of the intraoperative assays, such as

parathyroid hormone testing for example, require measuring baseline levels at low picomolar concentrations (Vasan, Blick et al. 2004; Friedman, Vidyasagar et al. 2005). A LOD of 10 pM was obtained for neat solutions of Alexa Fluor 647 with the prototype instrument. Online sample concentration can be achieved using immunoaffinity chromatography by loading relatively large injection volumes onto the column for antigen capture by an immobilized antibody support. The sample antigen can then be released from the column in a volume that is smaller than the injected volume for enhanced detection.

Immunoaffinity chromatography was demonstrated using immobilized rabbit anti-goat IgG and fluorescently labeled goat IgG as a model antibody-antigen system. The immunoaffinity stationary phase was comprised of antibody attached to glass beads via a streptavidin-biotin linkage. A chaotropic gradient was chosen for antigen elution and a concentration-dependent increase in fluorescence signal was observed. The device presented was laboratory-built from a combination of commercially available materials. The relatively simple construction and compact nature of instrument components may be advantageous in clinical and research settings where system flexibility and portability are desired.

CHAPTER 3 Demonstration of a direct capture immunoaffinity separation for C-reactive protein using a capillary-based microfluidic device

Drawn from manuscript published in Journal of Pharmaceutical and Biomedical

Analysis- Article in Press

3.1 Introduction

Immunoaffinity separations rely upon antibody-antigen reactions to selectively remove target analytes from sample matrices. The combination of immunoaffinity techniques with miniaturized analytical instrumentation provides a powerful tool for separating analytes of interest from complex matrices, while consuming minimal quantities of samples and reagents (Peoples and Karnes 2008). Microchip and capillary-based systems offer a reduction in diffusion distances that allow for faster antibody-antigen recognition versus traditional microplate immunoassays, especially when packed bead beds are used (Sato, Tokeshi et al. 2000; Sato, Tokeshi et al. 2001; Verpoorte 2003; Lim and Zhang 2007). Two common immunoaffinity techniques include competitive and noncompetitive immunoassays. In a competition assay, sample antigens and labeled antigens compete for a limited amount of antibody sites. Large antigens, capable of possessing two distinct epitopes, may be analyzed by a noncompetitive immunoassay (Hage 1999). An immobilized antibody is used to capture the antigen and a detection antibody is introduced to form a sandwich complex. Competitive and sandwich

74

immunoassay techniques require the labeling of secondary compounds, such as analogous antigens or detection antibodies prior to sample analysis. A direct capture immunoassay uses an immobilized capture antibody and directly measures the signal of the antigen either bound to the antibody or after dissociation from the antibody. In many clinical applications the antigen is present in trace amounts or does not readily provide a measurable signal; labeling of the antigen is then performed to enhance the response. In direct capture immunoaffinity chromatography, samples are applied to a separation column and the target antigen binds to a stationary support of immobilized antibodies. Extraneous components in the matrix, including unused labeling reagents, are pumped to waste and the antigen is then eluted in a dissociation buffer for detection (Hage 1998).

C-reactive protein (CRP) was selected as a model antigen for proof-of-concept demonstration of direct capture immunoaffinity using a miniaturized chromatography device. CRP is a serum protein and an acute phase reactant whose levels become elevated during injury or infection (Ledue and Rifai 2003). The native conformation of CRP is a 115 kDa pentamer made of five noncovalently bonded 23 kDa subunits (Wang, Wu et al. 2002; Hu, Hsu et al. 2006). CRP has been measured as a general biomarker of inflammation and may be used to assess cardiovascular disease (CVD) risk (Myers, Rifai et al. 2004). Low, medium, and high CVD risk categories have been identified corresponding to CRP levels of less than 1.0 μg/mL, 1.0 to 3.0 μg/mL, and greater than 3.0 μg/mL, respectively. CRP concentrations greater than 10 μg/mL indicate trauma, infection, or other sources of inflammation (Myers, Rifai et al. 2004).

CRP is frequently employed as a model analyte for demonstrating innovative microfluidic and small-scale immunoaffinity separation technologies (Shin, Lee et al. 2007). A microfluidic sandwich immunoassay for CRP in human plasma was performed using capillary action to generate sample flow (Wolf, Juncker et al. 2004). Fluorescently labeled detection antibodies were used to measure CRP from one microliter sample volumes. Hosokawa et al. (Hosokawa, Omata et al. 2007) developed a microchip immunoassay of CRP in human serum based on dendritic amplification and fluorescence detection. The amplification technique relied upon a sandwich complex that included a biotinylated second antibody. Fluorescein isothiocyanate (FITC)-streptavidin and biotinylated anti-streptavidin were introduced to produce a layered, dendritic structure. A microfluidic competition immunoaffinity separation of CRP was demonstrated with on-chip detection of fluorescein-labeled CRP after an acid elution step (Shin, Lee et al. 2007). Sandwich immunoassays of CRP have been demonstrated in human serum with on-chip chemiluminescence detection using an imager or photographic film (Bhattacharyya and Klapperich 2007). Kriz et al. (Kriz, Ibraimi et al. 2005) applied magnetic permeability detection of anti-CRP nanoparticles for CRP immunoassays in whole blood samples. CRP was sandwiched between antibody-coated silica microparticles and antibody-coated magnetic nanoparticles in a glass vial. The silica particles were allowed to sediment and the magnetic permeability was measured after placing the vial into a magnetic coil. Tsai et al. (Tsai, Hsu et al. 2007) developed a magnetic-based competitive immunoassay for CRP in serum using a flow-through channel design with a magnetic detection zone. Free CRP and CRP-conjugated silica

particles competed for binding of antibody-coated magnetic nanoparticles and the signal was generated by counting the CRP-silica particles under a microscope. Other formats for measuring CRP have included immunochromatographic test strips for whole blood sandwich immunoassays (Ahn, Choi et al. 2003) and surface plasmon resonance (SPR) biosensors (Hu, Hsu et al. 2006). The SPR method employed three separate monoclonal antibodies to detect both the native, pentamer conformation and the modified, subunit forms of CRP.

In the current research, a direct labeling/direct capture immunoaffinity separation of CRP is described. The antigen is labeled with a fluorescent dye reagent and separated on a capillary immunoaffinity column for detection with diode laser-induced fluorescence (LIF) detection. The system employs syringe pumps, a microfluidic mixing chip, a capillary injection loop, and a flexible capillary-scale column design to perform immunoaffinity chromatography with low sample and mobile phase requirements.

3.2 Experimental materials and methods

3.2.1 Reagents and materials

Highly pure C-reactive protein and corresponding monoclonal antibody were purchased from Fitzgerald Industries International, Inc. (Concord, MA). Streptavidin-coated 5.01 μm silica beads were obtained from Bangs Laboratories, Inc. (Fishers, IN). Sulfosuccinimidyl-6-(biotin-amido) hexanoate (Sulfo-NHS-LC-Biotin), 0.5 mL Zeba

Desalt Spin Columns and an EZ Biotin Quantitation Kit were obtained from Pierce Biotechnology (Rockford, IL). Alexa Fluor 647 carboxylic acid, succinimidyl ester (λ_{ex} = 650 nm, λ_{em} = 668 nm) was purchased from Invitrogen (Carlsbad, CA). SeraSub, a protein-free, buffered polymer solution with the same viscosity, specific gravity, and osmolality as serum was purchased from CST Technologies (Great Neck, NY). Purified water was prepared using a Barnstead Nanopure Diamond system (Dubuque, IW). All other reagents and chemicals were obtained from Sigma (St. Louis, MO). All solutions were filtered through 0.22 μm PVDF Durapore 13 mm syringe filters (Millipore, Billerica, MA) prior to use. Polyetheretherketone (PEEK) capillary tubing of 360 μm outer diameter (OD) and PEEK unions were purchased from Upchurch Scientific (Oak Harbor, WA).

3.2.2 Instrumentation

Immunoaffinity chromatography was performed on a laboratory-built system described previously (Peoples, Phillips et al. 2007). Two microliter OEM module syringe pumps (Harvard Apparatus, Inc., Holliston, MA) fitted with glass gastight 1700 series syringes (Hamilton, Reno, NV) were placed into a 0.22" acrylic cabinet enclosure. Mixing of mobile phases delivered by the syringe pumps was performed using a gradient mixing chip (NanoMixer, Upchurch Scientific). Samples were introduced into the system using a Microinjector (Upchurch Scientific) with a 250 nL injection loop made from 50 μm internal diameter (ID) PEEK capillary tubing. Fluid transfer lines

throughout the system from the pumps to the column inlet were made from PEEK capillary tubing.

A flow cell was made from 360 μm OD by 50 μm ID square fused-silica capillary tubing (Polymicro Technologies, Phoenix, AZ) and a 2 mm section of the polyimide coating was burned off using a capillary window maker (MicoSolv Technology Corporation, Long Branch, NJ). The flow cell was mounted onto a Zetalif laser-induced fluorescence detector (Picometrics, Ramonville, France) containing a Hamamatsu R928 red-sensitive photomultiplier tube (Bridgeport, NJ). The laser diode system consisted of a 650 nm, 20 mW laser diode (Lasermate Group, Inc., Pomona, CA), laser diode mount LDM 4412 with collimating lens (ILX Lightwave, Bozeman, MT), and an ILX Lightwave LDC-3722 laser diode controller. The diode was typically operated at 20°C and 60 mA and the PMT voltage was maintained at 730 V. A National Instruments (Austin, TX) USB-9215 data acquisition card with 16-bit resolution was used to interface the detector signal to a PC.

3.2.3 Column design

The column body was prepared from 175 μm ID x 1/16" OD PEEK tubing (Upchurch Scientific) cut to lengths of 19 and 18.5 mm for columns I and II, respectively. Stainless steel external column end fittings (Valco Instrument Co. Inc., Houston, TX) containing 0.5 μm frits (Upchurch Scientific) were tightened onto the columns. The frits were 0.038 in. x 0.030 in. x 0.062 in. made from stainless steel with a polymer ring. Columns were packed with stationary phase under negative pressure using a vacuum

pump. Slurries of beads were prepared at 3 mg/mL and added to the top of the column body with the inlet frit removed.

3.2.4 Software

A custom program written in LabVIEW 7.0 (National Instruments) was used to control the syringe pumps to perform step-gradients and acquire the detector signal as a chromatogram. SigmaPlot 10.0 (Systat software Inc., San Jose, CA) was used for data analysis and calibration modeling.

3.2.5 Antibody biotinylation

The monoclonal anti-CRP antibody was diluted in sodium phosphate buffer (pH 7.2; 10 mM) and biotinylated using a 30-fold molar excess of Sulfo-NHS-LC-Biotin. The reaction solution was mixed by rotation for 30 minutes at room temperature, followed by 30 minutes at 4 °C. Excess biotin was removed with 0.5 mL Zeba Desalt Spin Columns according to the manufacturer's instructions and the antibody concentration was measured at A_{280nm} using a NanoDrop ND-1000 spectrophotometer (NanoDrop Technologies, Wilmington, DE). The degree of biotinylation was determined with an EZ Biotin Quantitation Kit according to the manufacturer's instructions and a BioTek Synergy 2 microplate reader (BioTek Instruments, Inc., Winooski, VT). The kit relies on 4'-hydroxyazobenzene-2-carboxylic acid (HABA)/avidin absorbance at 500 nm. The biotin-labeled antibody displaces the HABA reagent causing a proportional decrease in the signal at 500 nm (Dotsikas and Loukas 2005). A positive control of biotinylated

horseradish peroxidase was used to normalize results and the biotin:anti-CRP molar ratio was determined to be 2.25 ± 0.08 (n = 3).

3.2.6 Stationary phase preparation

Streptavidin-coated silica beads (5 µm) were washed three times with sodium phosphate buffer (pH 7.2; 10 mM) prior to use. The beads were centrifuged at 1200g for 5 minutes at 7 °C and the supernatant discarded after each wash. Based on the biotin-binding capacity of the beads provided on the certificate of analysis, each mg of beads can bind approximately 2.4 µg of biotinylated antibody. A 7-fold excess of biotin-anti-CRP was added to 1.5 mg of streptavidin-coated silica beads in 0.5 mL and rotated overnight (19 hours) at 4 °C. The beads were washed 3 times as before and reacted with 60 ng/mL biotin for 1.5 hours at 4 °C to block any remaining reactive sites. The antibody-coated beads were washed 5 times and stored in sodium phosphate buffer (pH 7.2; 10 mM) at 4 °C until use.

3.2.7 C-reactive protein binding

C-reactive protein was labeled with a primary amine-reactive laser dye to assess the activity of columns and develop an immunoaffinity chromatography separation using the microfluidic system. CRP (2.21 mg/mL in a buffer of 100 mM Tris, 2 mM calcium chloride, and 0.1% sodium azide at pH 7.5) was desalted to remove the amine-containing buffer Tris and exchanged into sodium bicarbonate (pH 8.4; 100 mM). A 34-fold molar excess of Alexa Fluor 647 carboxylic acid, succinimidyl ester dye was added to the CRP

solution and rotated 1 hour at room temperature. After desalting the reaction mixture into phosphate buffered saline (pH 7.4; 10 mM phosphate, 2.7 mM potassium chloride, and 137 mM sodium chloride) (PBS), the absorbance at 280 nm and 650 nm was measured on a NanoDrop ND-1000 spectrophotometer. The degree of labeling was calculated according to the dye manufacturer's instructions and determined to be 5.1 ± 0.7 moles of dye per mole of CRP ($n = 6$). The extinction coefficient used for CRP was $E_{mg/mL} = 1.7$ (Scripps Laboratories, http://www.scrippslabs.com/datatables/protein_absorbance.html). Labeled CRP at 1 mg/mL in PBS containing 1% bovine serum albumin (BSA) was stored at -20 °C.

Two physiological buffers were evaluated as sample solutions and loading mobile phase buffers, PBS and Dulbecco's PBS (DPBS). Unlike PBS, Dulbecco's PBS is a balanced salt solution containing additional salts of calcium chloride dihydrate (0.9 mM) and magnesium chloride hexahydrate (0.5 mM). The pH of the DPBS buffer was measured at 7.2. CRP was prepared at a concentration of 10 μg/mL in PBS or DPBS containing 0.1 % BSA. Each solution was injected (250 nL) into the system using a loading mobile phase (pump A) of PBS or DPBS for the PBS- or DPBS-based sample solutions, respectively. The elution mobile phase (pump B) was glycine-HCl (pH 1.8; 200 mM) for all injections. The flow rate was 2.0 μL/min and the temperature was maintained at 6-8 °C by pumping ice water though a copper coil wrapped around the column. The initial gradient used was 98.75 % pump A for 2.5 min followed by a step gradient to 98.75 % pump B over 3 seconds. After 2 minutes, the mobile phase was returned to pump A for 2 minutes to equilibrate the column.
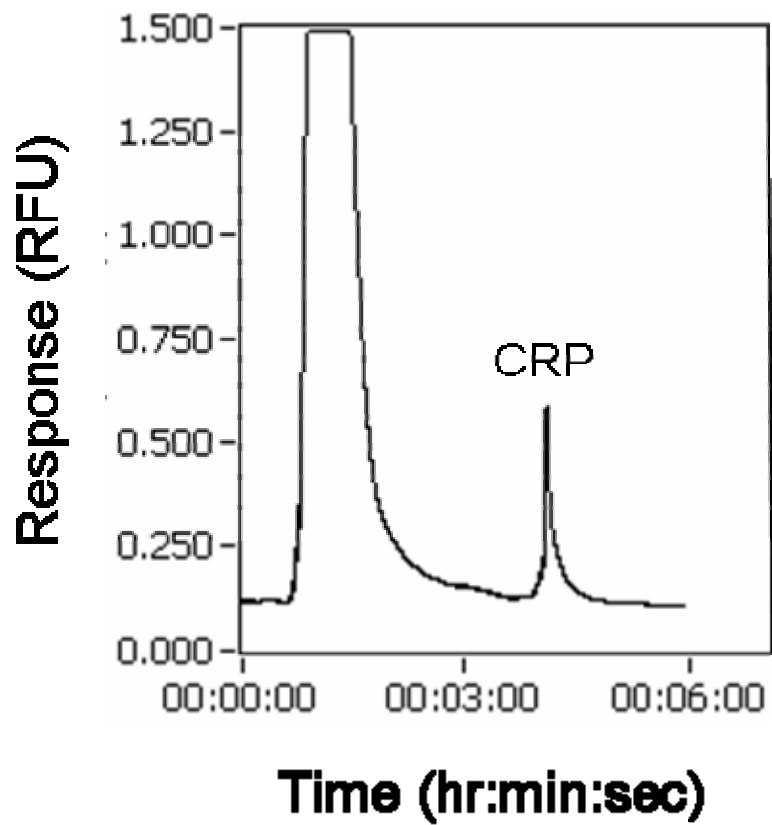
Figure 14: Typical immunoaffinity chromatogram for a 250 nL injection of C-reactive

protein. Conditions are described in the text and RFU = relative fluorescence units.
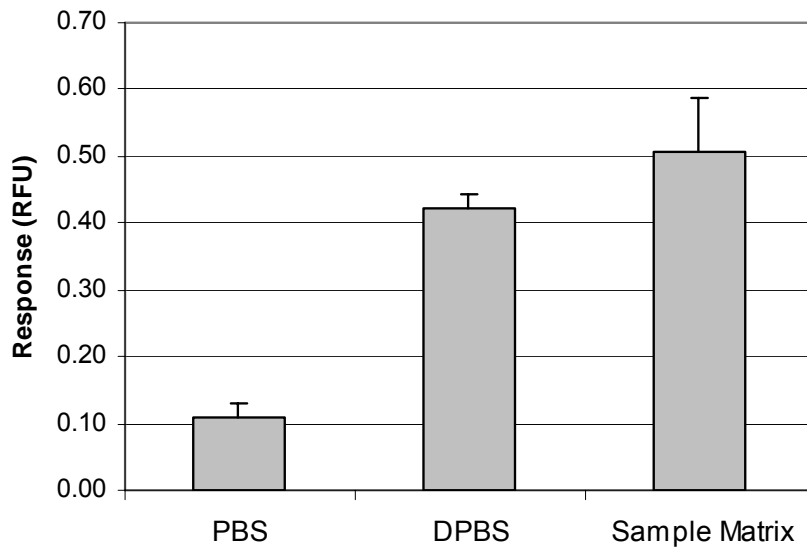
Figure 15: Effect of mobile phase and sample buffer solution on C-reactive protein-antibody binding. The shaded bars represent the CRP signal (n = 3, mean + standard deviation) in different mobile phase A and sample solutions. The "sample matrix" bar represents a mobile phase A of DPBS and a sample solution of DPBS:serum matrix 1:1 (v:v). Running conditions are described in the text and RFU = relative fluorescence units.

C-reactive protein has been shown to undergo conformational changes in the absence of calcium (Wang, Wu et al. 2002) and the PBS and DPBS systems were used to compare common physiological buffers with and without calcium. Figure 14 shows a typical chromatogram observed for a 250 nL injection of CRP in the DPBS sample solution with DPBS as the running mobile phase. The first peak represents nonreactive material and the second, sharper peak corresponds to immunoaffinity captured CRP. When PBS was used as the running buffer and sample solution, the recovered CRP peak intensity was approximately 4 times lower than the DPBS system. Therefore, DPBS was selected as the mobile phase used for sample application and also as a sample diluent. Figure 15 shows the effect of mobile phase and sample solution buffer on the immunoaffinity capture of CRP.

3.2.8   *Labeling and analysis of samples*

Prior to fluorescently labeling CRP in a simulated serum matrix, 10 µg/mL of pre-labeled CRP was spiked into a 1:1 (v:v) DPBS:SeraSub mixture containing 0.1 % BSA. The immunoaffinity chromatography conditions were the same as in section 2.7 with DPBS as the mobile phase in pump A. As shown in Figure 15, the column was capable of binding CRP in the presence of the sample matrix. The simulated serum was a buffered polymer solution with the same viscosity, specific gravity, and osmolality as serum. These properties may contribute to stability of endogenous proteins such as CRP and favorable binding conditions for antibody-antigen reactions by providing an environment resembling human serum. Polymers have also been reported to enhance

immunoassay binding and stabilize immunoreagents, including antibodies and proteins (Studentsov, Schiffman et al. 2002).

The experimental design for fluorescent dye labeling of the antigen and direct capture immunoaffinity separation is illustrated by Figure 16. CRP was desalted into DPBS and used to prepare calibration levels of 0.475, 0.950, 3.27, 6.65, 15.0, 23.5, 47.5, and 95.0 µg/mL in the simulated serum sample matrix. Alexa Fluor 647 carboxylic acid, succinimidyl ester dye was prepared at 40 µg/mL in DPBS and mixed 1:1 with each CRP calibrator and a blank. The reaction mixture was incubated for 1 hour at room temperature with gentle shaking. Samples were centrifuged at 10,000xg for 1 minute prior to injection and stored at 4 °C. The immunoaffinity chromatography conditions for the direct labeling/direct capture assay were adjusted to account for a larger unbound peak response due to excess dye and also a peak due to the matrix. The hold time of 98.75 % pump A after sample injection was increased to 5 minutes, followed by a step gradient to 98.75 % pump B over 15 seconds. The elution buffer of glycine-HCl (pH 1.8; 200 mM) was held for 2 minutes and the mobile phase was returned to DPBS for two minutes to equilibrate the column.

Each of the calibrators was injected n = 3 times to construct and evaluate calibrations models. Additionally, the 0.950, 6.65, and 47.5 µg/mL levels were injected in duplicate n = 6 times and the average of duplicate injections was used to assess accuracy and precision.

A. Fluorescent Labeling of Antigen:
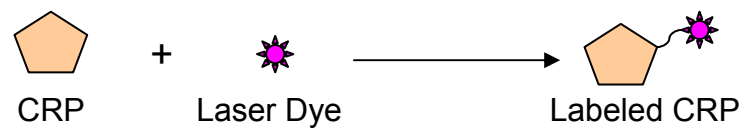
B. Direct Capture Assay:
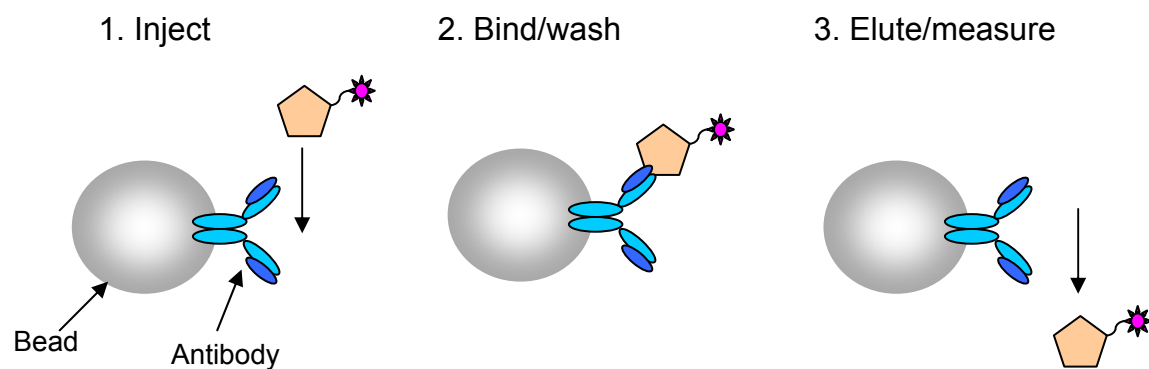
Figure 16: Procedure for direct fluorescent labeling and direct capture immunoaffinity

separation of C-reactive protein. Experimental details are described in the text.

3.3 Results and Discussion

3.3.1   *Immunoaffinity chromatography conditions*

Phosphate buffered saline and Dulbecco's phosphate buffered saline were evaluated during method development with respect to CRP binding in the immunoaffinity column. The presence of calcium and magnesium in the sample solutions and mobile phase resulted in a greater degree of antigen recognition by the anti-CRP antibodies in the capillary column. The DPBS buffer may help to maintain CRP in a favorable conformation for antibody recognition or may provide a more optimal environment for antibody-antigen association. The DPBS solution was used as sample diluent and antigen application mobile phase for all experiments.

3.3.2   *Direct capture immunoaffinity demonstration with C-reactive protein*

Samples were injected onto the immunoaffinity column with a loading/washing step of 5 minutes in pump A mobile phase. This allowed the large, unbound peak of excess dye to elute from the system prior to the gradient elution step. During the glycine-HCl elution step, the CRP was released from the immobilized antibodies and detected. A comparison of chromatograms for blank matrix and CRP injections is shown in Fig. 17. A small matrix peak is present in the blank just before 6 minutes and the CRP peak elutes at approximately 7 minutes.
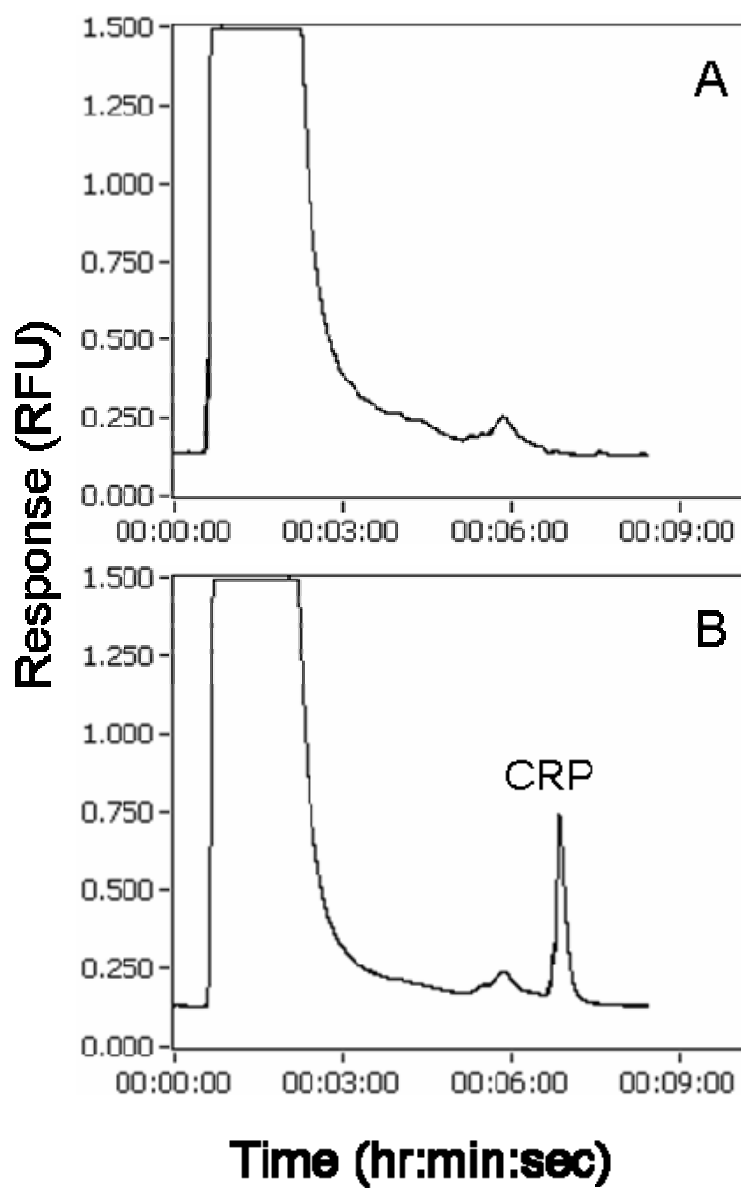
Figure 17: Typical chromatograms of a blank (A) and 6.65 µg/mL C-reactive protein standard (B) in the sample matrix. Running conditions are described in the text and RFU = relative fluorescence units.
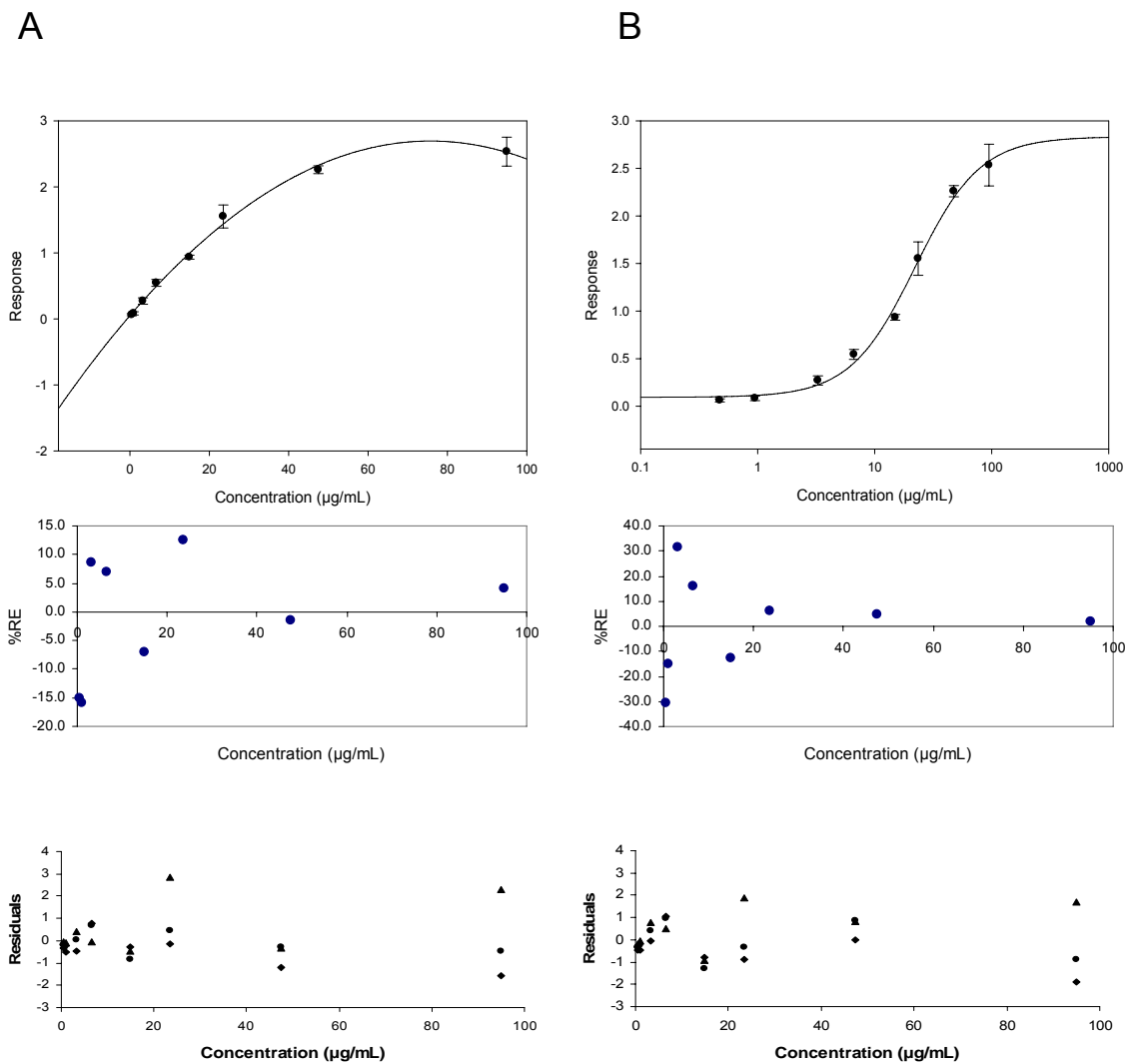
Fig. 18: Comparison of quadratic (A) and 4-parameter logistic (B) models. Each data point represents the mean ± standard deviation of n = 3 injections and the response is in relative fluorescence units (RFU). The % relative error (%RE) versus concentration (duplicate injections) is shown below each model. The residuals for each model are shown below the %RE plots, with diamonds, circles, and triangles representing the 1st, 2nd, and 3rd replicates.

3.3.3 Calibration models and metrics

Quadratic and 4-parameter logistic (4PL) curves were evaluated using the data from the response of the 8 calibrators. To calculate figures of merit, including accuracy and precision, the best model was selected by plotting % relative error (%RE) against the concentration levels. The %RE represents the difference between back-calculated values and nominal values divided the nominal values and multiplied by 100% (Findlay and Dillard 2007). Figure 18 shows the two models with the plotted %RE versus standard concentration and residual plots. The residuals were evaluated for constant variance with an F-test ($\alpha = 0.05$) using the Microsoft Excel Two Sample for Variances test. Both the quadratic and 4PL models displayed unequal variance across the calibration range ($p < 0.05$). The quadratic model had an r^2 of 0.99 (0.11 standard error) with %RE ranging from -15.9 to 12.6 for the 8 levels. The 4PL model had an r^2 of 0.99 (0.12 standard error) with the %RE between -30.8 and 31.6. The current guidance for model selection of ligand binding assays, including immunoassays, recommends %RE be within 20% for back-calculated standards and 25% at the lower and upper limit of quantification (LLOQ and ULOQ, respectively) (Kelley and DeSilva 2007). Based on these guidelines, the quadratic model was chosen to describe the data and calculate accuracy. No weighting factor was applied since the quadratic fit represented the simplest model that passed the recommended %RE requirements.

The equation for the quadratic model was $y = y0 + ax + bx^2$ and the parameter estimates were $y = 0.05\ (0.03) + 0.070\ (0.003)x -0.00050\ (0.00003)x^2$, where standard error is shown in parenthesis. The limit of detection (LOD) was estimated to be 57.2

ng/mL (497 pM) at 2 times the standard deviation of the blank response, n = 3. The linear slope term, a, was used to convert the response into a concentration in ng/mL. Based on the 250 nL injection loop size, the on-column LOD was 14.3 pg (124 attomoles). Table 6 summarizes the accuracy and precision data represented as % difference from nominal value (%DFN) and % relative standard deviation (%RSD), respectively.

Table 6: Accuracy and precision of C-reactive protein by direct capture immunoassay (3 levels, n = 6 replicates).

CRP Concentration (µg/mL)	Precision (%RSD)	Accuracy (%DFN)
0.95	2.0	-8.8
6.65	12.3	-11.1
47.5	17.0	4.8

The equation for the 4PL model was $y = min + (max-min)/[1 + (x/EC50)^{Hillslope}]$, plotted with a logarithmic x-axis scale. The EC50 term represents the inflection point, the Hillslope is a slope factor, and the min and max terms represent the lower and upper asymptotes of the curve (Findlay and Dillard 2007). Parameter estimates with standard error in parenthesis for the 4PL model shown in Fig. 18 are as follows: min = 0.09 (0.05), max = 2.8 (0.2), EC50 = 22 (2), and Hillslope = -1.6 (0.2). The 4PL model was chosen to

estimate the maximum antigen-binding capacity of the columns. The useful range of this model can be extended on the upper end by achieving a higher degree of active immobilized antibody on the solid support (i.e., proper antibody orientation) and on the lower end by reducing background and nonspecific binding. Blocking agents or surfactants can be used in wash steps or added to the mobile phase to lower nonspecific binding of labeled matrix components.

3.3.4 Column characteristics

Using the 4PL model parameter estimates a maximum binding concentration of CRP was calculated. The concentration injected on column was adjusted for the dilution factor of the dye solution and the 250 nL injection volume. Column I (0.175 x 19 mm) and Column II (0.175 x 18.5 mm) could bind approximately 188 and 125 ng of C-reactive protein, respectively.

To preserve the working lifetime of the column, a column chiller consisting of a copper coil was pumped with ice water during operation and columns were stored at 4 °C when not in use. At greater than 100 injections, the response of the 47.5 µg/mL standard was approximately 50% of prior injections, while the 0.950 µg/mL standard response remained constant (See Figure 19). A two tailed t-test ($\alpha = 0.05$) assuming unequal variances was performed in Microsoft Excel for each concentration to compare the effect of injection number. The difference between standard responses after 35 or 100 injections was statistically significant ($p < 0.05$) for the 6.65 and 47.5 µg/mL concentrations and insignificant ($p > 0.05$) for the 0.950 µg/mL concentration. The

useful life of the column is reduced for the higher standard concentrations as the amount of active antibody is compromised; however, the columns would still be useful to measure CRP concentrations in the low µg/mL concentration ranges. Inactivity of binding sites may be caused by incomplete antigen elution or repeated acid elution cycles that damage antibodies and decrease the overall antigen-binding capacity (Yarmush, Antonsen et al. 1992).   On the 4PL model, this would result in a lowering of the upper asymptote and a reduction in range of measurable concentrations. Therefore, the lifetime of anti-CRP columns that could measure the entire calibration range was approximately 100 acid elution cycles stored and operated at refrigerated conditions.
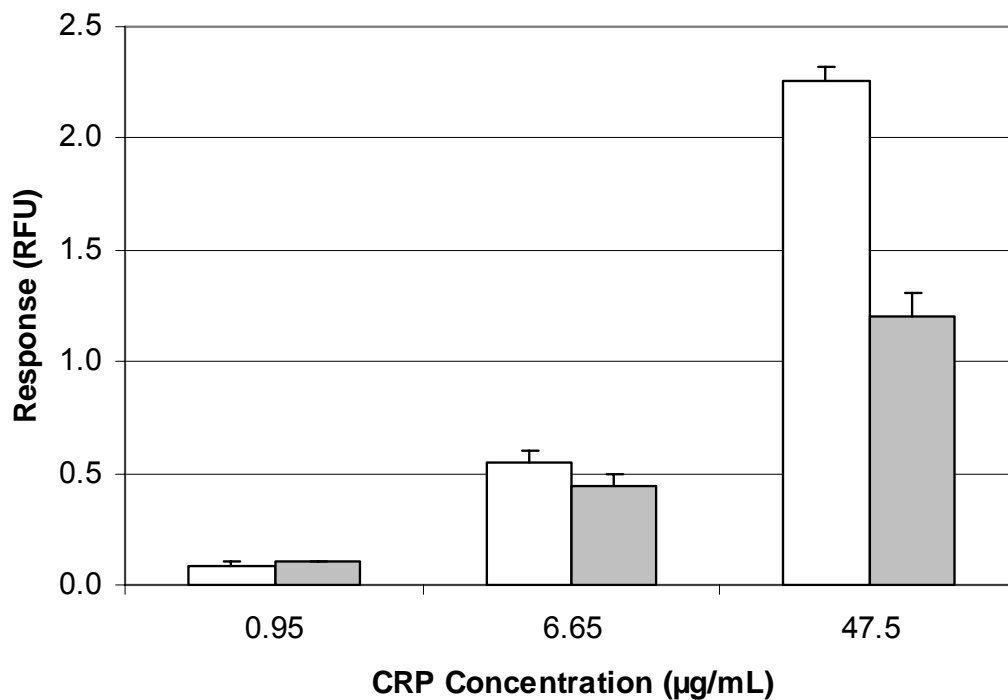
Figure 19: Effect of injection number on C-reactive protein response (at least n = 3, mean + standard deviation). The white bars represent CRP response after 35 elution cycles and the shaded bars represent CRP response after more than 100 injections. There was a statistically significant difference ($p < 0.05$) between the 35 and 100 injection responses for the 6.65 and 47.5 µg/mL concentrations.

3.4   Conclusions

A direct capture immunoaffinity separation of C-reactive protein was demonstrated using a miniaturized, capillary-based device. This simple, pump-driven microfluidic system was assembled from many commercially available materials. The basic components of the system include two syringe pumps for fluid delivery, a gradient chip for mobile phase mixing, a micro-injector with capillary injection loop, capillary columns packed with immunoaffinity beads, and a diode LIF detector containing a laboratory-constructed, fused-silica capillary flow cell. CRP was directly labeled with a fluorescent dye, bound to antibody-coated beads in a capillary column, and eluted for measurement by diode LIF. This procedure is straightforward and requires a one-step reaction prior to sample injection. The small injection volume (250 nL) and low mobile phase flow rate (2.0 µL/min) minimize reagent and sample consumption and offer the potential to analyze sub-microliter samples. The small-scale instrumentation and low sample volume requirements are advantageous in clinical applications that require portable systems such as patient point-of-care settings.

CHAPTER 4 Evaluation of direct capture immunoaffinity chromatography for parathyroid hormone in human serum

4.1   Introduction

Immunoassays are currently used in patient point-of-care monitoring and other diagnostic applications because of the simplicity and speed of the assay (von Lode 2005). Rapid immunoassays are of great value in intraoperative or point-of-surgery tests, where surgical success may be ascertained by the results (Sokoll, Wians et al. 2004). For example, a rapid intraoperative immunoassay for parathyroid hormone (PTH) is used for patients with hyperparathyroidism undergoing surgical resection of enlarged glands. PTH is measured at time zero (baseline before surgery) and 5, 10, and sometimes 20 minutes after removal of the suspect gland. The patient remains under anesthesia during the entire process. A fifty percent reduction in PTH values from baseline is generally used as a marker of successful excision (Inabnet 2004). Baseline PTH levels are routinely in the low pg/mL range (Sokoll, Wians et al. 2004; Vasan, Blick et al. 2004; Friedman, Vidyasagar et al. 2005) and commercial immunoassay high level calibrators are in the low ng/mL range (Sokoll, Wians et al. 2004).   Faster outcomes for intraoperative tests such as PTH result in a reduction in surgery time, less anesthesia, and increased patient welfare (Vasan, Blick et al. 2004).   Other rapid immunoassays are applied for similar procedures to monitor insulin, gastrin, adrenocorticotropin, cortisol, and growth hormone (Sokoll, Wians et al. 2004).

97

The combination of immunoassays with microfluidic systems allows for selective and rapid analysis of analytes from small sample sizes (Sato, Hibara et al. 2003). The dimensions of microfluidic channels or capillaries (less than 1 mm) result in reduced diffusion distances for antibody-antigen reactions. When packed beds of beads are used the reactive surface area to volume ratio is enhanced, producing faster reaction times (Verpoorte 2003; Lim and Zhang 2007). Additionally, microfluidic devices require low amounts of reagents and are composed of miniaturized components, making portability and point-of-care testing possible (Bange, Halsall et al. 2005).

Only one example of a microfluidic device for immunoassay of PTH has been reported (Hayes, Polson et al. 2001). Antibodies were immobilized to magnetic beads, pumped into fused silica capillaries, and held in place with a rare earth magnet. The PTH samples were pumped through the capillary, followed by the fluorescently-labeled detection antibody. A new packed bed was used for each experiment and the total analysis time was 60 minutes for each sample. The only concentration of PTH assayed was 1.4 ng/mL, which was noted as the upper physiological range. Successful sandwich assays for PTH in human plasma have been reported using conventional HPLC and chemiluminescent detection (Hage and Kao 1991; Hage, Taylor et al. 1992). The technique required 200 µL of plasma and the detection antibody was incubated with samples for one hour offline prior to injection.

In the current research, a direct labeling and direct capture immunoaffinity separation of PTH was demonstrated using a microfluidic capillary instrument. The system consisted of micro-syringe pumps, a gradient mixing chip, micro-injector,

capillary column, and diode laser detector. The aim of the work was to develop a rapid assay for PTH using minimal sample volume. PTH was fluorescently labeled in samples and directly injected into the system. The use of biological matrix revealed limitations with the direct labeling approach and a sandwich immunoassay was investigated as an alternative approach.

4.2 Experimental materials and methods

4.2.1 Reagents and materials

Highly purified PTH (amino acids (aa) 1-84) and polyclonal goat anti-human PTH (aa 1-34) antibody for the direct capture assay were purchased from United States Biological (Swampscott, MA). Monolclonal mouse anti-human PTH C-terminus (aa 53-83) and N-terminus (aa 1-34) were purchased from QED Bioscience Inc. (San Diego, CA). Human PTH (1-84) for the sandwich assay was purchased from Bachem (Torrance, CA). Zeba Desalt Spin Columns (0.5 mL), an EZ Biotin Quantitation Kit, and Sulfosuccinimidyl-6-(biotin-amido) hexanoate (Sulfo-NHS-LC-Biotin) were obtained from Pierce Biotechnology (Rockford, IL). Alexa Fluor 647 carboxylic acid, succinimidyl ester (λ_{ex} = 650 nm, λ_{em} = 668 nm) and rabbit anti-goat IgG (biotin conjugate) were purchased from Invitrogen (Carlsbad, CA). Streptavidin silica beads (5.01 µm and 4.82 µm) were obtained from Bangs Laboratories, Inc. (Fishers, IN). Pooled normal human serum was purchased from BioChemed Services (Winchester, VA). Molecular weight cutoff filters (MWCO) were obtained from Waters (Milford, MA) for 3 and 10 kDa, Pall Life Sciences (Ann Arbor, MI) for 30 and 100 kDa, and

Vivascience (Littleton, MA) for 50 kDa cutoffs. Human serum was filtered by centrifugation at 12000g for 20 minutes using the cutoff devices. Purified water was prepared in the laboratory with a Barnstead Nanopure Diamond system (Dubuque, IW). The remaining reagents were purchased from Sigma (St. Louis, MO). Buffers and solutions were filtered through 0.22 µm PVDF Durapore 13 mm syringe filters (Millipore, Billerica, MA) prior to use. Polyetheretherketone (PEEK) tubing (1/16 inch outer diameter (OD)), capillary tubing (360 µm OD), and PEEK unions were purchased from Upchurch Scientific (Oak Harbor, WA).

4.2.2 Instrumentation

The miniaturized chromatography system described previously (Peoples, Phillips et al. 2007) was used for all assays. Dual micro syringe pumps (Harvard Apparatus, Inc., Holliston, MA) with glass gastight 1700 series syringes (Hamilton, Reno, NV) were used for binary gradients and a gradient mixing chip (NanoMixer, Upchurch Scientific) was configured in the low pressure setting. A manual injector (Microinjector Upchurch Scientific) was fit with a 250 nL PEEK capillary injection loop. All tubing from the pumps to the column was made from PEEK capillary.

Square fused-silica capillary tubing (360 µm OD by 50 µm internal diameter (ID)) (Polymicro Technologies, Phoenix, AZ) was connected after the column and a 2 mm section of the polyimide coating was burned off to make the flow cell using a capillary window maker (MicoSolv Technology Corporation, Long Branch, NJ). The flow cell was positioned in a Zetalif laser-induced fluorescence detector (Picometrics,

Ramonville, France) with a Hamamatsu R928 photomultiplier tube (Bridgeport, NJ). A 650 nm, 20 mW laser diode (Lasermate Group, Inc., Pomona, CA) in a laser diode mount LDM 4412 (ILX Lightwave Bozeman, MT) was operated with an ILX Lightwave LDC-3722 laser diode controller (20°C; 60 mA). The photomultiplier tube voltage was set at 730 V. A USB-9215 data acquisition card with 16-bit resolution (National Instruments, Austin, TX) was used to relay the detector output to a PC.

4.2.3 *Capillary columns and chromatography*

The columns were prepared by placing an 18.5 mm section of 175 μm ID x 1/16" OD PEEK tubing (Upchurch Scientific) into stainless steel external column end fittings (Valco Instrument Co. Inc., Houston, TX) including 0.5 μm frits (Upchurch Scientific). Slurries of beads were prepared at 3 mg/mL and packed into the columns by vacuum. During operation, columns were maintained at 6-8 °C with ice water pumped through a copper coil. For all experiments the flow rate was 2.0 μL/min and samples were centrifuged at 10,000*g* for 1 minute before injection.

4.2.4 *Software*

LabVIEW 7.1 (National Instruments) programs were used to control step-gradients and acquire the chromatograms.

4.2.5 Antibody biotinylation

The polyclonal anti-PTH antibody was biotinylated using a 50-fold molar excess of Sulfo-NHS-LC-Biotin by rotating 1 hour at room temperature. The monoclonal anti-PTH was reacted with a 35-fold molar excess of Sulfo-NHS-LC-Biotin and the solution was mixed by rotation for 30 minutes at room temperature, followed by 30 minutes at 4 °C. Biotinlyated antibodies were purified with 0.5 mL Zeba Desalt Spin Columns according to the manufacturer's instructions. The antibodies were desalted into sodium phosphate buffer (pH 7.2; 10 mM) and the antibody concentration was measured at A_{280nm} (NanoDrop ND-1000, NanoDrop Technologies, Wilmington, DE). An EZ Biotin Quantitation Kit was used according to the manufacturer's instructions with a BioTek Synergy 2 microplate reader (BioTek Instruments, Inc., Winooski, VT). The biotin:anti-PTH molar ratio for the monoclonal antibody was determined to be 2.4 ± 0.2 (n = 6).

4.2.6 Stationary phase preparation

Streptavidin-coated silica beads were washed three times with sodium phosphate buffer (pH 7.2; 10 mM) by centrifuging at 1200x*g* for 5 minutes at 7 °C. The supernatant was discarded in between wash steps. A 20-fold excess of biotin-anti-PTH (polyclonal) was reacted with 5.01 µm streptavidin-coated silica beads in 0.5 mL of phosphate buffer and rotated 15 hours at 4 °C. For the biotin-monoclonal anti-PTH, 10-fold excess was reacted with 4.82 µm streptavidin-coated silica beads in 0.5 mL of phosphate buffer and rotated 19.5 hours at 4 °C. All beads were washed 3 times and reacted with 15 ng/mL biotin (polyclonal ant-PTH) or 47 ng/mL biotin (monoclonal anti-

PTH) at 4 °C for 1 or 0.5 hours, respectively. The beads were then washed 5 times and stored in sodium phosphate buffer (pH 7.2; 10 mM) at 4 °C. Clumping of the beads in solution was observed for the monoclonal antibody (sandwich assay).

4.2.7   *Direct capture/labeling and analysis of samples*

Pooled human serum was filtered through 30 kDa MWCO devices and diluted 1:10 in phosphate buffered saline (pH 7.4; 10 mM phosphate, 2.7 mM potassium chloride, and 137 mM sodium chloride) (PBS). PTH 1-84 was spiked into the diluted serum at 4 µg/mL and labeled by adding 1:1 400 µg/mL of Alexa Fluor 647 dye in PBS. The reactions were gently vortexed 1.5 hours at room temperature. Control serum (no PTH) and the PTH sample were injected in a phosphate buffer (pH 7.0, 100 mM, 0.01 % Brij-35)) for Pump A and sodium thiocyanate (2.5 M, 0.01% Brij-35) for Pump B. Pump A was held at 98.75% for 5.5 minutes before changing to 98.75% Pump B over 12 seconds and held for 2 minutes before returning to the phosphate buffer.

4.2.8   *Investigation of parathyroid hormone and matrix binding*

Rabbit anti-goat 5.01 µm silica beads were prepared adding a 10-fold excess of biotinylated antibody and reacting 15 hours at 4 °C. The beads were washed as described in section 2.6. This column was used to evaluate the binding of the fluorescent dye, serum control, and labeled PTH to a non-PTH antibody column (control column). A neat PTH solution was reacted with 50 µg/mL of Alexa Fluor 647 by rotation at 1.5 hours and room temperature. The PTH concentration was 1 µg/mL in PBS and was also injected on

the polyclonal anti-pth column. A dye control was prepared in PBS at 50 µg/mL and blank human serum (30 kDa MWCO, 1:10 in PBS) was reacted with 200 µg/mL of the dye. The mobile phase was the same as in section 2.7, but the sodium thiocyanate buffer was held at 2.5 minutes during the elution step.

4.2.9 Sandwich immunoassays

4.2.9.1 Antibody labeling

Anti-PTH (N-terminus) was labeled with a 45-fold molar excess of Alexa Fluor 647 dye in PBS (pH 7.9 with 100 mM sodium bicarbonate) by rotation at room temperature for 1.25 hours. The mixture was desalted into PBS and measured at A_{280nm} and A_{650nm} to determine the degree of labeling (NanoDrop ND-1000). The molar ratio of dye to antibody was determined to be 10.3 ± 0.2 (n = 6). The detection antibody was diluted to 412 µg/mL in PBS containing 0.1 % bovine serum albumin (BSA) and stored at -20 °C until use.

4.2.9.2 Conditions

Samples were injected and allowed to pump through the column before a sequential injection of detection antibody was made. Initial conditions employed PBS/0.1% BSA in Pump A and glycine-HCl (200 mM pH 2.0) in Pump B. After sample injection Pump A was held at 98.75% for 5 minutes before 10 µg/mL of detection antibody was injected. The PBS buffer was pumped through the system for 4 minutes and changed to 98.75% B over 1 minute. The elution step was held for 2 minutes before

returning back to pump A. A 2.5 M sodium thiocyanate buffer as Pump B and detection antibody concentrations of 25 and 100 µg/mL were also attempted. Parathyroid concentrations of 5 ng/mL, 40 ng/mL, and 1 µg/mL in PBS/0.1% BSA were injected during development.

4.3 Results and Discussion

4.3.1 *Direct capture immunoaffinity results*

PTH in serum was eluted from the immunoaffinity column after direct labeling in 1:10 human serum and Figure 20 shows an overlay of blank serum and PTH at 4 µg/mL. A peak for PTH was observed at approximately 7.5 minutes; however, a peak was also observed from diluted serum not spiked with PTH. The blank serum peak response was approximately half of the PTH peak response. Matrix components were labeled by the reactive dye in the same way that PTH was labeled, i.e., via primary amine groups. Nonspecific binding of some matrix components was strong enough to remain on the column until the elution buffer was applied.
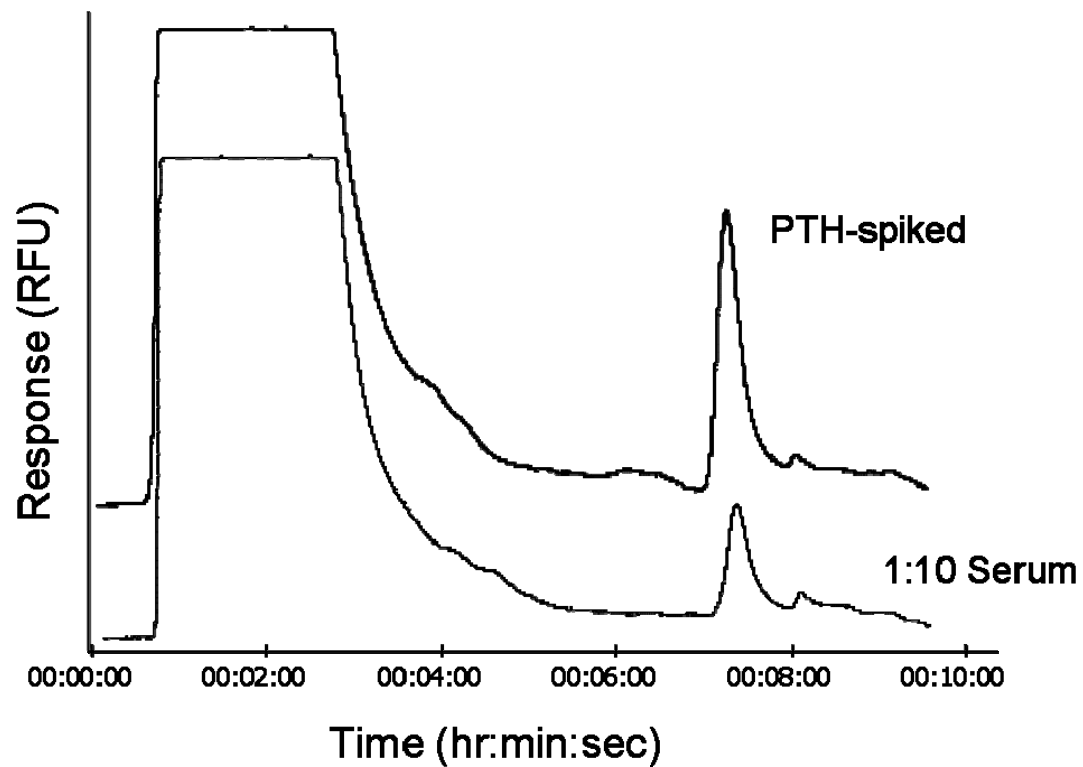
Figure 20: Parathyroid hormone in human serum by direct labeling/direct capture immunoaffinity chromatography. RFU = relative fluorescence units.

4.3.2 Parathyroid hormone binding

The reaction mixtures of Alexa Fluor 647 dye, dye/serum, and dye/PTH were allowed to sit at 4 °C overnight before collecting chromatograms on the non-PTH antibody control column. Initial injections of the dye resulted in several large peaks across the entire chromatographic window. The dye was still reactive after 1.5 hours of mixing and was likely binding to primary amine groups on immobilized antibodies. In order to achieve consistent dye labeling of unknown concentrations an excess of reactive dye was necessary. The excess dye was no longer active after allowing the reaction mixtures to incubate overnight. However, long waiting times are not ideal for point-of-care type applications. Practical use of the direct labeling approach would require stopping the reaction rapidly after antigen labeling. A discussion of strategies to improve the limitations associated with the reactive nature of the dye is included in Section 4.3.3.

The average peak response for each condition on the control column, along with the response of PTH on the anti-PTH column is shown in Figure 21. The peak response for 1 µg/mL PTH on the anti-PTH column was 3.9 RFU ± 0.1 (standard deviation) compared to 0.38 RFU ± 0.08 on the control column. Although PTH did bind nonspecifically to the control column, the binding to the anti-PTH column was approximately 11 times greater, indicating antibody binding. The average serum peak response was 0.15 relative fluorescence units (RFU) ± 0.02; however, this represents a 1:10 dilution.
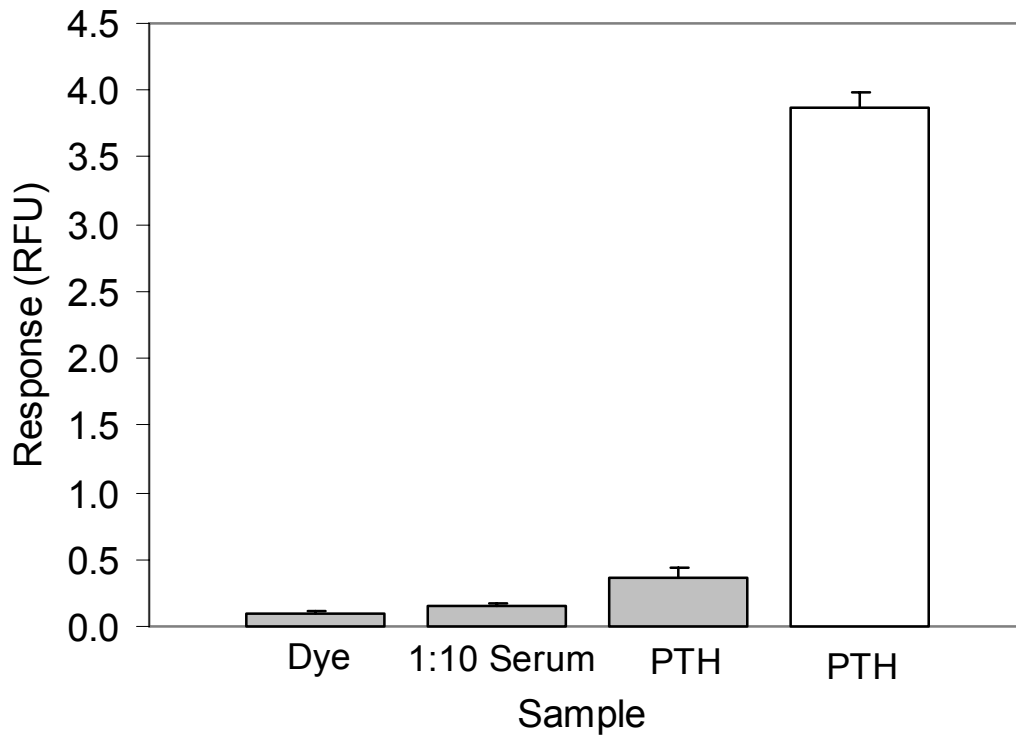
Figure 21: Peak response during elution step for Alexa Fluor 647 dye, diluted serum, and parathyroid hormone after fluorescent labeling. The shaded bars and white bar represent response on the control and anti-PTH columns, respectively. Each bar represents the average response (n = 3) + standard deviation. RFU = relative fluorescence units.

4.3.3 Limitations and strategies for parathyroid hormone direct capture immunoaffinity

Based on the experimental results, a direct capture immunoaffinity assay for PTH in human serum would not be practical with the current system. Although the technique was able to capture PTH from solution through antibody binding, the presence of human serum resulted in large amounts of nonspecific binding in the system (Figure 20). The nonspecific binding of labeled matrix components would prohibit measuring concentrations for normal PTH values (low picomolar).

The advantages of the direct labeling/direct capture technique include simplicity and potential speed of the assay. In order to use the direct capture immunoassay for PTH, the limitations presented in this study would need to be addressed. One of the key limitations observed was the reactive nature of the fluorescent dye. The dye contains an NHS reactive group that allows conjugation to compounds through primary amine groups. The dye is added to samples in an excess of expected antigen and primary amine-containing matrix components. Therefore, reactive dye may remain during the injection of samples and bind to immobilized antibodies in the column. A potential solution to excess reactive dye includes adding a stopping reagent with enough primary amine content to bind all reactive dye. A second solution would be to remove reactive dye by passing samples through a desalting column. The latter strategy would require that the antigen be large enough to pass through column faster than the dye. Each strategy would require extra sample processing steps, adding to the analysis time.

A second limitation related to the reactive dye involves the use of biological matrices such as human serum. During the labeling of PTH the reactive fluorescent dye

will also bind to endogenous proteins and other compounds that have a primary amine group. The matrix is then labeled and will give a nonspecific response if binding to the column occurs. A simple solution is to dilute the matrix prior to reacting with the dye and concentrating the sample online with the immunoaffinity column. The dilution factor must be taken into account when reporting the calibration range and in the case of PTH, the assay requires low picomolar levels. A 1:10 dilution of the matrix was applied and still demonstrated significant nonspecific binding. Larger injection volumes may be used to increase the PTH signal, but the nonspecific background may also increase proportionally. Another strategy to lower nonspecific matrix binding is to remove the large proteins from serum using MWCO filters. In the current research, 30 kDa MWCO filters were used for human serum before the labeling reaction. This strategy was appropriate for PTH since the molecular weight is 9424.5 (Bachem data sheet). This technique could only be used for compounds with a molecular weight below the cutoff filter. A chart of total protein content versus the range of MWCO filter is shown in Figure 22. The protein amount was calculated by measuring the absorbance at 260 and 280 nm using a NanoDrop ND-1000. The concentration in mg/mL was obtained by the formula $(1.55 \times A_{280nm}) - (0.76 \times A_{260nm})$ (Phillips and Dickens 2000). Figure 22 shows that greater than 2 mg/mL of total protein still remained for all filters used. The devices require centrifugation to remove matrix proteins and may add up to 30 minutes to the time of analysis. Additionally, the recovery of PTH or any antigen needs to be assessed before using the cutoff devices for sample preparation.
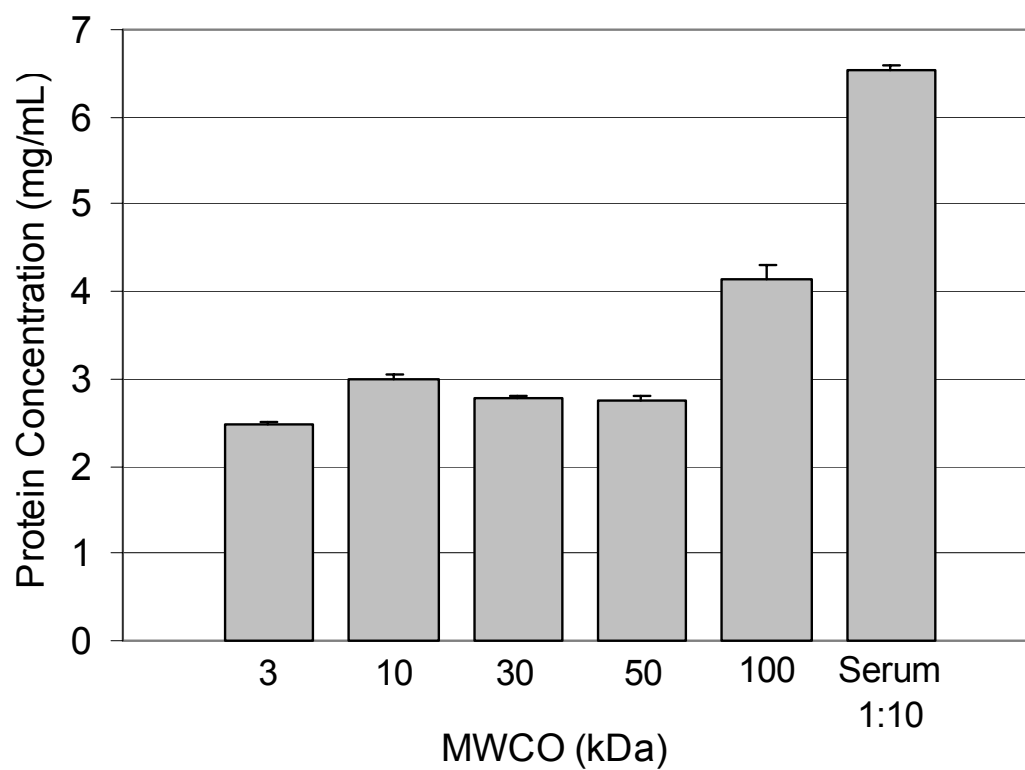
Figure 22: Total protein content of human serum after filtration with molecular weight cutoff devices. Each bar represents the average protein amount (n = 5) + one standard deviation.

Mobile phase additives, such as detergents or blocking agents may also be used to lower nonspecific binding. In the current microfluidic system, these reagents can lead to bubble formation in the syringes and mixer, causing spikes in the baseline. The affect of Brij-35 (a detergent) on PTH binding is shown in Figure 23. The addition of Brij-35 resulted in an increased PTH response at the concentrations tested, while the nonspecific binding remained present. The increased PTH response may be due to an improved antibody-antigen binding environment when detergents are added to the mobile phase (Wood 1993). For human plasma samples, the presence of Brij-35 allowed for an increased number of injections before adverse back pressure was observed. The detergent may help to keep matrix proteins from clogging the column frits and therefore extend the column lifetime.

A summary schematic of the direct capture approach is shown in Figure 24. The matrix components that bind to the immunoaffinity column will give a response during the elution of antigens if both are labeled. The reduction of nonspecific binding was discussed in Section 1.3.3 of Chapter 1.

4.3.4 Parathyroid sandwich immunoassay

A dual antibody sandwich assay was performed in an attempt to detect PTH in the presence of serum matrix compounds. The design of the sandwich assay and proposed matrix binding is shown in Figure 25. The measured response results from the dye-labeled detection antibody and is proportional to antigen binding. Nonspecific binding of matrix components will not give a measurable response.
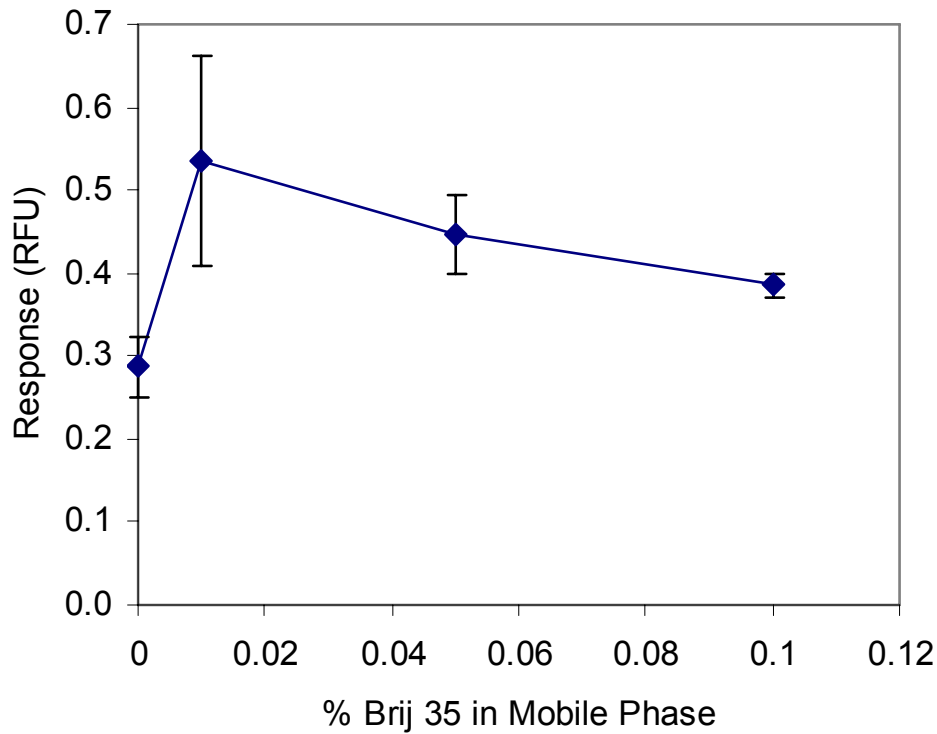
Figure 23: Percentage of Brij-35 in mobile phase A (100 mM phosphate, pH 7.0) and mobile phase B (2.5 M sodium thiocyanate). Each point represents the average peak response (n = 3 ± standard deviation) of parathyroid hormone at 1 µg/mL in PBS.
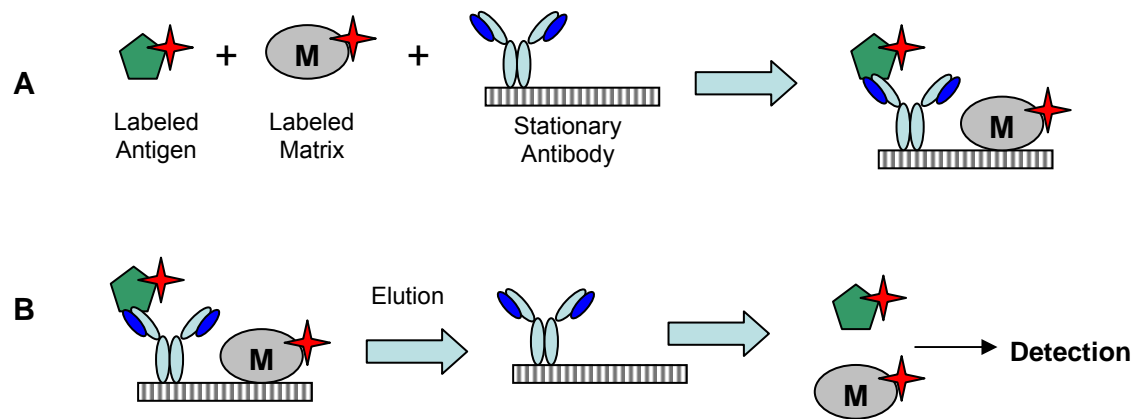
Figure 24: Proposed binding and detection of matrix components in the direct capture approach. In A, the antigen and labeled matrix components bind to the antibody and nonspecific sites, respectively. In B, both are eluted simultaneously for detection.
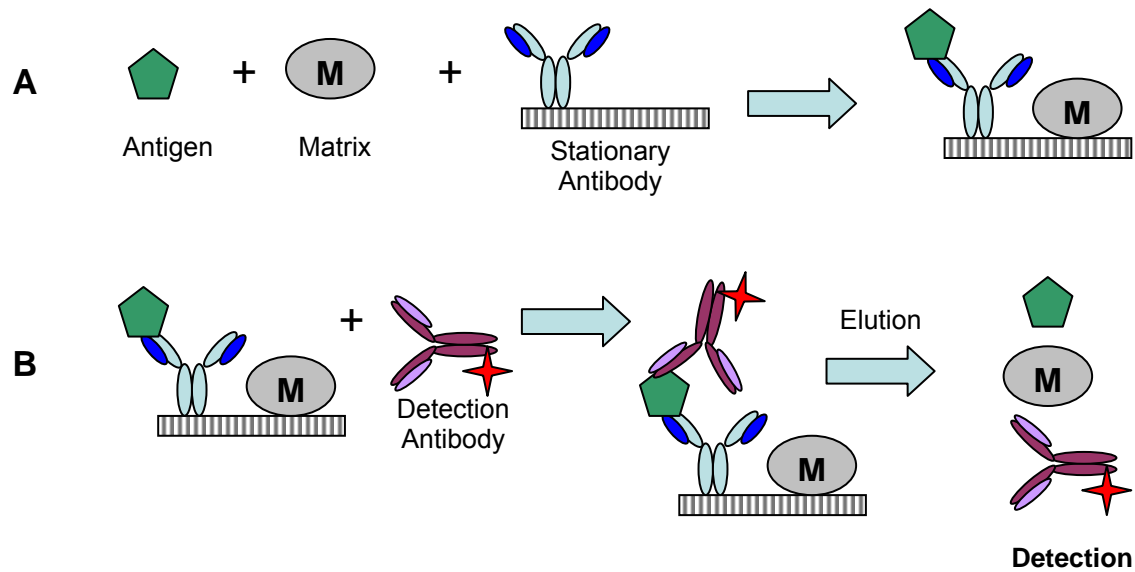
Figure 25: Proposed binding of sample antigen and matrix components in a sandwich immunoaffinity separation. In A, the antigen and matrix components bind but are not labeled. In B, a labeled detection antibody is introduced and measured during the elution step.

Positive formation of a sandwich complex with PTH was not observed under any of the development conditions in experimental section 2.9.2. Example chromatograms of blank and PTH for the sandwich immunoassay are shown in Figure 26. The successful formation of an antibody-PTH-antibody sandwich relies on the recognition of two distinct epitopes. The capture antibody recognized aa 53-84 and the detection antibody recognized aa 1-34. The PTH peptide was supplied at 92% purity and some amino acid content was partially destroyed during purification, as noted on the product data sheet. An incomplete or damaged amino acid sequence near one of the epitopes could have potentially prevented the sandwich complex formation. Another possibility is the general lack of quality reagents for development of a sandwich immunoassay for PTH. The pair of antibodies used in the current research was supplied from a manufacturer (QED Bioscience) that did not provide or specify an available matched antigen. The development of a sandwich immunoassay for PTH using the current bead-based system would require testing all available sources of antibodies with intact PTH (aa 1-84). The purchase of PTH reagents for screening matched antibody pairs is highly cost prohibitive versus other available clinical biomarkers. Quantities of 100 µg of PTH or anti-PTH cost greater than $300 for identified manufacturers.
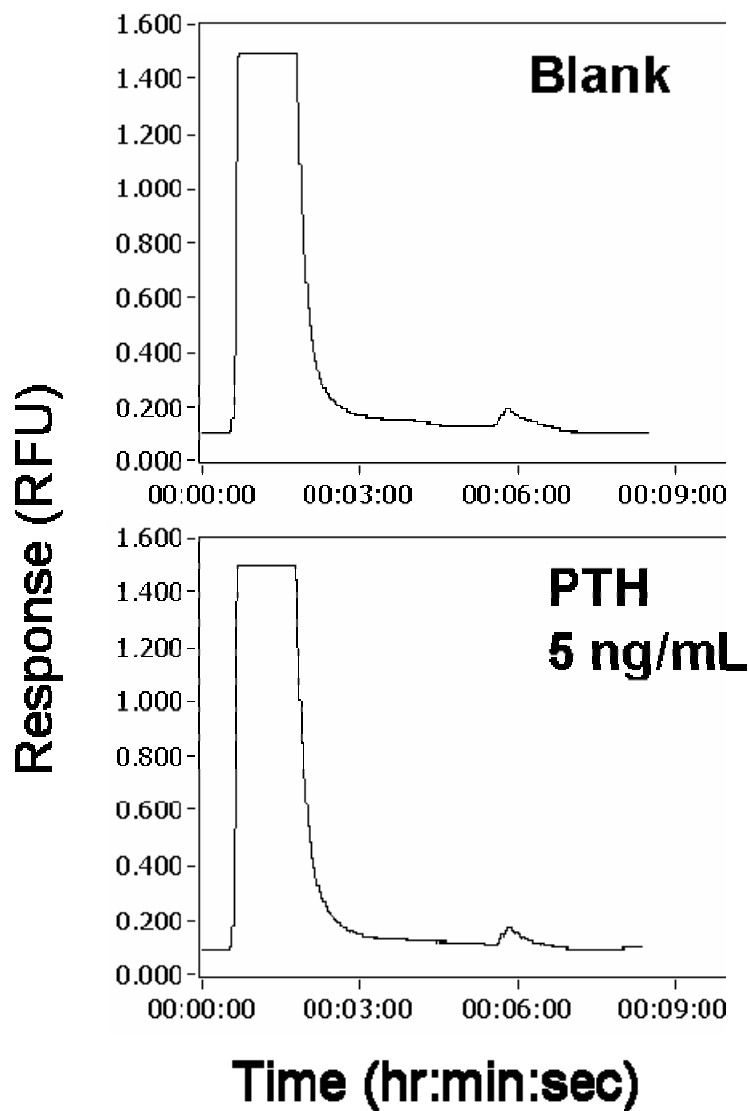
Figure 26: Sandwich immunoassay chromatograms of parathyroid hormone. Eluted peak response is at approximately 6 minutes. The mobile phase was PBS/0.1 % BSA in Pump A and glycine-HCl (200 mM; pH 2.0) in Pump B. The detection antibody concentration was 10 µg/mL.

4.4 Conclusions

A direct capture immunoaffinity separation of parathyroid hormone was initially successful in neat solutions, but suffered from nonspecific binding of labeled matrix compounds. A two antibody sandwich assay was attempted to overcome limitations of the direct labeling approach. The formation of PTH sandwiches with stationary phase and detection antibodies was not observed. An incomplete amino acid sequence for the peptide or lack of quality matched antibodies was assigned as the cause. The direct capture assay demonstrated that it was possible to immobilize an active antibody to PTH. The dual antibody approach required that PTH be present intact as the 84 amino acid peptide.   The detection antibody may not have been able to bind with the corresponding epitope due to the degree of Alexa Fluor 647 labeling. There were 10.3 ± 0.2 (n = 6) moles of dye per mole of antibody, which may have limited or interfered with antigen recognition. Additionally, any degradation of the intact PTH in solution would have prevented detection antibody binding. Truncated fragments of PTH would have been able to bind in the direct capture assay, which used a polyclonal antibody. Polyclonal antibodies could be used for the sandwich immunoassays as well, but would still need to recognize epitopes at opposite ends of the PTH peptide.

Established matched antibodies and purified antigen for sandwich immunoassays of C-reactive protein were available from Fitzgerald Industries, Inc. (Concord, MA). Sufficient quantities of the reagents were purchased previously and will be used to develop an immunoaffinity sandwich assay in biological matrices.

CHAPTER 5 A Microfluidic Capillary System for Immunoaffinity Separations of C-Reactive Protein in Human Serum and Cerebrospinal Fluid

Drawn from manuscript published in Analytical Chemistry- Article in Press

5.1 Introduction

Microfluidics and miniaturized analytical instrumentation result in fast analysis times, low consumption of reagents and sample volumes, and potential portability due to the small footprint of the equipment (Bange, Halsall et al. 2005; Whitesides 2006). The use of immunoaffinity separation mechanisms in microfluidic devices allows for the isolation of analytes from complex biological matrices based on the very selective nature of antibody-antigen reactions (Phillips and Smith 2002; Peoples and Karnes 2008). Employing capillaries or microchannels for immunoaffinity reactions results in reduced diffusion distances and a greater binding surface area to solution volume ratio (Sato, Tokeshi et al. 2000). Therefore, antibody-antigen reactions take place much faster in microfluidic systems versus conventional immunoassay platforms. The use of beads as solid phases further increases the reactive surface area and makes preconcentration of sample antigens possible (Verpoorte 2003; Lim and Zhang 2007). Analytes are bound and released in immunoaffinity chromatography rather than partitioning through the column and resolution is controlled by the elution gradient conditions (Erxleben and

119

Ruzicka 2005). The column dimensions can be readily miniaturized provided the binding capacity is adequate.

C-reactive protein (CRP) is a 115 kDa pentameric protein and acute phase reactant recognized as a biomarker of inflammation (Volanakis 2001; Wang, Wu et al. 2002; Meyer, Hartmann et al. 2007). CRP measured in human plasma or serum has been suggested as an indicator of cardiovascular disease (CVD) risk (Ledue and Rifai 2003; Myers, Rifai et al. 2004). Three categories have been defined for CVD risk assessment corresponding to CRP concentrations of < 1 µg/mL (low), 1 to 3 µg/mL (average), and > 3 µg/mL (high), with concentrations above 10 µg/mL indicating other causes of inflammation or infection (Ledue and Rifai 2003). CRP in human cerebrospinal fluid (CSF) in combination with serum measurements has been studied for monitoring severe head injury patients (Is, Coskun et al. 2007) and diagnosing shunt infections (Schuhmann, Ostrowski et al. 2005). Elevated levels of CSF CRP have also been observed in patients with meningitis and may aid in diagnosis of bacterial versus aseptic meningitis (Virji, Diven et al. 1985; Kanoh and Ohtani 1997; Rajs, Finzi-Yeheskel et al. 2002). Bacterial cultures of CSF can take as long as 24 hours to obtain results (Virji, Diven et al. 1985; Schuhmann, Ostrowski et al. 2005) and thus rapid testing of a relevant biomarker such as CRP may aid in preliminary diagnosis. The loss of CSF after patient sampling may be associated with adverse events including headaches (Grant, Condon et al. 1991; Mokri 2000; Turnbull and Shepherd 2003); therefore, assays of CSF with minimal sample volume requirements are potentially advantageous to patient welfare.

Additionally, CRP is commonly used to demonstrate the performance and utility of new miniaturized instrumentation (Shin, Lee et al. 2007).

Nephelometric and turbidimetric immunoassays are often used for the analysis of CRP in clinical laboratories (Kriz, Ibraimi et al. 2005; Bhattacharyya and Klapperich 2007). These assays are performed on automated but large clinical analyzers (Kriz, Ibraimi et al. 2005), with quantification limits of 3 to 8 µg/mL (Roberts, Moulton et al. 2001). Additionaly, the procedures are time consuming and not well suited for point-of-care type applications (Bhattacharyya and Klapperich 2007). Commercially available enzyme-linked immunosorbent assays (ELISA) are available for CRP and demonstrate adequate sensitivity for clinically relevant concentrations (Christodoulides, Mohanty et al. 2005; Meyer, Hartmann et al. 2006). The ELISA method offers high throughput due to parallel sample processing (Johns, Rosengarten et al. 1996); however, the technique also involves laborious wash steps (Tsai, Hsu et al. 2007) and can take several hours to complete (Meyer, Hartmann et al. 2006; Bhattacharyya and Klapperich 2007)

Microfluidic and small-scale immunoassay-based separations of CRP have been reported in various matrices. Most of the assay platforms have been in the form of microchips. CRP was separated from human serum with an affinity solid phase of phosphocholine in microchannels (Roper, Frisk et al. 2006), although a second step involving capillary electrophoresis-UV absorption detection was necessary for measurement. Competitive immunoassays in buffer (Shin, Lee et al. 2007) and sandwich immunoassays in human serum (Wolf, Juncker et al. 2004) have been demonstrated in microchips with fluorescent detection. Microchips for CRP immunoassays in human

serum have also been reported with dendritic amplification of the fluorescent signal (Hosokawa, Omata et al. 2007) and chemiluminescent detection (Bhattacharyya and Klapperich 2007) techniques. CRP in human saliva was detected by a fluorescence bead-based sandwich immunoassay on a microchip array (Christodoulides, Mohanty et al. 2005). The high sensitivity of the assay allowed for a 1000-fold dilution of samples and reduced viscosity-related matrix effects. Antibodies immobilized to magnetic nanoparticles or beads have been applied to detect CRP in 20 µL of human whole blood (Kriz, Ibraimi et al. 2005) or 500 µL of serum, saliva, and urine (Meyer, Hartmann et al. 2007).

We have previously described a microfluidic direct capture/direct labeling technique as a proof-of-concept immunoaffinity separation (Peoples, Phillips et al.). In the current work, sandwich immunoassays are presented in a microfluidic capillary as effective and simple alternatives to microfluidic chip platforms. The analysis of CRP is demonstrated in both human serum and CSF matrices, with dilution of serum as the only sample preparation. The miniaturized format is based on immunoaffinity chromatography and allows for highly-controlled fluid and reagent delivery without manual wash steps or excessive manipulation. This is the first known report of CSF CRP measurement in a microfluidic system. CSF is more difficult to obtain versus serum; however, the small sample volume requirement of the current approach (approximately 8 µL per sample) permits the use of CSF as a calibration matrix.

5.2 Experimental section

5.2.1 Reagents and materials

Monoclonal mouse anti-CRP clones M7111422 (stationary phase) and M701289 (detection), highly pure CRP (>95%), and CRP-free serum (affinity purified, pooled normal human serum) were purchased from Fitzgerald Industries International, Inc. (Concord, MA). Normal human serum and CSF (pooled/mixed gender) were obtained from BioChemed Services (Winchester, VA). Sulfosuccinimidyl-6-(biotin-amido) hexanoate (Sulfo-NHS-LC-Biotin), EZ Biotin Quantitation Kit, and 0.5 mL Zeba Desalt Spin Columns were purchased from Pierce Biotechnology (Rockford, IL). Alexa Fluor 647 carboxylic acid, succinimidyl ester (λ_{ex} = 650 nm, λ_{em} = 668 nm) was obtained from Invitrogen (Carlsbad, CA). Streptavidin-coated 4.82 µm silica beads were purchased from Bangs Laboratories, Inc. (Fishers, IN). SeraSub, a simulated serum matrix, was obtained from CST Technologies (Great Neck, NY). A Barnstead Nanopure Diamond (Dubuque, IW) system was used to prepare purified water. All remaining chemicals and reagents were obtained from Sigma (St. Louis, MO). Buffer solutions were filtered through 0.22 µm PVDF Durapore (13 mm syringe filters) (Millipore, Billerica, MA) prior to use. All polyetheretherketone (PEEK) tubing and connectors were purchased from Upchurch Scientific (Oak Harbor, WA).

5.2.2 Apparatus- pumping, mixing, injecting

A pump-based device for capillary immunoaffinity chromatography was constructed and described previously (Peoples, Phillips et al. 2007). Dual microliter

OEM syringe pumps (Harvard Apparatus, Inc., Holliston, MA) containing glass gastight 1700 series syringes (Hamilton, Reno, NV) were mounted in an acrylic cabinet enclosure. Each syringe was connected to a microfluidic mixing chip (NanoMixer, Upchurch Scientific) via a section of PEEK capillary tubing (360 µm outer diameter (OD)). The low pressure configuration was used, requiring 30 nL of mixing volume in the branching channels. The mixing chip was linked to a Microinjector (Upchurch Scientific) where samples were introduced via a 5 µL syringe. An injection loop of 250 nL was prepared from PEEK capillary tubing (50 µm internal diameter (ID)). PEEK capillary tubing was used for all fluidic connections pre-column.

5.2.3 Apparatus- capillary columns

PEEK tubing was used to make the column body by cutting to a desired length. An 18.5 mm long column was prepared from tubing with dimensions of 175 µm ID x 1/16" OD. Stainless steel 0.5 µm frits (Upchurch Scientific) were placed into stainless steel external column end fittings (Valco Instrument Co. Inc., Houston, TX) and wrench-tightened onto the column. The column was connected to a vacuum pump and negative pressure was applied to pull slurries of stationary phase through an open end of the tubing. The open end was sealed with a frit-containing end fitting and stored at 4 °C until use. During operation, the column was maintained at 6-8 °C by a pumping ice water through a copper column jacket.

5.2.4 Detection and software

A 650 nm, 20 mW laser diode (Lasermate Group, Inc., Pomona, CA), was placed in an ILX Lightwave laser diode mount LDM 4412 (Bozeman, MT) with collimating lens and controlled by an ILX Lightwave LDC-3722 laser diode controller. A fiber optic was attached from the diode laser to a Zetalif laser-induced fluorescence detector (Picometrics, Ramonville, France) with a Hamamatsu R928 photomultiplier tube (Bridgeport, NJ). The flow cell was made by burning a 2 mm section of polyimide coating from 360 μm OD by 50 μm ID square fused-silica capillary tubing (Polymicro Technologies, Phoenix, AZ). The laser diode was maintained at 20°C and 60 mA, and the PMT voltage was set at 730 V. During operation, the capillary column was placed between the injector and flow cell. The detector was connected to a computer using a National Instruments (Austin, TX) USB-9215 data acquisition card with 16-bit resolution. LabVIEW 7.0 (National Instruments) was used to write a run program for control of syringe pump step-gradients and an analysis program to process chromatograms. Calibration modeling of immunoassay data was performed with SigmaPlot 10.0 (Systat software Inc., San Jose, CA).

5.2.5 Immunoaffinity materials preparation

5.2.5.1 Biotinylation of capture antibody

Monoclonal mouse anti-CRP clone M7111422 was biotinylated using a 32-fold molar excess of Sulfo-NHS-LC-Biotin in a solution of sodium phosphate buffer (10 mM, pH 7.2). The reaction was performed on a rotator for 30 minutes at both room

temperature and at 4 °C. Zeba Desalt Spin Columns were used according to the manufacturer's instructions to remove excess biotin and unreacted material. A NanoDrop ND-1000 spectrophotometer (NanoDrop Technologies, Wilmington, DE) was used to measure the antibody concentration at A_{280nm}. An EZ Biotin Quantitation Kit was used according to the manufacturer's instructions with a BioTek Synergy 2 microplate reader (BioTek Instruments, Inc., Winooski, VT); the molar ratio of biotin:anti-CRP was determined to be 2.7 ± 0.2 (n = 3).

5.2.5.2. Preparation of stationary phase

A 7-fold potential excess of biotin-anti-CRP was added to 1.5 mg of 4.82 μm streptavidin-coated silica beads in phosphate buffer (10 mM, pH 7.2) and mixed by rotation at 4 °C overnight (22.5 hours). The beads were centrifuged 3 times (1200g, 5 minutes, 7 °C) to wash and the supernatant was discarded after each step. The beads were then reconstituted to 0.5 mL with 70 ng/mL biotin in phosphate buffer (10 mM, pH 7.2) and rotated for 1 hour at 4 °C to block any remaining biotin receptors. The beads were washed 5 times as before and stored at 4 °C until use. The antibody-coated beads were brought to a final concentration of 3 mg/mL for column packing.

5.2.5.3. Fluorescent labeling of detection antibody

Monoclonal mouse anti-CRP clone M701289 was reacted with a 26-fold molar excess of Alexa Fluor 647 dye by rotating 1 hour at room temperature, followed by 30 minutes at 4 °C. The reaction solution was phosphate buffered saline (10 mM phosphate,

2.7 mM potassium chloride, 137 mM sodium chloride, pH 7.4) (PBS) and excess dye was removed by desalting spin columns. Absorbance readings at 280 nm and 650 nm were measured on a NanoDrop ND-1000 spectrophotometer and the extent of labeling was calculated according to the dye manufacturer's instructions. The molar ratio of dye:antibody was determined to be 3.5 ± 0.1 (n = 6). The detection antibody was brought to a concentration of 575 µg/mL in Dulbecco's PBS (DPBS) containing 0.1 % bovine serum albumin (BSA) and aliquots were stored at -20 °C until use. DPBS contains calcium chloride dihydrate (0.9 mM) and magnesium chloride hexahydrate (0.5 mM) and has a pH of 7.2.

5.2.5.4. Capillary sandwich immunoassay design

Each reactant of the assay was sequentially injected into the microfluidic system. The overall reaction scheme of the assay inside the capillary is illustrated in Figure 27. In step 1 a sample is injected onto the column and the immobilized antibodies capture CRP from solution. During this phase, all matrix components and nonretained material are washed to waste. In step 2 the detection antibody is injected and binds with the isolated CRP, forming the sandwich complex. In the third and final step, an acidic elution gradient is applied and the dissociated detection antibody is measured. The amount of detection antibody is directly proportional to the amount of CRP in the sample solution.
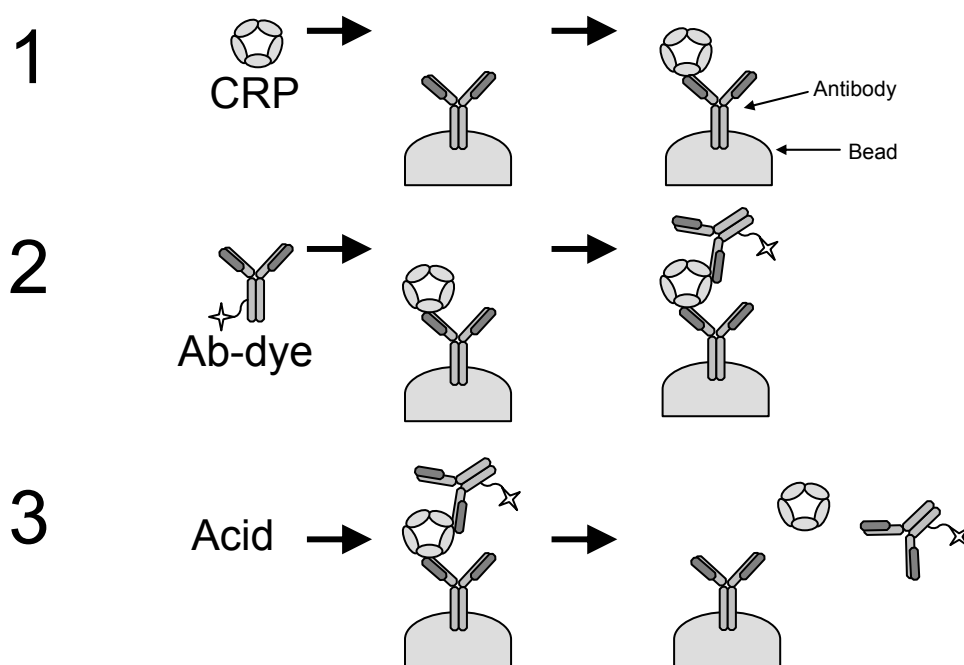
Figure 27:   Representation of sandwich immunoaffinity separation steps inside the capillary format. Ab-dye corresponds to the fluorescent-labeled detection antibody.

5.2.5.5. *Immunoaffinity Chromatography Conditions*

Pump A (application buffer) contained either Tris/CaCl$_2$ (50 mM Tris, 5 mM CaCl$_2$, pH 7.2) with 0.01% Brij-35 for human serum assays or DPBS for assays in CSF. Pump B (elution buffer) contained a glycine-HCl buffer (200 mM, pH 1.8) for all assays. The samples were injected and 98.75% Pump A was applied for 4 minutes before injection of the detector antibody. This step allowed extraneous matrix components to pump to waste. The detector antibody was injected and Pump A was applied for either 4.5 or 2.5 minutes for serum or CSF samples, respectively. Next the gradient was changed to 98.75 % Pump B over 24 seconds (serum samples) or 6 seconds (CSF samples) and held for 2 minutes to dissociate and elute the labeled antibody. The total runtimes for serum and CSF assays were approximately 12 and 10 minutes, respectively. The flow rate for all assays was programmed at 2.0 µL/min. A 5 µL syringe was used to make injections and only approximately 8 µL of sample was required to prime the injection system.

The 50 mM Tris/5 mM CaCl$_2$ buffer was originally selected for the plasma CRP assay because it gave a higher CRP response (1 µg/mL injections) versus DPBS or Tris with 2 mM CaCl$_2$. The use of greater than 5mM CaCl$_2$ in the mobile phase resulted in precipitation of salt in the syringes and therefore was not used as a practical consideration. Figure 28 shows the response 1 µg/mL of CRP in different mobile phases during development of the serum assay.
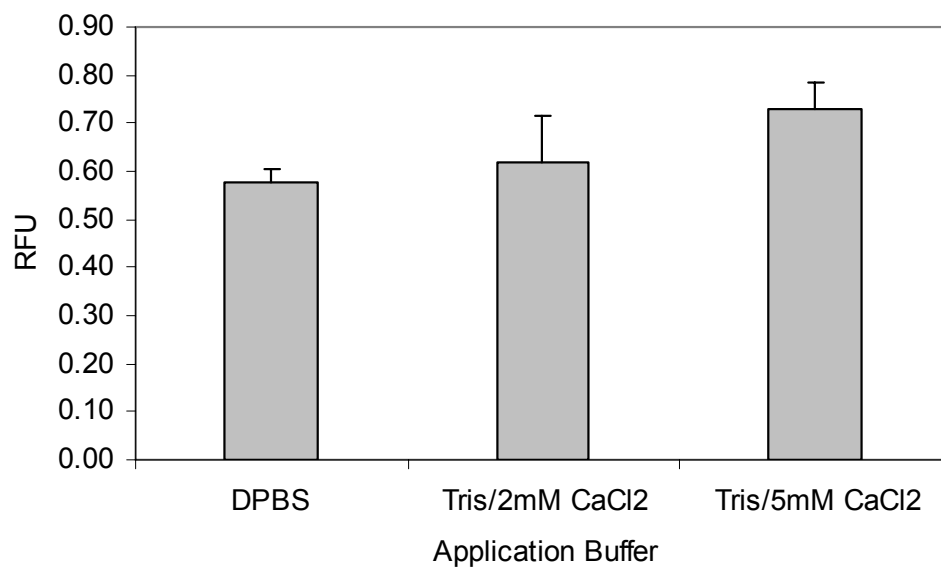
Figure 28: C-reactive protein response (n = 3) in different mobile phases. CRP was at 1 µg/mL in the mobile phase with 0.1% BSA. The detection antibody was 11.5 µg/mL in DPBS/0.1% BSA. The response is the average of three injections + the standard deviation. RFU = relative fluorescence units.

5.3 Results and discussion

5.3.1. Evaluation of detection antibody

CRP was prepared at 1 µg/mL in Tris/CaCl$_2$ /0.1% BSA and injected under the serum assay conditions, except no Brij-35 was present in the mobile phase. The detection antibody was injected (n = 3) at concentrations of 0.500, 1.00, 5.00, 11.5, 23.0, and 98.6 µg/mL in DPBS/0.1% BSA and these results are shown in Figure 29. At 23.0 and 98.6 µg/mL the error bars (± one standard deviation) become greatly increased relative to the lower concentrations. This could be the result of a steric effect in which detection antibody binding interferes with subsequent detection antibody binding at high antibody concentrations. Additionally, the runtimes must be increased at higher antibody concentrations to account for a lager unbound peak of excess labeled antibody in the chromatogram. For the reasons listed above and to conserve immunoreagents, a detection antibody concentration of 11.5 µg/mL was selected for all assays.

5.3.2 Matrix effects

The introduction of human serum caused clogging in the syringes and capillary tubing. Consequently, a minimum dilution factor of 1:10 was required for the injection of serum samples. The 1:10 diluted serum (in Tris/CaCl$_2$ /0.1% BSA) was compared to both neat solutions and 1:1 diluted simulated serum (SeraSub). CRP at 1 µg/mL was injected (n = 3) in each solution (Figure 30) and the 1:10 serum dilution had a response 73% and 64% of the neat and simulated serum solutions, respectively. Therefore, 1:10 diluted serum was used as the calibration matrix instead of a surrogate.
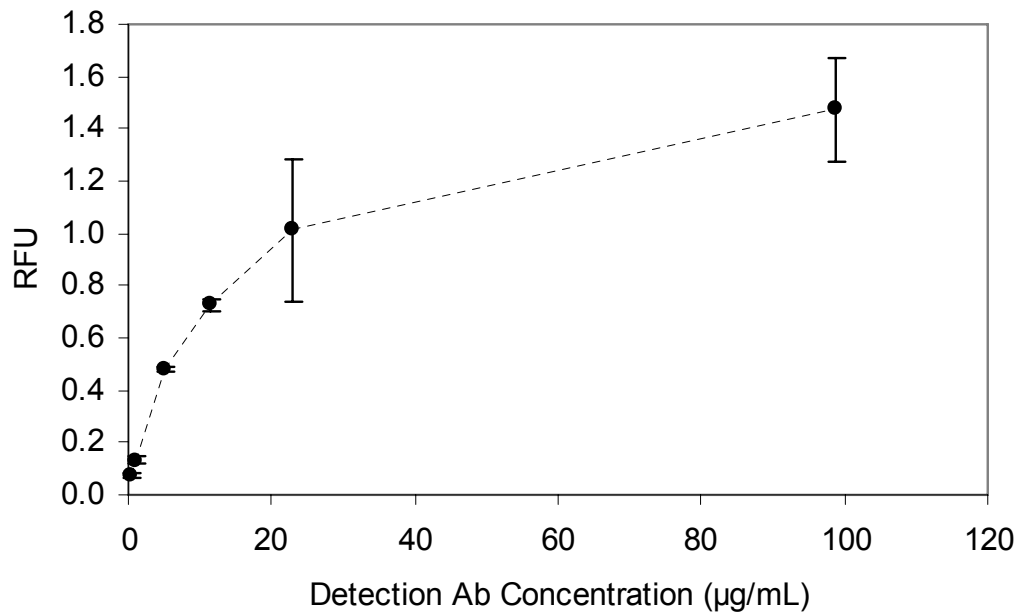
Figure 29:   Effect of increasing detection antibody concentration with C-reactive protein

fixed at 1 μg/mL. Response is the average of three injections ± the standard deviation.

RFU = relative fluorescence units.
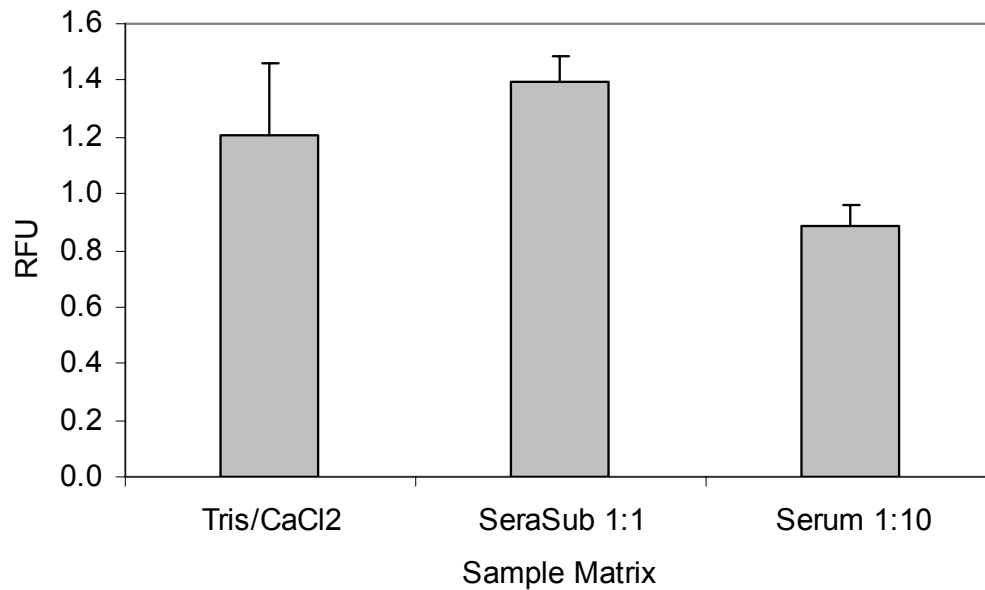
Figure 30: Comparison of C-reactive protein response (average of $n = 3$ + standard deviation) in surrogate matrices and human serum. RFU = relative fluorescence units.

The total protein content of 1:10 diluted human serum and 100 % CSF was determined by direct spectrophotometry at 260/280 nm using a NanoDrop ND-1000. The measured protein amount was 0.82 ± 0.03 mg/mL (n = 6) in pooled CSF matrix and 6.9 ± 0.2 mg/mL (n = 6) in pooled serum diluted 1:10. CSF could be injected at 100% with no adverse observations because of the low total protein content. CSF calibration standards were prepared in 100% matrix.

5.3.3. Immunoaffinity chromatography

Representative chromatograms produced by the capillary system are shown in Figure 31 with response in relative fluorescence units (RFU). The top chromatograms represent injections of blank 1:10 serum (a) and 100% CSF (c). The bottom chromatograms represent 1 µg/mL CRP in 1:10 serum (b) and 0.5 µg/mL CRP in CSF (d). In each, the first off-scale peak corresponds to excess detection antibody and the second peak represents CRP. The serum assay required a slightly longer hold time before the elution gradient due to occasional small peaks in the baseline.
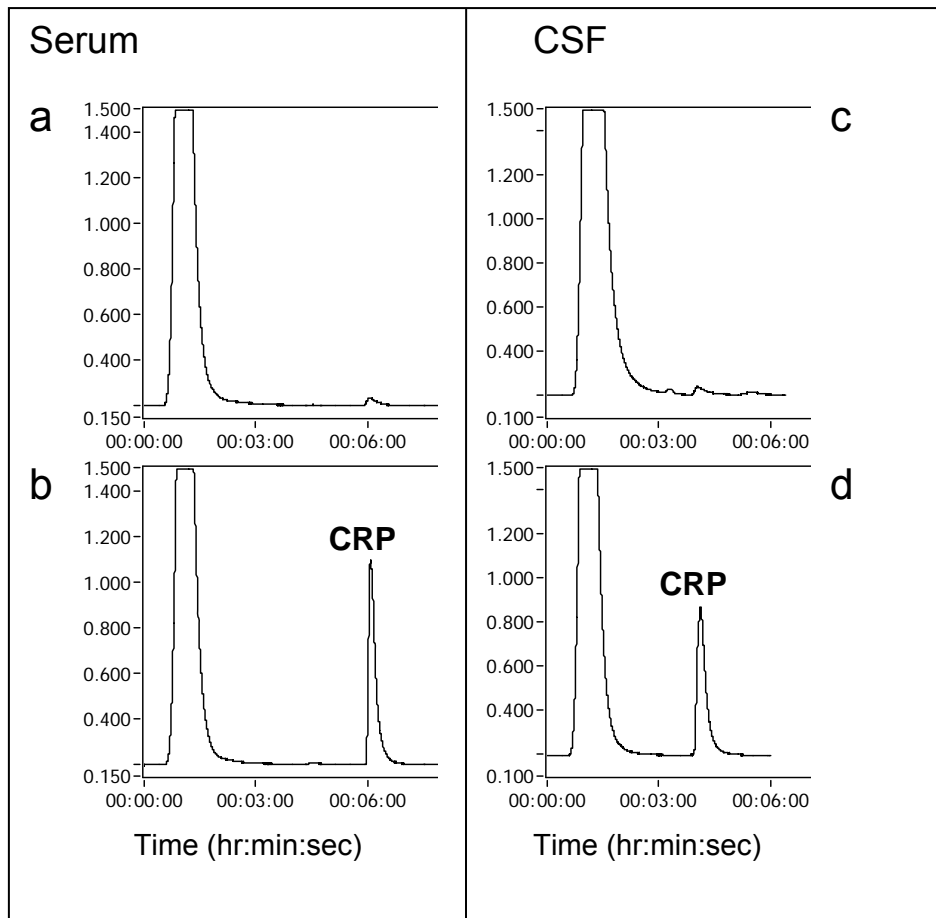
Figure 31: Representative immunoaffinity chromatograms of (a) blank 1:10 serum, (b) 1 µg/mL C-reactive protein in 1:10 serum, (c) blank CSF, and (d) 0.5 µg/mL C-reactive protein in CSF. The response units are in RFU (relative fluorescence units).

5.3.4. Calibration and assay performance

Calibration curves were constructed from triplicate injections of CRP-spiked solutions. The serum assay included CRP concentrations of 0.0540, 0.107, 0.322, 0.504, 1.02, and 3.00 µg/mL. CRP concentrations of 0.0100, 0.0750, 0.198, 0.509, 1.02, 4.98, and 29.5 µg/mL were used as CSF calibration standards. A nonlinear response was observed across the entire calibration range for both assays when plotting the data on a linear x-scale. A linear calibration fit would have required truncating data at the high concentrations and resulted in a limited range. Therefore, a nonlinear model was selected to describe the data. A 4 parameter logistic function (4-PL) was used to model the data and demonstrated an equation of $y = min + (max-min)/[1 + (x/EC50)^{Hillslope}]$. The model used a logarithmic x-axis scale and parameters to describe the minimum and maximum asymptotes (min and max), inflection point (EC50), and slope factor (Hillslope). The percent relative error (%RE) of each calibration point was plotted against the CRP concentration. The difference between back-calculated values and nominal values was divided by the nominal values and multiplied by 100% to give %RE (Findlay and Dillard 2007). The results of both assay calibrations are shown in Figure 32. The %RE data ranged from -1.6 to 2.2 for the serum assay and -7.4 to 5.5 for the CSF assay. The accuracy represented as % difference from the nominal value (%DFN) and precision represented as % relative standard deviation (%RSD) are shown for serum and CSF concentrations (n = 6) in Table 7. All values are less than 15.8%. The current recommended acceptance limits for accuracy and precision in ligand binding assays is ± 25% at the lower and upper limits of quantification and ± 20% at all other levels

(Viswanathan, Bansal et al. 2007). The concentration of CRP included in the calibration at the lowest standard was based on precision and %RE. The lowest injected CRP concentration response in each sample matrix demonstrated a %RE of < 25%. Additionally, the %RSD (n = 3) at the lowest CRP concentrations was 14.1% (CSF) and 19.5% (serum).

Table 7: Accuracy and precision of C-reactive protein by sandwich immunoassays (n = 6).

Matrix	Concentration (µg/mL)	Accuracy (%DFN)	Precision (%RSD)
1:10 Serum	0.504	1.1	15.1
	1.02	-6.1	11.3
CSF	0.198	9.6	15.8
	0.509	7.3	11.0
	1.02	2.9	9.3

The parameter estimates with standard error for the human serum assay (Figure 32 A) were min = 0.08 (0.02), max = 1.20 (0.05), EC50 = 0.72 (0.05), Hillslope = -3.2 (0.4), and r^2 = 0.98 (0.08). The adjusted assay range correcting for the dilution factor was from 0.540 to 30.0 µg/mL, which encompassed the relevant range for cardiovascular disease risk assessment (Ledue and Rifai 2003). Based on the parameter estimate for the upper asymptote, the CRP concentration that would saturate the system would be 17 µg/mL in 1:10 diluted serum (170 µg/mL, undiluted). The serum assay is capable of assessing cardiovascular disease risk as well as general inflammation, although extreme

cases may require dilution into the assay range. A separate source of pooled normal human serum (not CRP free) was injected (n = 2) and determined to have a concentration of 2.48 µg/mL of CRP. This value falls into the average cardiovascular disease risk bracket and compares with the expected normal range.

The parameter estimates with standard error for the CSF assay (Figure 32 B) were min = 0.14 (0.07), max = 3.1 (0.1), EC50 = 1.5 (0.2), Hillslope = -1.5 (0.2), and r^2 = 0.98 (0.18). Normal CRP levels in human CSF are much lower than in serum and thus an undiluted matrix was advantageous for this application. The CSF used to prepare the calibration was not CRP free and a background subtraction of the calibration was necessary. Based on the subtracted background, a pooled normal human CSF sample contained 164 ng/mL of CRP (n = 4 injections). This is in agreement with values for CRP in control patient CSF established in the literature (Rajs, Finzi-Yeheskel et al. 2002; Is, Coskun et al. 2007). The total range of the CSF assay encompasses the relevant CRP levels associated with conditions such as bacterial meningitis (Kanoh and Ohtani 1997; Rajs, Finzi-Yeheskel et al. 2002; Is, Coskun et al. 2007) and may have application in detecting sources of inflammation in human CSF.

Both the response and range of the CSF assay were greater than those of the human serum assay. The upper asymptote parameter estimate for the CSF calibration was 2.6 times higher than the upper estimate of the serum calibration. These results could be attributed to the differences in sample matrix and a slope error. The serum matrix contains high levels of large proteins and other macromolecules that could interfere (possibly compete) with antibody-antigen recognition. Because CRP is also a
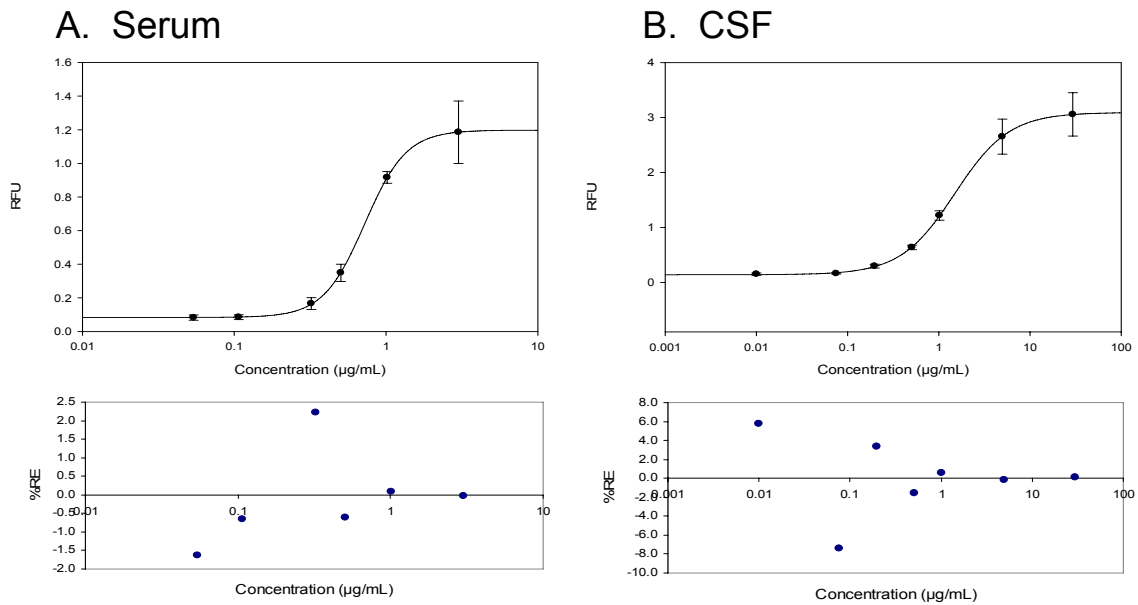
Figure 32: Calibration curves and % relative error plots of C-reactive protein in 1:10

serum and undiluted CSF. RFU = relative fluorescence units.

large protein, sample preparation to remove matrix components was limited to sample dilution.

The saturation of the calibration curves were used as an estimate of maximum antigen binding and column capacity. To eliminate the possibility of detector saturation, the detection antibody was pumped through the detector flow cell at concentrations below and above the working concentration (11.5 µg/mL). Detection antibody was prepared at 1.97, 2.81, 39.9, 144, and 288 µg.mL and analyzed in duplicate. A log-scale x-axis was used to plot the data since the calibration curves were also plotted with a log-scale x-axis. The response from 1.97 µg/mL to 288 µg/mL did not appear to saturate and a linear regression resulted in an equation of $y = 4.9 (0.2)x - 0.3 (0.4)$, with an r^2 of 0.99 (0.48). The detector response was linear beyond the working concentration of the detection antibody used in the sandwich immunoassays; therefore, the saturation of the 4PL calibration curves represents maximum antigen binding rather than detector saturation.

Sandwich immunoassays of clinical markers using immunoaffinity chromatography have been reported previously. A flow injection sandwich immunoassay for serum carcinoembryonic antigen was demonstrated using time-resolved fluorescence detection (Yan, Zhou et al. 2005). The antigen and detection antibody were injected sequentially and the detection was performed offline. A high performance immunoaffinity separation of parathyroid hormone in human plasma was presented in a sandwich format with chemiluminescent detection (Hage and Kao 1991). The sample antigen and labeled antibody were injected simultaneously and the useful column lifetime was 200 injections of clinical samples. The simultaneous injection of reagents was

reported to provide better detection limits versus sequential injection, but required an incubation step for all samples prior to analysis. Chromatographic sandwich immunoassays of thyroid-stimulating hormone and human chorionic gonadotropin in human serum were demonstrated as alternatives to ELISA methods (Johns, Rosengarten et al. 1996). The samples and detection antibody were simultaneously injected after incubation and the immunoaffinity columns could be regenerated at least 1000 times.

The use of liquid chromatography systems for sandwich immunoassays results in lower throughput than conventional microplate assays, but offers advantages of assay speed and precision, with a reduction in laborious preparation steps (Hage and Kao 1991; Johns, Rosengarten et al. 1996). In the current study, a microfluidic capillary sandwich immunoassay was presented with sequential reagent injections and assay times as low as 10 minutes. The immunoaffinity capillary column lifetime was at least 185 injection cycles operated and stored at refrigerated conditions. During the sandwich and direct capture immunoassays (Chapter 3), the PEEK capillary columns demonstrated no failures once the packing procedure was established. The packing procedure described in Chapter 2 resulted in columns that remained active for greater than 100 elution cycles operated and stored at refrigerated conditions. The column used for sandwich immunoassays did not display any loss in antigen binding after 185 injections. This lifetime may be attributed to the clean nature of the CSF and diluted serum samples.

Table 8 compares features of recent microfluidic immunoassays for CRP, including the work presented in the current chapter (Peoples and Karnes 2008).

Table 8: Miniaturized or microfluidic immunoassays for CRP.

System/ Detection	Matrix (Injected volume)	Analysis time (min)	Detectability	Precision/ Accuracy within 20%	Reference
Chip/ Fluorescence	Human plasma (1 µL)	10	30 ng/mL (LOD)	Precision- Yes Accuracy- NR	Wolf et al. 2004
Chip/ Fluorescence	Buffer (20-40 µL)	NR	1.4 nM (LOD)	Precision- No Accuracy- NR	Shin et al. 2007
Chip/ Fluorescence	Human serum (0.5 µL)	23	17 pg/mL (LOD)	NR	Hosokawa et al. 2007
Chip/ LIF	Human saliva	12	5 fg/mL (LOD)	NR	Christodoulides et al. 2007
Chip/ CL	Human serum	25	100 ng/mL (LOD)	Precision- Yes Accuracy- NR	Bhattacharya and Klapperich 2007
Chip/ Particle Counting	Human serum (10 µL)	<10	1.2 µg/mL (LLOQ)	NR	Tsai et al. 2007
Vial/ Magnetic Permeability	Human Blood (20 µL)	11.5	200 ng/mL (LOD)	Precision- Yes Accuracy- NR	Kriz et al. 2005
Capillary/ LIF	Human CSF/serum (250 nL)	10 (CSF) 12 (serum)	10.0 ng/mL (CSF) 540 ng/mL (serum) (LLOQ)	Precision- Yes Accuracy- Yes	Peoples and Karnes 2008

Abbreviations: Chemiluminescence (CL), laser-induced fluorescence (LIF), limit of detection (LOD), and lower limit of quantification (LLOQ).

5.4 Conclusions

Immunoaffinity chromatography of CRP in human serum and CSF was performed in a sandwich format. The separations were achieved in microfluidic capillaries, consuming low amounts of reagents and samples. Capillaries were presented as simple,

readily available alternatives to standard microchip platforms. Capillary tubing is relatively inexpensive and produced in a variety of internal and outer diameters. The dimensions of separation zones may therefore be changed or evaluated rapidly by simply changing the tubing size.

The sandwich immunoassay format allowed biological matrices to be used with minimal sample preparation. The detection antibody was introduced only after the sample matrix was pumped through the column to waste. The appropriate sensitivity of CRP assays was achieved without necessarily reaching equilibrium conditions, resulting in faster assay times compared to standard immunoassays. The flow-through capillary format also allowed the same antibodies to be reused multiple times. During the course of the current study 185 injections were made on a single column with no appreciable loss of antibody activity. The small dimensions of the column used (175 µm x 18.5 mm) required minimal amounts of stationary phase, yet had sufficient antigen-binding capacity to perform CRP assays in clinically-relevant ranges. Additionally, the low sample volume requirements of the system may contribute to less invasive patient sampling for obtaining blood serum or CSF.

CHAPTER 6 Summary and Conclusions

A prototype microfluidic analytical system was developed and presented for the analysis of biological matrices in clinical and research applications. Microfluidics has been defined in this work as moving fluid through capillaries or channels with internal dimensions less than one millimeter. Patient point-of-care and clinical testing may benefit from portable, miniaturized equipment and small volume sample requirements. The reduction of sample volumes required in microfluidic assays could lead to less invasive patient sampling techniques and preservation of limited sample material. The described microfluidic approach relied on antibody-antigen reactions as the basis for isolating compounds from complex matrices. All immunoaffinity separations presented employed a stationary antibody to selectively capture the target antigen from samples in a pump-generated flow through format. The use of immunoaffinity chromatography in microdevices provides a selective, rapid, and potentially portable means of measuring clinically relevant markers in biological matrices.

The instrumentation assembled in the current work was presented in detail, along with performance testing and initial proof-of-concept results. The miniaturized system for immunoaffinity chromatography was constructed from two micro syringe pumps, a gradient mixing chip, micro-injector capillary injection loop, a capillary column, and a diode laser-induced fluorescence (LIF) detector fitted with a fused-silica capillary flow

cell. A custom program written with LabVIEW software controlled the syringe pumps to perform step gradient elution and collected the LIF signal as a chromatogram. Optimization of the device was achieved by measuring flow accuracy with respect to column length and particle size. Syringe size and pressure effects were also used to characterize the capability of the pumps and system failure due to pressure limitations was observed as leaking around the syringe plungers. Based on test results, 500-µL syringes were selected as mobile phase reservoirs and columns were prepared at 25 mm lengths and 200 µm internal diameters. Columns were initially made from polyetheretherketone (PEEK)-fused silica tubing and packed under negative pressure by vacuum. The system was tested for mixer proportioning by pumping different compositions of buffer and fluorescent dye solutions in a stepwise fashion. A linear response was achieved for increasing concentrations of fluorescent dye by online mixing (r^2 = 1.0000 ± 0.0004 standard error). The effectiveness of an acidic gradient was confirmed by monitoring pH post-column and measuring premixed solutions offline. Finally, assessment of detectability was achieved by injecting fluorescent dye solutions and measuring the signal from the LIF detector. The limit of detection for the system with these solutions was 10.0 picomolar or 10.0 attomoles on-column. As proof-of-principle, immunoaffinity chromatography was demonstrated with immobilized rabbit anti-goat IgG and a fluorescent dye-goat IgG conjugate as a model antigen. The samples were injected using a 1.0 µL loop and the flow rate was 1.5 µL/min.

C-reactive protein (CRP), a biomarker of inflammation and cardiovascular disease risk assessment, was selected as a model antigen to demonstrate a direct

labeling/direct capture immunoaffinity separation using the microfluidic system. In this application, the columns were made from 175 μm internal diameter PEEK tubing, the injection loop was 250 nL, and the flow rate was 2.0 μL/min. Monoclonal anti-CRP was biotinylated and attached to 5.0 μm streptavidin-silica beads to make the solid support for separation columns. CRP in simulated serum matrix was fluorescently labeled in a one-step reaction and directly injected onto the immunoaffinity capillary. The purified antigen was then eluted in an acid gradient and measured. The antibody binding of CRP was evaluated in two physiological buffers, phosphate buffered saline (PBS) and Dulbecco's PBS (DPBS). The binding was enhanced in calcium-containing DPBS, indicating that the anti-CRP antibody may have been sensitive to conformational changes of CRP. A quadratic calibration model produced % relative errors of -15.9 to 12.6 for CRP concentration levels ranging from 0.475 to 95.0 μg/mL. The accuracy (% difference from nominal) and precision (% relative standard deviation (RSD)) of replicate injections were within 17.0%. The limit of detection was 57.2 ng/mL and chromatographic run times were less than 10 minutes. A 4-parameter logistic model was chosen to estimate the maximum antigen-binding capacity of two columns. Column I (0.175 x 19 mm) and Column II (0.175 x 18.5 mm) could bind approximately 188 and 125 ng of C-reactive protein, respectively. The useful column lifetime was observed to be greater than 100 injection cycles operated and stored at refrigerated conditions.

The measurement of parathyroid hormone (PTH) during the removal of parathyroid tumors is an intraoperative assay used to assess surgical success. A simple direct capture immunoaffinity separation of PTH in human serum was performed using a

capillary microfluidic approach. Antibodies were biotinylated and attached to silica prior to vacuum packing into capillary columns. PTH was fluorescently labeled with an amine-reactive dye in diluted human serum, injected onto the capillary column, and eluted by a dissociation buffer for measurement by diode LIF. Although the direct capture approach was capable of separating PTH from human serum, the assay was compromised by nonspecific binding of matrix components. Strategies to improve the background signal included removing large proteins by molecular weight cutoff filters and dilution of the matrix. It was determined that the required clinical range could not readily be obtained by the direct capture method and therefore a two antibody sandwich assay was attempted to overcome matrix effects. The sandwich assay was unsuccessful for isolating PTH from solution due to either an incomplete PTH amino acid sequence or lack of quality reagents.

Capillary sandwich immunoassays for C-reactive protein were demonstrated in human serum and cerebrospinal fluid (CSF), which are relevant matrices for cardiovascular disease risk and meningitis research, respectively. Capillaries packed with antibody-coated silica beads were used to capture CRP from the matrix and a second, dye-labeled antibody was introduced to form a sandwich complex. An acidic elution buffer dissociated the antibody-antigen complexes and the labeled antibody was detected with diode laser-induced fluorescence. Four parameter logistic functions and % relative error plots were used to model and assess the data. The calibration ranges for CRP were 0.0540-3.00 μg/mL in 1:10 diluted serum and 0.0100–29.5 μg/mL in undiluted CSF. The % relative error of back calculated standards for the serum and CSF assays was -1.6 to

2.2 and -7.4 to 5.5, respectively. All precision and accuracy data, expressed as % RSD and % difference from nominal values, was less than 15.8%. The microfluidic apparatus employed a flow rate of 2 µL/min and a sample injection volume of 250 nL. Since it was not necessary to reach antibody-antigen reaction equilibrium and the assay platform dimensions were minimal, run times were as short as 10 minutes.

The prototype instrument design involved commercially available materials and is potentially portable, making the goal of clinical and point-of-care testing possible. Furthermore, the assay procedure may be modified for other clinically relevant markers by changing the antibodies. The direct labeling and direct capture immunoaffinity approach was demonstrated to be simple and rapid, but suffered from matrix effects that limited the overall assay range. The reactive nature of the dye may cause labeled matrix components to interfere with detection in the direct capture mode. A two antibody sandwich immunoassay was performed in the capillary chromatography format for the analysis of a biomarker in biological matrices. The labeling of the detection antibody occurred offline, allowing purification and removal of unreacted fluorescent dye. C-reactive protein was analyzed in both human serum and cerebrospinal fluid matrices using the sandwich immunoaffinity separation. Reagent and sample consumption was minimal due to sub-microliter injection volumes and low µL flow rates. As proof-of-principle, the microfluidic capillary-based system was capable of separating and measuring analytes (antigens) from biological matrices.

References

Ahn, J. S., S. Choi, et al. (2003). "Development of a point-of-care assay system for high-sensitivity C-reactive protein in whole blood." Clin Chim Acta **332**(1-2): 51-9.

Amundsen, L. K. and H. Siren (2007). "Immunoaffinity CE in clinical analysis of body fluids and tissues." Electrophoresis **28**(1-2): 99-113.

Bange, A., H. B. Halsall, et al. (2005). "Microfluidic immunosensor systems." Biosens Bioelectron **20**(12): 2488-503.

Bangs, L. B. (1996). "New Developments in particle-based immunoassays: introduction." Pure and Applied Chemistry **68**(10): 1873-1879.

Bhattacharyya, A. and C. M. Klapperich (2007). "Design and testing of a disposable microfluidic chemiluminescent immunoassay for disease biomarkers in human serum samples." Biomed Microdevices **9**(2): 245-51.

Bhoopathy, S. and H. T. Karnes (2002). "Determination of (3S)-3-hydroxy quinidine for metabolism screening experiments using direct injection capillary electrophoresis and laser-induced fluorescence detection." Biomed Chromatogr **16**(1): 1-6.

Bi, H., W. Zhong, et al. (2006). "Construction of a biomimetic surface on microfluidic chips for biofouling resistance." Anal Chem **78**(10): 3399-405.

Bogusiewicz, A., N. I. Mock, et al. (2004). "Instability of the biotin-protein bond in human plasma." Anal Biochem **327**(2): 156-61.

149

Brogan, K. L., J. H. Shin, et al. (2004). "Influence of surfactants and antibody immobilization strategy on reducing nonspecific protein interactions for molecular recognition force microscopy." Langmuir **20**(22): 9729-35.

Buranda, T., J. Huang, et al. (2002). "Biomolecular recognition on well-characterized beads packed in microfluidic channels." Anal Chem **74**(5): 1149-56.

Butler, J. E. (2000). "Solid supports in enzyme-linked immunosorbent assay and other solid-phase immunoassays." Methods **22**(1): 4-23.

Cappiello, A., G. Famiglini, et al. (2003). "Variable-gradient generator for micro- and nano-HPLC." Anal Chem **75**(5): 1173-9.

Cheng, S. B., C. D. Skinner, et al. (2001). "Development of a multichannel microfluidic analysis system employing affinity capillary electrophoresis for immunoassay." Anal Chem **73**(7): 1472-9.

Chiem, N. H. and D. J. Harrison (1998). "Microchip systems for immunoassay: an integrated immunoreactor with electrophoretic separation for serum theophylline determination." Clin Chem **44**(3): 591-8.

Chilkoti, A. and P. S. Stayton (1995). "Molecular Origins of the slow streptavidin-biotin dissociation kinetics." J. Am. Chem. Soc. **117**: 10622-10628.

Cho, I. H., E. H. Paek, et al. (2007). "Site-directed biotinylation of antibodies for controlled immobilization on solid surfaces." Anal Biochem **365**(1): 14-23.

Christodoulides, N., S. Mohanty, et al. (2005). "Application of microchip assay system for the measurement of C-reactive protein in human saliva." Lab Chip **5**(3): 261-9.

Clarke, W. and D. S. Hage (2001). "Development of sandwich HPLC microcolumns for analyte adsorption on the millisecond time scale." Anal Chem **73**(6): 1366-73.

Dai, J., G. L. Baker, et al. (2006). "Use of porous membranes modified with polyelectrolyte multilayers as substrates for protein arrays with low nonspecific adsorption." Anal Chem **78**(1): 135-40.

Delaunay-Bertoncini, N. and M. C. Hennion (2004). "Immunoaffinity solid-phase extraction for pharmaceutical and biomedical trace-analysis-coupling with HPLC and CE-perspectives." J Pharm Biomed Anal **34**(4): 717-36.

Dodge, A., K. Fluri, et al. (2001). "Electrokinetically driven microfluidic chips with surface-modified chambers for heterogeneous immunoassays." Anal Chem **73**(14): 3400-9.

Dotsikas, Y. and Y. L. Loukas (2005). "Application of avidin-biotin technology for the characterization of a model hapten-protein conjugate." J Immunoassay Immunochem **26**(4): 285-93.

Ducret, A., N. Bartone, et al. (1998). "A simplified gradient solvent delivery system for capillary liquid chromatography-electrospray ionization mass spectrometry." Anal Biochem **265**(1): 129-38.

Erxleben, H. and J. Ruzicka (2005). "Sequential affinity chromatography miniaturized within a "lab-on-valve" system." Analyst **130**(4): 469-71.

Findlay, J. W. and R. F. Dillard (2007). "Appropriate calibration curve fitting in ligand binding assays." Aaps J **9**(2): E260-7.

Friedman, M., R. Vidyasagar, et al. (2005). "Intraoperative intact parathyroid hormone level monitoring as a guide to parathyroid reimplantation after thyroidectomy." Laryngoscope **115**(1): 34-8.

Gardas, A. and A. Lewartowska (1988). "Coating of proteins to polystyrene ELISA plates in the presence of detergents." Journal of Immunological Methods **106**(2): 251-255.

Gotz, S. and U. Karst (2007). "Recent developments in optical detection methods for microchip separations." Anal Bioanal Chem **387**(1): 183-92.

Grant, R., B. Condon, et al. (1991). "Changes in intracranial CSF volume after lumbar puncture and their relationship to post-LP headache." J Neurol Neurosurg Psychiatry **54**(5): 440-2.

Guzman, N. A. (2003). "Improved solid-phase microextraction device for use in on-line immunoaffinity capillary electrophoresis." Electrophoresis **24**(21): 3718-27.

Guzman, N. A. and T. M. Phillips (2005). "Immunoaffinity CE for proteomics studies." Anal Chem **77**(3): 61A-67A.

Guzman, N. A. and R. J. Stubbs (2001). "The use of selective adsorbents in capillary electrophoresis-mass spectrometry for analyte preconcentration and microreactions: a powerful three-dimensional tool for multiple chemical and biological applications." Electrophoresis **22**(17): 3602-28.

Hage, D. S. (1998). "Survey of recent advances in analytical applications of immunoaffinity chromatography." J Chromatogr B Biomed Sci Appl **715**(1): 3-28.

Hage, D. S. (1999). "Affinity chromatography: a review of clinical applications." Clin Chem **45**(5): 593-615.

Hage, D. S. and P. C. Kao (1991). "High-performance immunoaffinity chromatography and chemiluminescent detection in the automation of a parathyroid hormone sandwich immunoassay." Anal Chem **63**(6): 586-95.

Hage, D. S., B. Taylor, et al. (1992). "Intact parathyroid hormone: performance and clinical utility of an automated assay based on high-performance immunoaffinity chromatography and chemiluminescence detection." Clin Chem **38**(8 Pt 1): 1494-500.

Hahn, Y. K., Z. Jin, et al. (2007). "Magnetophoretic immunoassay of allergen-specific IgE in an enhanced magnetic field gradient." Anal Chem **79**(6): 2214-20.

Hatch, A., A. E. Kamholz, et al. (2001). "A rapid diffusion immunoassay in a T-sensor." Nat Biotechnol **19**(5): 461-5.

Hayes, M. A., T. N. Polson, et al. (2001). "Flow-based microimmunoassay." Anal Chem **73**(24): 5896-902.

Hennion, M. C. and V. Pichon (2003). "Immuno-based sample preparation for trace analysis." J Chromatogr A **1000**(1-2): 29-52.

Herrmann, M., T. Veres, et al. (2006). "Enzymatically-generated fluorescent detection in micro-channels with internal magnetic mixing for the development of parallel microfluidic ELISA." Lab Chip **6**(4): 555-60.

Ho, J. A., H. W. Hsu, et al. (2004). "Liposome-based microcapillary immunosensor for detection of Escherichia coli O157:H7." Anal Biochem **330**(2): 342-9.

Hodgson, R. J., M. A. Brook, et al. (2005). "Capillary-scale monolithic immunoaffinity columns for immunoextraction with in-line laser-induced fluorescence detection." Anal Chem **77**(14): 4404-12.

Hosokawa, K., M. Omata, et al. (2007). "Immunoassay on a power-free microchip with laminar flow-assisted dendritic amplification." Anal Chem **79**(15): 6000-4.

Hu, W. P., H. Y. Hsu, et al. (2006). "Immunodetection of pentamer and modified C-reactive protein using surface plasmon resonance biosensing." Biosens Bioelectron **21**(8): 1631-7.

Inabnet, W. B. (2004). "Intraoperative parathyroid hormone monitoring." World J Surg **28**(12): 1212-5.

Is, M., A. Coskun, et al. (2007). "High-sensitivity C-reactive protein levels in cerebrospinal fluid and serum in severe head injury: relationship to tumor necrosis factor-alpha and interleukin-6." J Clin Neurosci **14**(12): 1163-71.

Jia, M., Z. He, et al. (2002). "Capillary electrophoretic enzyme immunoassay with electrochemical detection for cortisol." Journal of Chromatography A **966**: 1857-194.

Jiang, G., S. Attiya, et al. (2000). "Red diode laser induced fluorescence detection with a confocal microscope on a microchip for capillary electrophoresis." Biosens Bioelectron **14**(10-11): 861-9.

Jiang, T., R. Mallik, et al. (2005). "Affinity monoliths for ultrafast immunoextraction." Anal Chem **77**(8): 2362-72.

Johns, M. A., L. K. Rosengarten, et al. (1996). "Enzyme-linked immunosorbent assays in a chromatographic format." J Chromatogr A **743**(1): 195-206.

Johnson, M. E. and J. P. Landers (2004). "Fundamentals and practice for ultrasensitive laser-induced fluorescence detection in microanalytical systems." Electrophoresis **25**(21-22): 3513-27.

Kanoh, Y. and H. Ohtani (1997). "Levels of interleukin-6, CRP and alpha 2 macroglobulin in cerebrospinal fluid (CSF) and serum as indicator of blood-CSF barrier damage." Biochem Mol Biol Int **43**(2): 269-78.

Kelley, M. and B. DeSilva (2007). "Key elements of bioanalytical method validation for macromolecules." Aaps J **9**(2): E156-63.

Kriz, K., F. Ibraimi, et al. (2005). "Detection of C-reactive protein utilizing magnetic permeability detection based immunoassays." Anal Chem **77**(18): 5920-4.

Kurita, R., Y. Yokota, et al. (2006). "On-chip enzyme immunoassay of a cardiac marker using a microfluidic device combined with a portable surface plasmon resonance system." Anal Chem **78**(15): 5525-31.

Kuswandi, B., Nuriman, et al. (2007). "Optical sensing systems for microfluidic devices: a review." Anal Chim Acta **601**(2): 141-55.

Ledue, T. B. and N. Rifai (2003). "Preanalytic and analytic sources of variations in C-reactive protein measurement: implications for cardiovascular disease risk assessment." Clin Chem **49**(8): 1258-71.

Lim, C. T. and Y. Zhang (2007). "Bead-based microfluidic immunoassays: the next generation." Biosens Bioelectron **22**(7): 1197-204.

Lim, T. K. and T. Matsunaga (2001). "Construction of electrochemical flow immunoassay system using capillary columns and ferrocene conjugated immunoglobulin G for detection of human chorionic gonadotrophin." Biosens Bioelectron **16**(9-12): 1063-9.

Liu, Y. and Y. Li (2001). "An antibody-immobilized capillary column as a bioseparator/bioreactor for detection of Escherichia coil O157:H7 with absorbance measurement." Anal Chem **73**(21): 5180-3.

Lu, B., M. R. Smyth, et al. (1996). "Oriented immobilization of antibodies and its applications in immunoassays and immunosensors." Analyst **121**(3): 29R-32R.

Luppa, P. B., L. J. Sokoll, et al. (2001). "Immunosensors--principles and applications to clinical chemistry." Clin Chim Acta **314**(1-2): 1-26.

Malek, A. and M. G. Khaledi (1999). "Steroid analysis in single cells by capillary electrophoresis with collinear laser-induced fluorescence detection." Anal Biochem **270**(1): 50-8.

Mallik, R. and D. S. Hage (2006). "Affinity monolith chromatography." J Sep Sci **29**(12): 1686-704.

Malmstadt, N., A. S. Hoffman, et al. (2004). ""Smart" mobile affinity matrix for microfluidic immunoassays." Lab Chip **4**(4): 412-5.

Mastichiadis, C., S. E. Kakabakos, et al. (2002). "Simultaneous determination of pesticides using a four-band disposable optical capillary immunosensor." Anal Chem **74**(23): 6064-72.

Meyer, M. H., M. Hartmann, et al. (2006). "SPR-based immunosensor for the CRP detection--a new method to detect a well known protein." Biosens Bioelectron **21**(10): 1987-90.

Meyer, M. H., M. Hartmann, et al. (2007). "CRP determination based on a novel magnetic biosensor." Biosens Bioelectron **22**(6): 973-9.

Moelbert, S., B. Normand, et al. (2004). "Kosmotropes and chaotropes: modelling preferential exclusion, binding and aggregate stability." Biophys Chem **112**(1): 45-57.

Mokri, B. (2000). "Cerebrospinal fluid volume depletion and its emerging clinical/imaging syndromes." Neurosurg Focus **9**(1): e6.

Murakami, Y., T. Endo, et al. (2004). "On-chip micro-flow polystyrene bead-based immunoassay for quantitative detection of tacrolimus (FK506)." Anal Biochem **334**(1): 111-6.

Myers, G. L., N. Rifai, et al. (2004). "CDC/AHA Workshop on Markers of Inflammation and Cardiovascular Disease: Application to Clinical and Public Health Practice: report from the laboratory science discussion group." Circulation **110**(25): e545-9.

Nagaraj, S. and H. T. Karnes (2000). "Visible diode laser induced fluorescence detection of doxorubicin in plasma using pressurized capillary electrochromatography." Biomed Chromatogr **14**(4): 234-42.

Nelson, K. E., J. O. Foley, et al. (2007). "Concentration gradient immunoassay. 1. An immunoassay based on interdiffusion and surface binding in a microchannel." Anal Chem **79**(10): 3542-8.

Nisnevitch, M. and M. A. Firer (2001). "The solid phase in affinity chromatography: strategies for antibody attachment." J Biochem Biophys Methods **49**(1-3): 467-80.

Okanda, F. M. and Z. El Rassi (2007). "Biospecific interaction (affinity) CEC and affinity nano-LC." Electrophoresis **28**(1-2): 89-98.

Peoples, M. C. and H. T. Karnes (2008). "Microfluidic Capillary System for Immunoaffinity Separations of C-Reactive Protein in Human Serum and Cerebrospinal Fluid." Anal Chem.

Peoples, M. C. and H. T. Karnes (2008). "Microfluidic immunoaffinity separations for bioanalysis." J Chromatogr B Analyt Technol Biomed Life Sci **866**(1-2): 14-25.

Peoples, M. C., T. M. Phillips, et al. "Demonstration of a direct capture immunoaffinity separation for C-reactive protein using a capillary-based microfluidic device." Journal of Pharmaceutical and Biomedical Analysis **In Press, Corrected Proof**.

Peoples, M. C., T. M. Phillips, et al. (2007). "A capillary-based microfluidic instrument suitable for immunoaffinity chromatography." J Chromatogr B Analyt Technol Biomed Life Sci **848**(2): 200-7.

Petrou, P. S., S. E. Kakabakos, et al. (2002). "Multi-analyte capillary immunosensor for the determination of hormones in human serum samples." Biosens Bioelectron **17**(4): 261-8.

Phillips, K. S. and Q. Cheng (2005). "Microfluidic immunoassay for bacterial toxins with supported phospholipid bilayer membranes on poly(dimethylsiloxane)." Anal Chem **77**(1): 327-34.

Phillips, T. M. (1985). "High performance immunoaffinity chromatography." <u>LCGC</u> **3**: 962-972.

Phillips, T. M. (1998). "Determination of in situ tissue neuropeptides by capillary immunoelectrophoresis." <u>Analytica Chimica Acta</u> **372**: 209-218.

Phillips, T. M. (2001). "Multi-analyte analysis of biological fluids with a recycling immunoaffinity column array." <u>J Biochem Biophys Methods</u> **49**(1-3): 253-62.

Phillips, T. M. (2004). "Rapid analysis of inflammatory cytokines in cerebrospinal fluid using chip-based immunoaffinity electrophoresis." <u>Electrophoresis</u> **25**(10-11): 1652-9.

Phillips, T. M. and B. F. Dickens (2000). <u>Affinity and Immnuoaffinity Purification Techniques</u>. Natick, MA, Eaton Publishing.

Phillips, T. M. and J. M. Krum (1998). "Recycling immunoaffinity chromatography for multiple analyte analysis in biological samples." <u>J Chromatogr B Biomed Sci Appl</u> **715**(1): 55-63.

Phillips, T. M. and P. D. Smith (2002). "Immunoaffinity Analysis of Substance P in Complex Biological Fluids: Analysis of Sub-microliter Samples." <u>Journal of Liquid Chromatography & Related Technologies</u> **25**(19): 2889-2900.

Phillips, T. M. and E. Wellner (2006a). "Measurement of neuropeptides in clinical samples using chip-based immunoaffinity capillary electrophoresis." <u>J Chromatogr A</u> **1111**(1): 106-11.

Phillips, T. M. and E. F. Wellner (2006). "Measurement of naproxen in human plasma by chip-based immunoaffinity capillary electrophoresis." Biomed Chromatogr **20**(6-7): 662-7.

Phillips, T. M. and E. F. Wellner (2006b). "Measurement of naproxen in human plasma by chip-based immunoaffinity capillary electrophoresis." Biomed Chromatogr **20**(6-7): 662-7.

Piyasena, M. E., T. Buranda, et al. (2004). "Near-simultaneous and real-time detection of multiple analytes in affinity microcolumns." Anal Chem **76**(21): 6266-73.

Qu, Q., X. Hu, et al. (2004). "Packing capilllary electrochromatography columns using vacuum--a preliminary study." J Sep Sci **27**(14): 1229-32.

Rahavendran, S. V. and H. T. Karnes (1993). "Solid-state diode laser-induced fluorescence detection in high-performance liquid chromatography." Pharm Res **10**(3): 328-34.

Rahavendran, S. V. and H. T. Karnes (1996). "An oxazine reagent for derivatization of carboxylic acid analytes suitable for liquid chromatographic detection using visible diode laser-induced fluorescence." J Pharm Biomed Anal **15**(1): 83-98.

Rajs, G., Z. Finzi-Yeheskel, et al. (2002). "C-reactive protein concentrations in cerebral spinal fluid in gram-positive and gram-negative bacterial meningitis." Clin Chem **48**(3): 591-2.

Rhemrev-Boom, M. M., M. Yates, et al. (2001). "(Immuno)affinity chromatography: a versatile tool for fast and selective purification, concentration, isolation and analysis." J Pharm Biomed Anal **24**(5-6): 825-33.

Roberts, W. L., L. Moulton, et al. (2001). "Evaluation of nine automated high-sensitivity C-reactive protein methods: implications for clinical and epidemiological applications. Part 2." Clin Chem **47**(3): 418-25.

Roper, M. G., M. L. Frisk, et al. (2006). "Extraction of C-reactive protein from serum on a microfluidic chip." Analytica Chimica Acta **569**(1-2): 195-202.

Salim, M., B. O'Sullivan, et al. (2007). "Characterization of fibrinogen adsorption onto glass microcapillary surfaces by ELISA." Lab Chip **7**(1): 64-70.

Salvi, G., P. De Los Rios, et al. (2005). "Effective interactions between chaotropic agents and proteins." Proteins **61**(3): 492-9.

Sapsford, K. E., P. T. Charles, et al. (2002). "Demonstration of four immunoassay formats using the array biosensor." Anal Chem **74**(5): 1061-8.

Sato, K., A. Hibara, et al. (2003). "Microchip-based chemical and biochemical analysis systems." Adv Drug Deliv Rev **55**(3): 379-91.

Sato, K., M. Tokeshi, et al. (2001). "Determination of carcinoembryonic antigen in human sera by integrated bead-bed immunoassay in a microchip for cancer diagnosis." Anal Chem **73**(6): 1213-8.

Sato, K., M. Tokeshi, et al. (2000). "Integration of an immunosorbent assay system: analysis of secretory human immunoglobulin A on polystyrene beads in a microchip." Anal Chem **72**(6): 1144-7.

Sato, K., M. Yamanaka, et al. (2002). "Microchip-based immunoassay system with branching multichannels for simultaneous determination of interferon-gamma." Electrophoresis **23**(5): 734-9.

Schuhmann, M. U., K. R. Ostrowski, et al. (2005). "The value of C-reactive protein in the management of shunt infections." J Neurosurg **103**(3 Suppl): 223-30.

Schwarz, M. A. and P. C. Hauser (2001). "Recent developments in detection methods for microfabricated analytical devices." Lab Chip **1**(1): 1-6.

Sebra, R. P., K. S. Masters, et al. (2006). "Detection of antigens in biologically complex fluids with photografted whole antibodies." Anal Chem **78**(9): 3144-51.

Shin, K. S., S. W. Lee, et al. (2007). "Amplification of fluorescence with packed beads to enhance the sensitivity of miniaturized detection in microfluidic chip." Biosens Bioelectron **22**(9-10): 2261-7.

Sibarani, J., M. Takai, et al. (2007). "Surface modification on microfluidic devices with 2-methacryloyloxyethyl phosphorylcholine polymers for reducing unfavorable protein adsorption." Colloids and Surfaces B: Biointerfaces **54**(1): 88-93.

Snyder, L. R., J. J. Kirkland, et al. (1997). Practical HPLC Method Development. New York, John Wiley & Sons, Inc.

Sokoll, L. J., F. H. Wians, Jr., et al. (2004). "Rapid intraoperative immunoassay of parathyroid hormone and other hormones: a new paradigm for point-of-care testing." Clin Chem **50**(7): 1126-35.

Soo Ko, J., H. C. Yoon, et al. (2003). "A polymer-based microfluidic device for immunosensing biochips." Lab Chip **3**(2): 106-13.

Strachan, E., A. K. Mallia, et al. (2004). "Solid-phase biotinylation of antibodies." J Mol Recognit **17**(3): 268-76.

Studentsov, Y. Y., M. Schiffman, et al. (2002). "Enhanced enzyme-linked immunosorbent assay for detection of antibodies to virus-like particles of human papillomavirus." J Clin Microbiol **40**(5): 1755-60.

Su, P., X. X. Zhang, et al. (2005). "Development and application of a multi-target immunoaffinity column for the selective extraction of natural estrogens from pregnant women's urine samples by capillary electrophoresis." J Chromatogr B Analyt Technol Biomed Life Sci **816**(1-2): 7-14.

Subramanian, A. (2002). "Immunoaffinity chromatography." Mol Biotechnol **20**(1): 41-7.

Tang, Z. and H. T. Karnes (2000). "Coupling immunoassays with chromatographic separation techniques." Biomed Chromatogr **14**(6): 442-9.

Torabi, F., H. R. Mobini Far, et al. (2007). "Development of a plasma panel test for detection of human myocardial proteins by capillary immunoassay." Biosens Bioelectron **22**(7): 1218-23.

Tsai, H. Y., C. F. Hsu, et al. (2007). "Detection of C-reactive protein based on immunoassay using antibody-conjugated magnetic nanoparticles." Anal Chem **79**(21): 8416-9.

Turnbull, D. K. and D. B. Shepherd (2003). "Post-dural puncture headache: pathogenesis, prevention and treatment." Br J Anaesth **91**(5): 718-29.

Vasan, N. R., K. E. Blick, et al. (2004). "The dilemma of the normal baseline parathyroid hormone level using the intraoperative PTH assay." Otolaryngol Head Neck Surg **131**(5): 610-5.

Verpoorte, E. (2003). "Beads and chips: new recipes for analysis." <u>Lab Chip</u> **3**(4): 60N-68N.

Virji, M. A., W. F. Diven, et al. (1985). "CSF alpha 2-macroglobulin and C-reactive protein as aids to rapid diagnosis of acute bacterial meningitis." <u>Clin Chim Acta</u> **148**(1): 31-7.

Viswanathan, C. T., S. Bansal, et al. (2007). "Quantitative bioanalytical methods validation and implementation: best practices for chromatographic and ligand binding assays." <u>Pharm Res</u> **24**(10): 1962-73.

Vogt, R. V., D. L. Phillips, et al. (1987). "Quantitative differences among various proteins as blocking agents for ELISA microtiter plates." <u>Journal of Immunological Methods</u> **101**(1): 43-50.

Volanakis, J. E. (2001). "Human C-reactive protein: expression, structure, and function." <u>Molecular Immunology</u> **38**(2-3): 189-197.

von Lode, P. (2005). "Point-of-care immunotesting: approaching the analytical performance of central laboratory methods." <u>Clin Biochem</u> **38**(7): 591-606.

Wang, H. W., Y. Wu, et al. (2002). "Polymorphism of structural forms of C-reactive protein." <u>Int J Mol Med</u> **9**(6): 665-71.

Wang, J., A. Ibanez, et al. (2001). "Electrochemical enzyme immunoassays on microchip platforms." <u>Anal Chem</u> **73**(21): 5323-7.

Wang, X., O. Hofmann, et al. (2007). "Integrated thin-film polymer/fullerene photodetectors for on-chip microfluidic chemiluminescence detection." <u>Lab Chip</u> **7**(1): 58-63.

Waterboer, T., P. Sehr, et al. (2006). "Suppression of non-specific binding in serological Luminex assays." Journal of Immunological Methods **309**(1-2): 200-204.

Weller, M. G. (2000). "Immunochromatographic techniques--a critical review." Fresenius J Anal Chem **366**(6-7): 635-45.

Whitesides, G. M. (2006). "The origins and the future of microfluidics." Nature **442**(7101): 368-73.

Wolf, M., D. Juncker, et al. (2004). "Simultaneous detection of C-reactive protein and other cardiac markers in human plasma using micromosaic immunoassays and self-regulating microfluidic networks." Biosens Bioelectron **19**(10): 1193-202.

Wood, W. G. (1993). Assay Components. Methods of Immunological Analysis. R. F. Masseyeff. New York, VCH Publishers, Inc. **1:** 607-610.

Yacoub-George, E., W. Hell, et al. (2007). "Automated 10-channel capillary chip immunodetector for biological agents detection." Biosens Bioelectron **22**(7): 1368-75.

Yamauchi, M., K. Mawatari, et al. (2006). "Circular dichroism thermal lens microscope for sensitive chiral analysis on microchip." Anal Chem **78**(8): 2646-50.

Yan, F., J. Zhou, et al. (2005). "Flow injection immunoassay for carcinoembryonic antigen combined with time-resolved fluorometric detection." J Immunol Methods **305**(2): 120-7.

Yang, C. Y., E. Brooks, et al. (2005). "Detection of picomolar levels of interleukin-8 in human saliva by SPR." Lab Chip **5**(10): 1017-23.

Yarmush, M. L., K. P. Antonsen, et al. (1992). "Immunoadsorption: strategies for antigen elution and production of reusable adsorbents." Biotechnol Prog **8**(3): 168-78.

Yeung, W. S., G. A. Luo, et al. (2003). "Capillary electrophoresis-based immunoassay." J Chromatogr B Analyt Technol Biomed Life Sci **797**(1-2): 217-28.

Zeleke, J. M., G. B. Smith, et al. (2006). "Enantiomer separation of amino acids in immunoaffinity micro LC-MS." Chirality **18**(7): 544-50.

Zhou, J., F. Rusnak, et al. (2000). "Quasi-linear gradients for capillary liquid chromatography with mass and tandem mass spectrometry." Rapid Commun Mass Spectrom **14**(6): 432-8.

APPENDIX A

The pump control and read programs in LabVIEW are presented as front panels and descriptive information. Front panels represent the computer screen views of the software. The actual running programs are attached to this dissertation as media files on a compact disc compatible with the LabVIEW software. The CD is located in the back cover.

The program manuals for each program are also presented.

PUMPCONTROL.vi

Front Panel

Controls and Indicators

`I/O` **PUMP A** A string that uniquely identifies the resource to be opened and
written to as well as read from. The grammar for the resource name is
shown below. Optional string segments are shown in square brackets ([])

Interface	Syntax
VXI	VXI[board]::VXI logical address[::INSTR]
GPIB-VXI	GPIB-VXI[board]::VXI logical address[::INSTR]
GPIB	GPIB[board]::primary address[::secondary address][::INSTR]
Serial	ASRL[board][::INSTR]

The following table shows the default value for optional string segments.

Optional String Segments	Default Value
board	0
secondary address	none

The following table shows examples of address strings.

Address String	Description
VXI0::1	A VXI device at logical address 1 in VXI interface VXI0.
GPIB-VXI::9	A VXI device at logical address 9 in a GPIB-VXI controlled system.
GPIB::5	A GPIB device at primary address 5.
ASRL1	A serial device attached to interface ASRL1.

`I/O` **PUMP B** A string that uniquely identifies the resource to be opened and
written to as well as read from. The grammar for the resource name is
shown below. Optional string segments are shown in square brackets ([])

Interface	Syntax
VXI	VXI[board]::VXI logical address[::INSTR]
GPIB-VXI	GPIB-VXI[board]::VXI logical address[::INSTR]
GPIB	GPIB[board]::primary address[::secondary address][::INSTR]
Serial	ASRL[board][::INSTR]

The following table shows the default value for optional string segments.

Optional String Segments	Default Value
board	0
secondary address	none

The following table shows examples of address strings.

Address String	Description
VXI0::1	A VXI device at logical address 1 in VXI interface VXI0.
GPIB-VXI::9	A VXI device at logical address 9 in a GPIB-VXI controlled system.
GPIB::5	A GPIB device at primary address 5.
ASRL1	A serial device attached to interface ASRL1.

`abc` **Initial Flow Rate A   (uL/min)**

`abc` **Initial Flow Rate B   (uL/min)**

`TF` **POWER**

`I/O` **Physical Channel 2 physical channels** specifies the names of the physical channels to use to create virtual channels.

Important! This is a **DAQmx Physical Channel** control and does not contain device information relevant to the DAQmx Base driver. The control is populated with device information maintained by the DAQmx driver. To use this control with DAQmx Base VIs use the **NI-DAQmx Base Configuration Utility** to determine the device numbers and type Physical Channel information in the control.

`DBL` **DURATION FOR DATA ACQUISITION   (min)**

`DBL` **SAMPLING RATE   (Hz) rate** specifies the sampling rate in samples per channel per second. If you use an external source for the Sample Clock, set this input to the maximum expected rate of that clock.

`DBL` **TIME 1**

`abc` **FLOW A1**

`abc` **FLOW B1**

`DBL` **TIME 2**

`abc` **FLOW A2**

`abc` **FLOW B2**

`DBL` **TIME 3**

`abc` **FLOW A3**

`abc` **FLOW B3**

`DBL` **TIME 4**

`abc` **FLOW A4**

`abc` **FLOW B4**

`DBL` **TIME 5**

`abc` **FLOW A5**

`abc` **FLOW B5**

`DBL` **TIME 6**

`abc` **FLOW A6**

`abc` FLOW B6

`DBL` TIME 7

`abc` FLOW A7

`abc` FLOW B7

`DBL` TIME 8

`abc` FLOW A8

`abc` FLOW B8

`DBL` TIME 9

`abc` FLOW A9

`abc` FLOW B9

`DBL` TIME 10

`abc` FLOW A10

`abc` FLOW B10

`DBL` TIME 11

`abc` FLOW A11

`abc` FLOW B11

`DBL` TIME 12

`abc` FLOW A12

`abc` FLOW B12

`DBL` TIME 13

`abc` FLOW A13

`abc` FLOW B13

`DBL` TIME 14

`abc` FLOW A14

`abc` FLOW B14

DBL | **TIME 15**

abc | **FLOW A15**

abc | **FLOW B15**

DBL | **TIME 16**

abc | **FLOW A16**

abc | **FLOW B16**

DBL | **TIME 17**

abc | **FLOW A17**

abc | **FLOW B17**

DBL | **TIME 18**

abc | **FLOW A18**

abc | **FLOW B18**

DBL | **TIME 19**

abc | **FLOW A19**

abc | **FLOW B19**

DBL | **TIME 20**

abc | **FLOW A20**

abc | **FLOW B20**

TF | **START**

TF | **nothing**

P~a | **PATH**

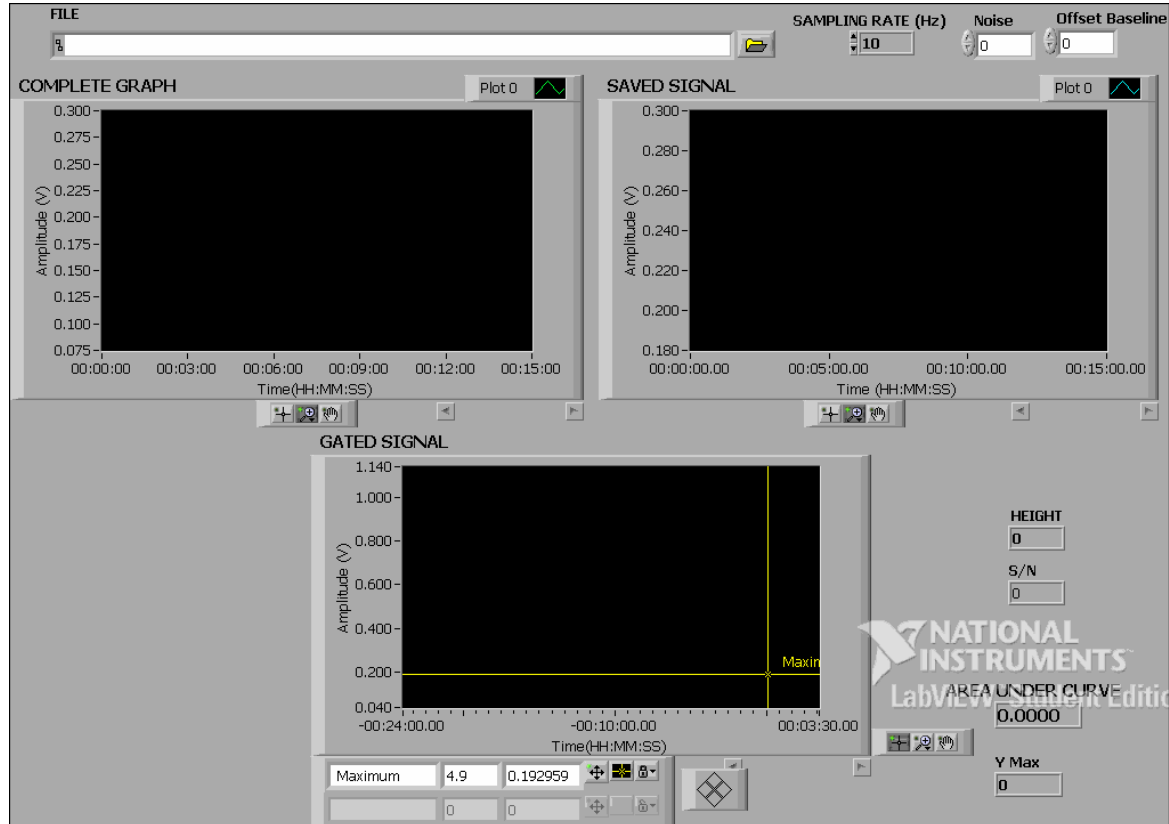[DBL] | **Measurement**

I32 | **TIME(s)**

ReadProgram.vi
Example of the SubVI with Error Handling template.

This VI is used as a subvi in the Limit Example.vi (Example of the use of Single Loop Application template). If there is no error this VI calculates the area of the signal that is under/over the +-5 band.

If there is an error, then it outputs 0.

Front Panel

Controls and Indicators

`DBL`	**SAMPLING RATE (Hz)**
`□~□`	**FILE**
`DBL`	**Noise**
`DBL`	**Offset Baseline**
`[DBL]`	**GATED SIGNAL**
`[DBL]`	**SAVED SIGNAL**
`DBL`	**AREA UNDER CURVE result** contains the result of the numeric integration.

`[DBL]` **COMPLETE GRAPH**

`[DBL]` **HEIGHT**

`[DBL]` **Y Max**

`[I32]` **S/N**

Pump Control Program Manual

1. Run program once without collecting real data.
2. Set Path and File Name. Add .lvm as the extension.
3. Select ports to be called Pump A & B (COM1 & COM2).
4. Begin program with Power off and the Start button off.
5. Tab through remaining sections:
    A. Set initial flow rate for each pump. The program will return to these flow rates when the timed session has ended. Once these rates have been set, the power button to begin the initial flow rate can be turned on at any time.
    B. Device & Channel should be set to Dev1/ai0.
    C. Set desired time to run data acquisition (in minutes).
    D. Set sampling rate in Hz, samples per second.
    E. Set time and flow rates for timed session.
        i. Data acquisition begins at Time 2. So, set Time 1 accordingly.
        ii. Leave Times at end of run equal to 0 if not all time segments are used. When the program gets to these values it will run through them and return to initial flow rate.
    F. On Chart, edit the final time to be equal to the Duration for DAQ time. If chart begins to autoscale while running, right click on the chart and click on X Scale>>Autoscale X to unselect this option.
    G. To clear chart right click on the chart and select clear chart.
6. To begin timed session press the start button.
    - The Timer starts when timed session begins.
    - Data acquisition begins at Time 2.
7. When a timed session has ended, press the start button to the off mode.
8. Clear the chart before another timed session is run. Remember to rename your file after each timed session or it will automatically rename your original file name to the next available name. As many timed sessions as desired can be run without having to turn the program off.
9. To stop pumps, stop the program using the stop sign on the toolbar and rerun program with the power button off. Then stop the program again using the stop sign.
10. If error code –200361 appears, unplug USB port from A\D converter and put back in and rerun program.

Read and Analyze Program Manual

1. To set the threshold, go to the block diagram (Window>>Show Block Diagram) and double click on the blue box titled Trigger and Gate. Set the start level and stop level to the threshold desired and press OK. Save the program. The program will collect all points above the threshold and integrate under the curve down to the baseline set by the threshold.
2. On front panel select File to read.
3. Set sampling rate to the sample rate at which the data was collected.
4. Set Offset Baseline to the (-) threshold used.
5. Run program.
6. The program will first graph the complete signal.
7. Next the signal will begin running on the second graph.
8. As the signal reaches above the threshold data will appear on the third graph.
9. Once the start threshold and stop threshold have been reached a box will pop up asking if this is the desired signal. If no is selected, the program will continue running until it has reached the signal desired. When yes is selected the program will stop running.
10. The area under the curve is calculated using the gated signal.
11. The height is calculated on the saved signal by taking the difference between the lowest and highest point on the graph. It is not the measurement of the height of the curve used to calculate the area. The height of the curve used to find area can be determined by subtracting the threshold from the max height of the curve.
12. Use the cursor to find the maximum y value. The cursor is the first box in the graph palette. The max y value and time at this value are displayed in the box below the graph.
13. To print the front panel, go to File>>Print Window.
14. If any errors occur while signal is reading, select continue. Otherwise, select stop.
15. To verify accuracy of integration run triangletest.lvm or squaretest.lvm and set sample rate to 20 Hz. Set trigger to 0. Then run read program.

VITA

Michael C. Peoples was born on January 8, 1975 in Quantico, Virginia. He received a Bachelor of Science degree in Chemistry from Virginia Commonwealth University in Richmond, Virginia in 1998. He worked as an analytical chemist in the pharmaceutical industry for over 3 years prior to joining the VCU Bioanalytical Core Laboratory Service Center in 2003. Mike currently holds the title of Technical Group Leader and is responsible for method development and validation, technical report writing, and supervision of projects. Mike has authored or coauthored 6 invited presentations and 5 posters related to his graduate research. He has written 6 accepted manuscripts to date in publications such as *Journal of Chromatography B*, *Journal of Pharmaceutical and Biomedical Analysis*, *Biomedical Chromatography*, and *Analytical Chemistry*, including a review of the field of microfluidic immunoaffinity separations. He was a co-organizer of a special issue for *Journal of Chromatography B*, volume 827, issue 1, November 15 2005: Analysis of antioxidants and biomarkers of oxidative stress. Mike was co-winner of the 2008 John Wood Award for Excellence in Pharmaceutical Sciences, Department of Pharmaceutics.